Development of an LC-MS/MS method for the analysis of *Saccharomyces cerevisiae* lipidome to determine the mechanism through which plant extract 21 delays aging by remodeling lipid composition

Karamat Mohammad

A Thesis

in

The Department

of

Biology

Presented in Partial Fulfillment of the Requirements for the Degree of Master of Sciences at Concordia University

Montreal, Quebec, Canada

December 2017

CONCORDIA UNIVERSITY

School of Graduate Studies

This is to certify that the thesis prepared

By: Karamat Mohammad

Entitled: Development of an LC-MS/MS method for the analysis of *Saccharomyces cerevisiae* lipidome to determine the mechanism through which plant extract 21 delays aging by remodeling lipid composition.

and submitted in partial fulfillment of the requirements for the degree of

Master of Sciences (Biology)

complies with the regulations of the University and meets the accepted standards with respect to originality and quality.

Signed by the final examining committee:

_____ Chair

Dr. Dayanandan Selvadurai

_____ External Examiner

Dr. William Zerges

_____ Examiner

Dr. Madoka Gray-Mitsumune

_____ Examiner

Dr. Jin Suk Lee

_____ Supervisor

Dr. Vladimir Titorenko

Approved by _____

Chair of Department or Graduate Program Director

_____

Dean of Faculty of Arts and Science

Date _____

Abstract

Development of an LC-MS/MS method for the analysis of *Saccharomyces cerevisiae* lipidome to determine the mechanism through which plant extract 21 delays aging by remodeling lipid composition

Karamat Mohammad

Aging is a multifactorial process that occurs in all biological organisms. The biological aspects of aging are evolutionary conserved across eukaryotes. *Saccharomyces cerevisiae* being a unicellular eukaryote has been used as a model organism to study aging. This unicellular eukaryote has a short lifespan, a fully sequenced genome and it is easy to manipulate genetically to make changes in metabolic pathways. Hence, it has been historically used to identify genes, metabolic pathways and chemical compounds that have influence on aging process. An extract from white willow bark (which is called PE21) was discovered in Dr. Vladimir Titorenko's lab as the plant extract capable of extending the chronological lifespan (CLS) of *Saccharomyces cerevisiae*. Previous studies in the lab have shown that PE21 considerably alters the lipid composition of *Saccharomyces cerevisiae*. Lipids play crucial roles in many important pathways related to cellular signaling network, energy storage, membrane trafficking, membrane dynamics and apoptosis. Lipidomics is a relatively new research field that aims at characterizing lipid profiles. The characterization of lipids is a difficult process because of their diverse chemical and physical properties and due to lack of sensitive tools to study them. Only with the advent of mass spectrometry it became possible to characterize individual lipid species of various lipid classes. Herein, I have developed an optimized LC-MS/MS method to successfully identify and quantify many individual

species of 10 different lipid classes of *Saccharomyces cerevisiae.* The developed method was used to analyze the effects of PE21 on the lipid composition of *Saccharomyces cerevisiae*. Our findings support previous studies, which stipulate that PE21 alters the lipid composition of yeast cells. PE21 markedly decreases the concentration of free fatty acids, thus it has been hypothesized that PE21 increases the CLS of yeast cells by decreasing the rate of liponecrosis known to be induced by free fatty acids. To further test this hypothesis, four single gene-deletion mutant strains differently affected in the metabolism of free fatty acids have been studied. More specifically, the lipid compositions and viabilities of such mutant strains were analyzed in yeast cultured in the presence or absence of PE21, and the results were compared to the results for wild-type strain.

Acknowledgements

First and foremost, thanks to my supervisor Dr. Vladimir Titorenko for his continuous mentorship, guidance, and support during my research career, beginning with my undergraduate Honours thesis and my master's thesis.

Special thanks to my thesis Committee members, Dr. Madoka Gray-Mitsumune and Dr. Jin Suk Lee for their help and support.

I would like to acknowledge the help and guidance of Dr. Heng Jiang from the Centre for Biological Applications of Mass Spectrometry (CBAMS) for the development of LC-MS/MS method and assistance with mass spectrometer instrumentation throughout my master's program.

My graduate studies were funded partially by the Concordia University Armand C. Archambault Fellowship award and the Concordia University Dean of Arts and Sciences Award of Excellence. I am sincerely thankful for both awards.

Thanks to all my lab colleagues for their cooperation and support.

Special thanks to Younes Medkour for his generous and affectionate help and support.

"The whole of science is nothing more than a refinement of everyday thinking".

Albert Einstein

Table of Contents

List of Tables

List of Figures

List of Abbreviations

AMPK/TOR, AMP-activated protein kinase/target of rapamycin; cAMP/PKA, cAMP/protein kinase A; CCO, cytochrome c oxidase; CL, cardiolipin; CLS, chronological life span; CR, caloric restriction; Cer, Ceramides; DAG, diacylglycerols; DR, dietary restriction; EE, ergosteryl esters; ESI/MS, electrospray ionization mass spectrometry; ER, endoplasmic reticulum; ERG, ergosterol; FA-CoA, fatty acids CoA; FFA, free fatty acids; GC/MS, gas chromatography followed by mass spectrometry; HPLC, high performance liquid chromatography; IGF-1, insulin/insulin-like growth factor 1; LBs, lipid bodies; LPA, lysophosphatidic acid; LC-MS/MS, liquid chromatography followed by tandem mass spectrometer; MS/MS, tandem mass spectrometer; PA, phosphatidic acid; PC, phosphatidylcholine; PE, phosphatidylethanolamine; PI, phosphatidylinositol; PI3K, phosphatidylinositol-3- kinase; PKC, protein kinase C; PS, phosphatidylserine; PG, phosphatidylglycerol; rDNA, ribosomal DNA; ROS, reactive oxygen species; RLS, replicative life span; SD, standard deviation; SO, Sphingosine; TAG, triacylglycerols; TLC, thin-layer chromatography; TORC1, TOR complex 1.

1.0 Introduction

1.1 Biological aging and its complexity

Aging is a highly complex multifactorial phenomenon that affects all biological organisms. It is marked by the progressive decline in the ability of an organism to resist stress and damage [1 - 4]. This continuous decrease in the organism's capacity to function leads to various pathologies such as neurodegenerative disorders, cancer and cardiovascular impairments and, ultimately, to death. Aging is orchestrated by an array of damage-producing and damage-repairing processes that are organized spatiotemporally throughout the life of an organism [2 – 9]. Current research aims at discovering and characterizing these processes to understand their integration by the organism and their specific roles in defining longevity. Another of current research's focus is the discovery of small molecules that exhibit a geroprotective effect by extending lifespan and healthspan. Previous research has enumerated nine hallmarks of aging that span across the entirety of the life domains. These are epigenetic alterations, deregulated nutrient sensing, cellular senescence, altered intercellular communication, stem cell exhaustion, mitochondrial dysfunction, loss of proteolysis, telomere attrition and genomic instability [10]. Although these hallmarks have been studied extensively, much of the molecular mechanisms underlying them remain unknown. The current challenge is to fully characterize the different pathways and molecular mechanisms underlying aging in evolutionarily distant organisms.

1.2 The signaling network that regulates longevity across phyla

Many single-gene mutations that extend longevity have been discovered and characterized in yeast, worms, flies and mice. These mutations affect an array of proteins that are involved in many cellular processes such as cell cycle, cell growth, stress response, protein folding, apoptosis, autophagy, proteasomal protein degradation, actin organization, signal transduction, nuclear DNA replication, chromatin assembly and maintenance, ribosome biogenesis and translation, lipid and carbohydrate metabolism, oxidative metabolism in mitochondria, NAD+ homeostasis, amino acid biosynthesis and degradation, and ammonium and amino acid uptake [2 - 4, 7, 11 – 14]. Interestingly, these processes are controlled by a limited set of nutrient and energy-sensing signaling pathways that converge into a complex network that defines and regulates longevity through organismal and intracellular nutrient and energy-sensing mechanisms [7, 15 - 18].

One of these intracellular nutrient and energy-sensing signaling pathways is the AMP-activated protein kinase/target of rapamycin (AMPK/TOR) pathway [17, 18]. This pathway is activated under conditions of low nutrient or energy supply by responding to high intracellular ratio of AMP to ATP. Under such conditions, TOR protein kinase is inhibited by AMPK. TOR protein kinase is known to associate with many other proteins into a complex known as TOR complex 1 (TORC1) [17, 18]. This complex responds to nutrient availability by phosphorylating and activating two nutrient-sensing protein kinases: Sch9 and protein kinase A (PKA) [14, 19]. TORC1 is a key player in many cellular processes; it regulates translation, transcription, ribosome formation, nutrient transport across membranes and autophagy [14, 20]. Inhibition of TORC1 slows down many

energy-consuming processes and orchestrates a pro-longevity program that promotes several protective cellular processes such as autophagy to remove damaged macromolecules and organelles [17, 21 – 23], and Msn2/4-dependent transcription of stress response genes [24]. It has been shown that yeast, worms, flies and mice with reduced TORC1 activity exhibit an increase in both replicative and chronological lifespans. Akin to this, mutations that impair Sch9 and PKA extend longevity in yeast. It is thought that the combined action of TORC1, Sch9 and PKA suppresses the Msn2/4-dependent transcription of stress response genes [19]. In fact, upon down-regulation of these kinases, both Msn2p and Msn4p translocate into the nucleus [25 - 27]. Upon their entry into the nucleus, these factors activate a transcriptional program that promotes the expression of many genes involved in stress protection, reactive oxygen species (ROS) detoxification, proteolysis, the tricarboxylic acid cycle, carbohydrate metabolism, trehalose biosynthesis and cell growth regulation [17 – 20].

The cAMP/protein kinase A (cAMP/PKA) pathway is known to regulate longevity in evolutionarily distant organisms such as yeast and mice. Upon glucose deprivation, cAMP/PKA signaling is decreased through the attenuation of adenylate cyclase activators [36, 37]. Reduced levels of cAMP/PKA pathway inhibits the phosphorylation of Rim15p and two stress response transcription factors, Msn2p and Msn4p. This restores the activity of Rim15p and allows for the translocation of Msn2p and Msn4p into the nucleus [29 - 31]. These two proteins then promote Rim15p-dependent transcription of stress response genes The establishment of this pro-longevity transcriptional program extends

yeast chronological lifespan. Interestingly, both the AMPK/TOR and cAMP/PKA pathways converge onto Rim15p making it a nutritional integrator.

1.3 Diets and pharmacological interventions that extend longevity across phyla

Extensive evidence supports the idea that intracellular nutrient levels and energy status play pivotal roles in modulating the lifespan of different organisms. Two dietary interventions have been shown to have a considerable longevity-extending effect in organisms ranging from yeast to rhesus monkey. The first intervention is caloric restriction (CR). The CR diet is low in calories but does not compromise the supply of nutrients [38 - 41]. The second intervention is dietary restriction (DR), which consists in reducing the levels of certain kinds of nutrients without compromising the intake of calories [42 - 45]. TORC1 plays the central role in the longevity-extending effects of CR and DR by 1) integrating the information on intracellular nutrient levels and energy status conveyed by AMPK, PKA and Sch9; and 2) serving as a control point that modulates a variety of longevity-defining processes.

Like dietary regimens, there is a variety of pharmacological interventions that extend lifespan and healthspan in organisms across phyla. Some of these anti-aging compounds improve the lifespan of organisms and delay the onset of aging-related pathologies by targeting the AMPK/TOR signaling pathway, which is responsive to the intracellular nutrient and energy status of the organism. Rapamycin, also known as sirolimus [49], is a macrocyclic lactone produced by *Streptomyces hygroscopicus* [24,

50]. This chemical was first used for its antifungal properties as well as an immunosuppressant in renal transplant [51], but has been recently demonstrated alsoto have some pro-longevity characteristics. It acts by inhibiting TORC1 and thus allows for the downstream Msn2/4-mediated transcriptional program to take place, thus extending RLS and CLS in yeast [29, 52, 53]. This drug also extends longevity in fruit flies and mice [54, 55], as well as increases the replicative lifespan of cultured rodent fibroblasts, human epithelium and human fibrosarcoma cells [56]. Metformin is a pro-longevity moleculethat targets the AMPK/TOR signaling pathway by activating the AMPK; this reduces the activity of TORC1 signaling and extends longevity in worms and mice [57, 58].

Most of the currently known anti-aging compounds act as CR or DR-mimetics in that they extend longevity by targeting the same nutrient and energy-sensing signaling pathways as caloric restriction and dietary restriction. They also mimic the effects of these dietary regimens on gene transcription, metabolic processes and stress response pathways [59, 60]. Such compounds only increase lifespan under non-CR and non-DR conditions and are unable to do so when the nutrients or calories intake is limited [57, 61 - 64].

Lithocholic acid (LCA), on the other hand, was found out to be a powerful CR mimetic that delays yeast chronological aging [65]. This anti-aging compound extends the lifespan of chronologically aging yeast via two mechanisms. The first mechanism works under non-caloric restriction conditions and extends the lifespan of yeast by activating the anti-aging capacity of PKA. LCA regulates housekeeping longevity assurance pathways by inhibiting lipid-induced cellular necrosis, decreasing mitochondrial degradation,

changing redox reactions in mitochondria, increasing resistance against thermal and oxidative stresses, suppressing mitochondria-driven apoptosis, and increasing the stability and integrity of genomic and mitochondrial DNA. The second mechanism works in a calorie-independent way by regulating housekeeping longevity pathways that do not interfere with cAMP/PKA and AMPK/TOR pathways. LCA accumulates in the inner mitochondrial membrane and causes a remodeling of mitochondrial morphology by disturbing the asymmetrical distribution of phospholipids. The concentrations of phosphatidic acid (PA), phosphatidylcholine (PC), phosphatidylserine (PS) and phosphatidylglycerol (PG) are increased, whereas the concentration of phosphatidylethanolamine (PE) and cardiolipin (CL) are decreased [65]. These changes lead to an increase in mitochondrial size, a decrease in mitochondrial numbers and in an increase of mitochondrial abundance of cristae [65]. All these changes promote mitochondrial respiration, maintain the mitochondrial membrane potential, and enhance the efficiency of ATP synthesis in chronologically old cells, thus delaying the process of aging [65].

Recent research has revealed six plant extracts that significantly extend the chronological lifespan of yeast [66]. One of these plant extracts is the most potent aging-delaying pharmacological intervention yet described in yeast. The detailed information about this plant extract and its effects can be found in Chapter 3.

1.4 Yeast is a valuable model organism to study the biology of aging and to uncover mechanisms that modulate aging

Growing evidence supports the idea that the fundamental aspects of biological aging are evolutionarily conserved. This made the budding yeast *Saccharomyces cerevisiae* a valuable model organism to study the mechanisms underlying aging [14, 18, 68]. Since this unicellular eukaryote has a short chronological lifespan, a fully sequenced genome and is easily amenable to genetic and biochemical manipulations [69], it has been successfully used for the discovery of genes, signaling pathways and dietary and pharmacological interventions that influence aging. In fact, baker's yeast proves itself quite important in the identification of numerous longevity-defining genes, such as those that form a complex network of nutrient and energy-sensing pathways that modulate aging. Interestingly, these pathways have been found to govern aging processes in higher-order eukaryotes as well [14, 18, 49, 68, 70 – 72]. In yeast, there are two ways to study aging; the first monitors the replicative lifespan (RLS) and the second monitors the chronological lifespan (CLS). RLS is a measure of the maximum number of daughter cells that a mother cell produces before senescence [73]. RLS in yeast models aging of mitotically active and dividing mammalian cells, such as lymphocytes. In contrast, CLS in yeast is a measure of the length of time that a cell remains alive after it has entered a non-diving state [73]. CLS in yeast models aging in mammalian non-dividing cells, such as neurons. Under laboratory conditions, yeast chronological aging is studied using a clonogenic assay. This assay consists in the recovery of yeast cells at different timepoints and then measuring the fraction of cells that are alive in the population [74].

1.5 Lipid metabolism in yeast

Lipids are known to be essential for many cellular processes including the synthesis of membrane bilayers, energy storage, signal transduction, vesicular trafficking and apoptosis [75 - 77]. The organelles involved in the biosynthetic pathways of these lipids are the endoplasmic reticulum, peroxisomes, mitochondria and lipid droplets. The synthesis of these lipids is organized in a highly-ordered network which involves bidirectional transport of precursors and intermediate between all the organelles [75 - 77]. Phospholipids, such as PC, PE, PI, PS, as well as sphingolipids, are the building blocks for organellar and plasma membranes. These lipids are found in all types of organellar membranes of the cell, and their relative abundance of different lipid classes differ between these various membranes. It is believed that such differences in the concentrations of various lipid classes play essential roles in determining the function of each of these organelles. For example, cardiolipin is a mitochondria-specific diphosphatidylglycerol that has been shown to serve in many mitochondria-specific processes. Cardiolipin associates with five protein complexes of the mitochondrial respiratory chain and regulates their activities [78 - 85]. It also plays an important role in regulating the activity of cytochrome *c* [78 - 85]. This cytochrome *c* is essential for mitochondria-controlled apoptosis [78 - 85]. In addition, cardiolipin plays an essential role in maintaining the homeostasis of protein transport across the inner mitochondrial membrane and in sustaining the electrochemical gradient across this mitochondrial membrane [78 - 85]. Interestingly, specific alterations in the levels of CL have been associated with many pathologies and disorders, such as diabetic cardiomyopathy, ataxia and non-alcoholic fatty liver disease [80 - 83]. Reduced levels of this lipid have been

shown to promote aging in rodents and humans [78, 80, 83]. Lastly, triacylglycerol and steryl esters are neutral lipids that serve as storage lipid forms, as well as the detoxification hubs for free fatty acids and sterols [76]. These neutral lipids are deposited in lipid droplets and remain there until their breakdown is triggered in response to certain stimuli.

1.6 Studying the lipid metabolism can provide insights on the mechanisms that underlie aging in yeast

A complex network that regulates lipid metabolism in yeast is divided into several metabolic pathways for various lipid classes, with each class being represented by many species that differ in the number of carbon atoms composing certain fatty acids and in the extent of unsaturation of these fatty acids [97, 98]. These lipids serve many function in cells such as, but not limited to, membrane dynamics, energy storage and signaling [98 - 101]. Many conditions that lead to changes in metabolism such as dietary alterations or environment conditions can cause changes in the levels of lipids in the cell and in their relative concentrations. These lipid changes can provide an insight into the mechanisms underlying aging. By studying the lipidomic signature of a cell, which consists of a snapshot of the lipid profile (relative concentrations of different lipid classes and species) at a specific time point under specific conditions, much can be learned about the mechanisms that define the rate of aging. The lipid signature of long-lived yeast cells can be used to 1) study the mechanisms underlying aging across phyla; and 2) design and develop drugs that can be used to extend longevity by emulating the changes in the lipid profile of these long-lived yeast cells in higher-order eukaryotes such as humans.

There are many methods for the identification and quantitation of lipids. The most predominant current technique to measure such lipid signatures is the electrospray ionization mass spectroscopy (ESI/MS), because of it high resolution, high sensitivity and high speed of execution [97, 98]. ESI/MS allows to identify different lipid classes and their relative abundance, but cannot identify individual species within these classes. This is due to the highly similar fatty acyl chains present in all major lipid classes [97, 98]. When combined with a well-developed sample extraction technique, intelligent selection of lipid standards, separation of the lipid classes prior to MS using HPLC and the use of bioinformatics tools to analyze the spectra obtained, ESI/MS allows an accurate characterization of the lipid signature of a yeast cell [102].

2.0 Development of an optimized LC-MS/MS method for the identification and quantification of various lipid classes and numerous lipid species in each class of *Saccharomyces cerevisiae*

2.1 Introduction.

2.1-1 Background

Lipidomics is a relatively new emerging research field due to its crucial role in studying many important pathways related to lipid-based cellular signaling networks, energy storage, membrane trafficking, membrane dynamics and apoptosis [103-106]. One of the most important group of lipids is the group of phospholipids, which are known to regulate most of the above pathways. Phospholipids are composed of a polar head group and a glycerol backbone for the attachment of different fatty acid moieties. The fatty acid moieties of different phospholipid classes of yeast cells are mostly the palmitic (C16:0), palmitoleic (C16:1) and oleic (C18:1) acids [107,108]. The fatty acid moieties of phospholipids found in yeast cells are either fully saturated or mono-unsaturated, since yeast cells have only one acyl desaturase enzyme [109,110]. Better understanding of the roles that different classes of phospholipids play in various cellular processes depends on their physical and chemical properties as well as on their concentrations.

Historically, the diverse structural and chemical properties of phospholipids and other lipid classes were obstacles in separating them from other impurities in the sample, identifying them and measuring their concentrations. For decades, high pressure liquid chromatography (HPLC) and thin layer chromatography (TLC) were the best choices to separate and characterize different lipid classes. However, it was impossible to use HPLC

and TLS for the identification and quantitation of individual species within each lipid class, due to low sensitivity and resolution of these techniques. Only with the advent of mass spectrometry technique, it became possible to identify individual phospholipid species with an accuracy of only one double bond difference in their fatty acid moieties [111]. Currently, there are many types of mass spectrometers used to analyze phospholipids and other lipid classes, such as triple quadrupole, quadrupole time of flight (TOF), LTQ orbitrap, ion trap and magnetic sector [112]. All these mass spectrometers have essentially three main components, including an ion source, mass analyzer and ion detector (as illustrated in Figure 1).

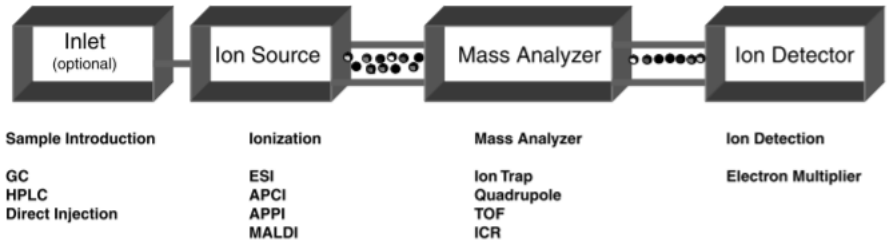

Figure 1. Components of a typical mass spectrometer, which contains an inlet where the sample in solution is injected, an ion source to ionize the sample, a mass analyzer that takes ionized masses and separates them based on mass-to-charge ratios, and an ion detector [113].

Therefore, they all operate on the same principle, but due to different type of ion source, mass analyzer and ion detector different mass spectrometers are used for analyzing different aspects of phospholipids. Reliable mass spectrometer data depends on the method of ionization and sample introduction. The use of mass spectrometer to analyze phospholipids was hindered due to extensive fragmentation by the ion source until the advent of electrospray ionization (ESI) which is a soft ionization method [114]. ESI cause almost no fragmentation of the parent ion, thus all phospholipids can be detected as molecular ions, which is necessary for structural analysis of lipid species [114]. The

principle of ionization in electrospray ionization is that sample passes through an extremely think capillary tube at a slow rate. At the end of the capillary tube a strong voltage difference nebulizes the sample together with mobile phase intro small charged droplets [114]. In the ESI lipid ions are produced by addition of a proton or any other cation, or multiple charge cation or by removal of a proton [115].

Although the combination of ESI with mass spectrometry was a big success in the field of lipidomics, but the advent of tandem mass spectrometry and its combination with ESI truly revolutionized the analysis of phospholipids [116, 117]. Tandem mass spectrometry (MS/MS) is the most recent technology which has an extra step of inducing collision of molecular ions between the two mass analyzers with a neutral atom or molecule as its illustrated in figure 2.

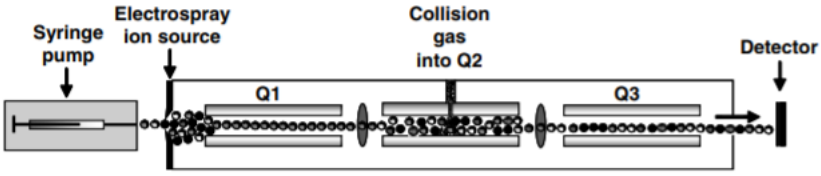

Figure 2. Tandem mass spectrometer in CID fragmentation setting. Q1 and Q3 quadrupoles are acting as mass analyzers, Q2 is a collision cell. The parent ion studied is chosen by Q1 and passes to the collision cell Q2. The molecular ion is fragmented by collision-induced dissociation (CID) and the mass-to-charge rations are read by Q3 [113].

The fragmentation of molecular ions in the collision chamber is referred to as collision induced dissociation (CID) [115]. In tandem mass spectrometry, we can easily assign a mass spectrometer peak to a specific lipid species, since the first mass analyzer selects the precursor or molecular ion, then it is passed to collision chamber where it dissociates into many smaller fragments. The structural information can be obtained through analysis of precursor ion and the fragments generated by collision, since each phospholipid has a

specific pattern of fragments [111]. The task of putting together the fragments back is done by computer software such as lipid-search or any other MS/MS compatible software. Even though ESI combined with tandem mass spectrometer can deduce the structural information of a lipid species, but if the lipid sample is not purified well enough and if you infuse the sample directly into mass spectrometer; there will be many problems assigning the mass spectrometer peaks to their corresponding lipid species.

2.1-2 Comparison of the shot gun and LC-MS/MS techniques of lipid analysis.

In the direct infusion or famously known as shot gun lipidomics, the purified sample is directly injected in the inlet of mass spectrometer, after passing through the ionization capillary a selected range of molecular ions will pass through the first mass analyzer into the collision chamber [107 – 111]. The problem is that the first mass analyzer does not pass the ions one by one to the collision chamber, so that we deduce the structural information of each individual lipid species based on its unique fragmentation pattern. Instead many ions are passed at once to collision chamber, and we can only determine the different types of phospholipid classes within a sample due to distinct fragment patterns of the polar head groups of each phospholipid class; it is not possible to associate the fragment of different fatty acid moieties to the right lipid species to which it belongs to. Therefore, shotgun technique is only good to quickly determine the different classes of phospholipids in a sample, but it is not possible to identify and quantify individual lipid species within each class if a mixture of lipid species is injected at once. However, it is possible to deduce the structure of a target phospholipid if we have the prior knowledge

of that phospholipid. In the first mass analyzer, a specific molecular ion mass corresponding to the target molecular ion can be selected, so that only that specific molecular ion pass to the collision chamber not the lipid species present in the mixture. This procedure of lipid identification needs prior knowledge of lipid species m/z value also it is very time consuming.

LC-MS/MS on the other hand can solve the problems encountered by the direct infusion. In the LC-MS/MS as the name suggest high pressure liquid chromatography HPLC is attached to a tandem mass spectrometer. The advantage of such setup is that HPLC will elute lipid species separately if the right column, mobile phase and the additives are chosen. The reverse phase –HPLC (RP-HPLC) which has a hydrophobic stationary phase separates lipid species based on their lipophilicity. Therefore RP-HPLC separation is based on the fatty acid moieties; it will elute two species of same molecular weight and charge if they differed by only one single double bond [115]. The high resolving power of HPLC also eliminates the problem of isobaric species. Isobaric species are those species with identical molecular weight, but differ in their structure [118].

2.1-3 Selection of an appropriate HPLC column for lipid analysis.

Phospholipids can be separate by both normal phase HPLC (NP-HPLC) and reverse phase HPLC (RP-HPLC). Phospholipids are amphiphilic molecules which have a hydrophilic head group and hydrophobic fatty acid moiety [108]. NP-HPLC has a polar stationary phase and it separates phospholipids based on their increasing head group polarity. So, the elution starts with least polar head phosphatidylglycerol (PG) and other lipid classes will elute in the following sequence: phosphatidylinositol (PI),

phosphatidylethanolamine (PE), phosphatidylserine (PS), phosphatidylcholine (PC) and sphingomyelin (Sph). NP-HPLC is good choice for separation and quantification of different classes of phospholipids, since a single phospholipid class will elute at one time, but it is not a good choice if the purpose of the study is to analyze individual lipid species within a specific class.

RP-HPLC is the column of choice if the goal is to analyze individual lipid species in various classes. RP-HPLC elutes the phospholipids classes in the reverse order compare to the NP-HPLC. Therefore, the phospholipid with least polar head such as PG will be eluted at last. A specific type of RP-HPLC is charged-surface-hybrid (CSH) which has slightly charged surface can elute molecules based on both the hydrophilic and hydrophobic characteristics. Thus, CSH column elutes phospholipid classes both based on their polar head groups and hydrophobic fatty acid moieties. Therefore, CSH column has a very high resolving power, which elutes the members of the same lipid class if they differ by a single double bond [112]. The drawback of RP-HPLC is that the polar impurities elutes with target molecules together. The polar impurities reduce the efficiency of ESI ionization through process known as ion suppression [115].

2.1-4 Selection of appropriate mobile phases and mobile phase additives

In general LC-MS/MS efficiency and sensitivity depends on ionization of target molecules. If a sample has a mixture of lipid classes, then each of the class will have an ideal ionization condition. Therefore, it is difficult to find a single ionization condition to achieve the optimal ionization of all lipid classes. As a result, the bet ionization condition is the one which result in a good ionization of overall lipid classes. The only two salts

which are incompatible with electrospray ionization are phosphate and sulfate containing salts [117]. mostly ammonium formate and ammonium acetate are used together with minute quantities of formic acid or acetic acid to obtain best ionization by altering the pH. The effect of different salts and acids on ionization of lipid classes are further discussed in tables 5 and 6.

The choice of mobile phase is strictly dependent on the sample type and on the column type [119]. the extensively used mobile phases for lipid analysis are acetonitrile, isopropanol, methanol and water. Almost always each specific sample has a unique HPLC gradient due to difference in MS peak quality and retention time of individual molecules within in a sample. For details of HPLC gradient please refer to the material and method section.

2.2 Detailed Materials and Methods

2.2-1 Yeast strains, media and growth conditions

The wild-type strain *Saccharomyces cerevisiae* BY4742 (*MATα his3Δ1 leu2Δ0 lys2Δ0 ura3Δ0*) from Thermo Scientific/Open Biosystems was grown in a synthetic minimal YNB medium (0.67% Yeast Nitrogen Base without amino acids) initially containing 2% (w/v) glucose and supplemented with 20 mg/l histidine, 30 mg/l leucine, 30 mg/l lysine and 20 mg/l uracil. Cells were cultured at 30 ^{O}C with rotational shaking at 200 rpm in Erlenmeyer flasks at a “flask volume/medium volume” ratio of 5:1.

2.2-2 Cell collection and counting

A hemocytometer (Hausser Scientific Catalog# 3200) was used to count yeast cells and to calculate the volume of cell culture containing 5.0 x 10^7 cells. Appropriate volume of cell culture was taken, and the cells were harvested by centrifugation in a Centra CL2 clinical centrifuge at 3,000 × g for 5 min at room temperature. The cell pellet was washed once in ice-cold Nano-pure water and once in ice-cold 155 mM ammonium bicarbonate (pH 8.0), and the cells were subjected to centrifugation at 20000 × g for 1 min at room temperature. The cell pellet was stored at -80 ^{o}C until lipid extraction.

2.2-3 Dichloromethane/Methanol lipid extraction method

For lipid extraction, the pelleted cells kept at -80 ^{o}C were thawed on ice before being re-suspended in 200 µl of ice-cold Nano-pure water. The re-suspended sample which contained 5 × 10^7 cells was transferred to a 15-mL high-strength glass screw top centrifuge tube with a Teflon lined cap (#0556912; Fisher Scientific). To each 15-mL high-strength glass tube the following was added: 1) 25 µL of the internal standard mix prepared in mixture of dichloromethane: methanol (both OPTIMA grade from Fisher Scientific used for LC-MS with CAS# 75-09-2 and 67-56-1), 2) 100 µL of 425-600 µM acid-washed glass beads to break open the cells (#G8772; Sigma-Aldrich) and 600 µL of dichloromethane : methanol at a 17:1 ratio both from Fisher Scientific with OPTIMA grade and CAS# 75-09-2 and 67-56-1. The samples were then vortexed vigorously for 5 minute at room temperature to breakdown the cells and subjected to centrifugation in a Centra CL2 clinical centrifuge at 3,000 × g for 5 min at room temperature; this centrifugation allowed to separate the upper aqueous phase from the lower organic phase, which

contained nonpolar lipids TAG, PC, PE and PG. The lower organic phase (400 µL) was then transferred to another 15-mL high-strength glass screw top centrifuge tube using pipette with polypropylene gel loading tips (Fisher scientific catalog# 13-611-115) with careful attention not to disrupt the glass beads or upper aqueous phase. 300 µL of Dichloromethane:methanol (2:1) solution was added to the remaining upper aqueous phase to allow the extraction of sphingolipids and of polar lipids PA, PS, PI and CL. The samples were again vortexed vigorously at room temperature for 5 minutes. The initial separated organic band was kept at under the flow of nitrogen gas for the duration of the second vortexing. The samples were again centrifuged for 5 min at 3,000 × rpm at room temperature; the lower organic phase (200 µL) was then separated and added to the corresponding initial organic phase with pipette using the polypropylene gel loading tips. With both lower organic phases combined, the solvent was evaporated off by nitrogen gas flow. Once all solvent was evaporated, the tubes containing the lipid film were closed under the flow of nitrogen gas and stored in -80^{o}C.

2.2-4 Chloroform/Methanol lipid extraction method

For lipid extraction, the pelleted cells kept at -80 ^{o}C were thawed on ice before being re-suspended in 200 µl of ice-cold Nano-pure water. The re-suspended sample which contained 5 × 10^{7} cells was transferred to a 15-mL high-strength glass screw top centrifuge tube with a Teflon lined cap (#0556912; Fisher Scientific). To each 15-mL high-strength glass tube the following was added: 1) 25 µL of the internal standard mix prepared in mixture of chloroform: methanol (both OPTIMA grade from Fisher Scientific used for LC-MS with CAS# 76-09-3 and 67-56-1), 2) 100 µL of 425-600 µM acid-washed

glass beads to break open the cells (#G8772; Sigma-Aldrich) and 600 µL of chloroform : methanol at a 17:1 ratio both from Fisher Scientific with OPTIMA grade and CAS# 76-09-3 and 67-56-1. The samples were then vortexed vigorously for 5 minute at room temperature to breakdown the cells and subjected to centrifugation in a Centra CL2 clinical centrifuge at 3,000 × g for 5 min at room temperature; this centrifugation allowed to separate the upper aqueous phase from the lower organic phase, which contained nonpolar lipids TAG, PC, PE and PG. The lower organic phase (400 µL) was then transferred to another 15-mL high-strength glass screw top centrifuge tube using pipette with polypropylene gel loading tips (Fisher scientific catalog# 13-611-115) with careful attention not to disrupt the glass beads or upper aqueous phase. 300 µL of chloroform-methanol (2:1) solution was added to the remaining upper aqueous phase to allow the extraction of sphingolipids and of polar lipids PA, PS, PI and CL. The samples were again vortexed vigorously at room temperature for 5 minutes. The initial separated organic band was kept at under the flow of nitrogen gas for the duration of the second vortexing. The samples were again centrifuged for 5 min at 3,000 × rpm at room temperature; the lower organic phase (200 µL) was then separated and added to the corresponding initial organic phase with pipette using the polypropylene gel loading tips. With both lower organic phases combined, the solvent was evaporated off by nitrogen gas flow. Once all solvent was evaporated, the tubes containing the lipid film were closed under the flow of nitrogen gas and stored in -80^{O}C.

2.2-5 Methyl-tert-butyl-ether (MTBE)/Methanol lipid extraction method

For lipid extraction, the pelleted cells kept at -80 ^{o}C were thawed on ice before being re-suspended in 200 µl of ice-cold Nano-pure water. The re-suspended sample which contained 5 × 10^{7} cells was transferred to a 15-mL high-strength glass screw top centrifuge tube with a Teflon lined cap (#0556912; Fisher Scientific). To each 15-mL high-strength glass tube the following was added: 1) 25 µL of the internal standard mix prepared in mixture of MTBE: methanol (both OPTIMA grade from Fisher Scientific used for LC-MS with CAS# 78-01-5 and 67-56-1), 2) 100 µL of 425-600 µM acid-washed glass beads to break open the cells (#G8772; Sigma-Aldrich) and 1.5 ml of ice-cold methanol was added. The samples were then vortexed vigorously for 5 minute at room temperature to breakdown the cells. 5 ml of ice-cold MTBE was added to sample and the sample was incubated at room temperature in a shaker for 1 hour. Phase separation was induced by addition of 1.25 ml ice-cold water and incubated on ice for 10 minutes. After the sample was subjected to centrifugation in a Centra CL2 clinical centrifuge at 3,000 × g for 5 min at room temperature; this centrifugation allowed to separate the upper organic phase from the lower aqueous phase. The upper organic phase was then transferred to another 15-mL high-strength glass screw top centrifuge tube using pipette with polypropylene gel loading tips (Fisher scientific catalog# 13-611-115) with careful attention not to disrupt the glass beads or lower aqueous phase. 2 ml of extraction solvent was added to remaining sample in aqueous phase to re-extract the lipids. The extraction solvent mixture contains MTBE/methanol/water at ratio of 10:3:2.5 (v/v/v). The initial separated organic band was kept at under the flow of nitrogen gas for the duration of the second vortexing. The upper organic phase was added to the corresponding initial organic phase with pipette using the

polypropylene gel loading tips. With both organic phases combined, the solvent was evaporated off by nitrogen gas flow. Once all solvent was evaporated, the tubes containing the lipid film were closed under the flow of nitrogen gas and stored in -80^{o}C.

Detection mode	Lipid classes	Lipid chain composition	Calculated M/Z values	Moles in samples
Negative	Ceramide	(18:1/17:0)	550.5204675	2.26E-09
	Cardiolipin	(14:0/14:0/14:0/14:0)	1239.839755	1.96E-09
	Free Fatty Acid	19:0	297.2799035	8.37E-09
	phosphatidylethanolamine	(15:0/15:0)	662.4766305	3.77E-09
	Phosphatidylglycerol	(15:0/15:0)	693.4712115	3.49E-09
	phosphatidylinositol	(17:0/20:4)	871.5342065	3.00E-11
	phosphatidylserine	(17:0/17:0)	762.5290605	3.18E-09
Positive	phosphatidylcholine	(13:0/13:0)	650.4755335	3.85E-09
	phytosphingosine	(16:1)	272.2584055	2.25E-09
	triacylglycerol	(28:1/10:1/10:1)	818.7232155	3.67E-09

Table 1. Internal lipid standards used for the experiment. Note: Internal lipid standards CL, CER, PI, SO, PE, PG, FFA, PS and PC were all from Avanti Polar Lipid, Alabaster, AL, USA. TAG internal standard originates from Larodan, Malmo, Sweden.

2.2-6 Sample preparation for LC-MS/MS

500 µL of acetonitrile: 2-propanol: H2O with ratio of (65:35:5) all with LC-MS grade from Fisher Scientific (catalog# A9551, A4611 and W6212) added to tubes containing the lipid film. Each tube was vortexed 3 times for 10 seconds each time and then all the samples were sonicated for 15 minutes and vortexed again as above and 100 µL from each sample was added to glass vials with inserts used for Agilent1100 Wellplate (note: it is important to eliminate all the air bubbles in the insert before putting the vials in the Agilent1100 Wellplate).

2.2-7 Liquid chromatography conditions

The LC–MS experiments were performed using an Agilent 1100 series LC system (Agilent Technologies) equipped with a binary pump, de-gaser and an autosamples. Lipid species were separated on a reverse-phase column CSH C18 (2.1 mm; 75 mm; pore size 130 Å; pH range of 1-11) (Waters, Milford, MA, USA) coupled to a CSH C18 VanGuard (Waters). The column was maintained at 55 °C at a flow-rate of 0.3 mL/min. The mobile phases consisted of (A) 60:40 (v/v) acetonitrile: water and (B) 90:10 (v/v) isopropanol: acetonitrile. For the positive mode ESI (+) both mobile phases A and B were mixed with 10 mM ammonium formate (0.631 g/L) from Fisher Scientific (catalog# A115-50). For the negative mode ESI (-) both mobile phases A and B were mixed with 10 mM ammonium acetate (0.771 g/L) from Fisher Scientific (catalog# 631-61-8). To enhance solubilizing of ammonium formate and ammonium acetate both salts were dissolved first in small volume of water (50 µl) before their addition in the mobile phases. Each mobile phase with modifiers (ammonium formate and ammonium acetate) was mixed, sonicated for 20 minutes to achieve complete dissolving of modifiers, mixed again, and then sonicated for

another 20 minutes.

The separation of different lipid species by HPLC was achieved under the following HPLC gradient: 0 to 4 min 90%(A); 4 to 10 min 40%(A); 10 to 21 min 32% (A); 21 to 24 min 3 % (A); 24 to 33 min 90 % (A). A sample volume of 5 µl and 10 µl was used for the injection in ESI (+) and ESI (-) respectively. Samples were kept in the Agilent1100 Wellplate.

2.2-8 Mass spectrometry

Extracted lipids were separated by HPLC and analyzed with Thermo Orbitrap Velos Mass Spectrometer equipped with ESI ion source (Thermo Scientific). Parent ions (MS-1) were detected in positive and negative modes using the FT analyzer at a resolution of 60,000. The MS-1 mass range used is from 150 – 2000 Dalton.

Ion Source type	ESI
Capillary Temperature ^{O}C	300
Source heater Temperature ^{O}C	300
Sheath Gas Flow	10
Aux Gas flow	5

Table 2. Thermo Orbitrap Velos mass spectrometer's tune file instrument settings. Legend: ESI stands for electrospray ionization.

Instrument polarity	Positive	Negative
Activation type	HCD	CID
Min. signal required	5000	5000
Isolation Width	2.0	2.0
Normalized Collision energy	55.0	35
Default charge state	2	2
Activation time	0.1	10

Table 3. Instrument method for MS-2 used in this experiment. Legend: HCD stands for High-energy-induced-collision-dissociation, and CID stands for collision-induced-dissociation.

2.2-9 Processing of raw data from LC-MS

Raw files from LC-MS were analyzed by Lipid Search software (V4.1) from Thermo Fisher. The Lipid Identification Software “Lipid Search” was used to identify different lipid classes with the help of Molecular Fragmentation Query Language based on the below (Table 4) parameters. In addition to the parameters below (Table 4) an extra manual filter was applied to eliminate any Fatty Acid with odd number of carbon and to eliminate any fatty acid with more than 1 double bond (polyunsaturated fatty acid).

Identification		
Database	Orbitrap	
Peak detection	Recall isotope (ON)	
Search option	Product search Orbitrap	
Search type	Product	
Experiment type	LC-MS	
Precursor tol	10 ppm	
Product tol	HCD (positive mode) 20 ppm	
	CID (negative mode) 0.5 da	
Quantitation		
Execute quantitation	ON	
Mz tol	-5.0; +5.0	
Tol type	ppm	
Filter		
Top rank filter	ON	
Main node filter	Main isomer peak	
m-score threshold	5.0	
c-score threshold	2.0	
FFA priority	ON	
ID quality filter	**A**	Lipid class & FA are completely identified
	B	Lipid class & some FA are identified
	C	Lipid class or FA are identified
	D	Lipid identified by other fragment ions (H_2O and others)
Lipid Class		
HCD (positive)	PC, SO, TG	
CID (negative)	CER, CL, FA, PE, PG, PI, PS	
Ions		
HCD (positive)	+H, +NH_4, +Na	
CID (negative)	-H, -2H, +HCOO	

Table 4. The parameters for lipid search software (V 4.1) used in the experiment for lipid detection. Legend: HCD stands for High-energy-induced-collision-dissociation, and CID stands for collision-induced-dissociation.

2.3 Results tables and figures.

Lipid Standard	ESI mode	AmF	AmF/FA	AmAc	AmAc/AA	AmAc/FA
Ceramide	-	49.6	38.8	77.7	73.4	70.2
Cardiolipin	-	78.8	73.2	88.	85.3	81.0
Free Fatty Acid	-	92.4	94	92.6	91.8	94.2
Phosphatidylethanolamine	-	73.4	61.5	77.7	74.5	75.6
Phosphatidylglycerol	-	34.5	38.8	43.2	45.3	42.1
Phosphatidylinositol	-	72.3	70.2	75.	76.6	73.4
Phosphatidylserine	-	75.6	74.5	81	77.7	69.1
Phosphatidylcholine	+	86.4	81	54	57.2	59.4
Phosphatidylsphingosine	+	88.5	84.2	74.5	75.6	70.2
Triacylglycerol	+	97.2	89.6	75.6	77.7	81

Table 5. The effect of different mobile phase additives on the efficiency of ionization of lipid standards: Ionization source used is electrospray ionization (ESI) and the HPLC column used is a normal phase column (NP-HPLC). The values in this table is from the average of 5 replicates as percentage (%) of the highest peak intensity value detected in each set. Legend: AmF ammonium formate, AmF/FA

ammonium formate with formic acid, AmAc ammonium acetate, AmAc/AA ammonium acetate with acetic acid, AmAc/FA ammonium acetate with formic acid. The highest values for ionization efficiencies in both + and - modes of ESI are highlighted in green.

Lipid Standard	ESI mode	AmF	AmF/FA	AmAc	AmAc/AA	AmAc/FA
Ceramide	-	74	75.2	85.8	77	74.8
Cardiolipin	-	72.9	75.1	78.3	68.4	74
Free Fatty Acid	-	77.1	77.2	75.5	84	72.9
Phosphatidylethanolamine	-	98	96	95	91.5	86
Phosphatidylglycerol	-	64	45.1	75.9	60.5	55
Phosphatidylinositol	-	79.3	76	82.5	80.3	77
Phosphatidylserine	-	73.7	61.6	85.8	81.4	73.7
Phosphatidylcholine	+	93.5	86.9	69.3	60.5	62.7
Phosphatidylsphingosine	+	89.1	79.2	78.1	73.7	69.3
Triacylglycerol	+	92.4	88	86.9	80.3	84.7

Table 6. The effect of different mobile phase additions on the efficiency of ionization of lipid standards: Ionization source used is electrospray ionization (ESI) and the HPLC column used is a reversed phase column (RP-HPLC). The values in this table is from the average of 5 replicates as percentage (%) of the highest peak intensity value detected in each set. Legend AmF ammonium formate, AmF/FA ammonium formate with formic acid, AmAc ammonium acetate, AmAc/AA ammonium acetate with acetic acid, AmAc/FA ammonium acetate with formic acid. The highest values for ionization efficiencies in both + and - modes of ESI are highlighted in green.

Lipid Standard	ESI mode	AmF	AmAc
Ceramide	-	48.1	57.4
Cardiolipin	-	47.3	52.4
Free Fatty Acid	-	50.1	50.5
Phosphatidylethanolamine	-	63.7	63.6
Phosphatidylglycerol	-	41.6	50.8
Phosphatidylinositol	-	0	0
Phosphatidylserine	-	0	0
Phosphatidylcholine	+	60.7	46.4
Phosphatidylsphingosine	+	57.9	52.3
Triacylglycerol	+	60.0	58.2

Table 7. The efficiencies of methyl-tert-butyl-ether (MTBE) and methanol extraction methods evaluated using commercial lipid standards: Ionization source used is electrospray ionization (ESI) and the HPLC column used is a reversed phase column (RP-HPLC). The values in this table is from the average 3 replicates and they represent percentage (%) recovery of lipid standards from the extraction compare to the same concentration of lipid standards spiked directly in the MS injection solvent. Legend AmF ammonium formate, AmAc ammonium acetate.

Lipid Standard	ESI mode	AmF	AmAc
Ceramide	-	59.9	71.2
Cardiolipin	-	59.0	64.9
Free Fatty Acid	-	62.4	62.6
Phosphatidylethanolamine	-	79.3	78.8
Phosphatidylglycerol	-	51.8	62.9
Phosphatidylinositol	-	64.2	68.4
Phosphatidylserine	-	59.6	71.2
Phosphatidylcholine	+	75.7	57.5
Phosphatidylsphingosine	+	72.1	64.8
Triacylglycerol	+	74.8	72.1

Table 8. The efficiency of 17:1 Dichloromethane:methanol and 2:1 Dichloromethane:methanol extraction method on the lipid standards: Ionization source used is electrospray ionization (ESI) and the HPLC column used is a reversed phase column (RP-HPLC). The values in this table is from the average 3 replicates and they represent percentage (%) recovery of lipid standards after the extraction compare to the same concentration of lipid standards spiked directly in the MS injection solvent. Legend AmF ammonium formate, AmAc ammonium acetate.

Lipid Standard	ESI mode	AmF	AmAc
Ceramide	-	64.3	77.2
Cardiolipin	-	63.4	70.4
Free Fatty Acid	-	67.0	67.9
Phosphatidylethanolamine	-	85.2	85.5
Phosphatidylglycerol	-	55.6	68.3
Phosphatidylinositol	-	68.9	74.2
Phosphatidylserine	-	64.1	77.2
Phosphatidylcholine	+	81.3	62.3
Phosphatidylsphingosine	+	77.5	70.2
Triacylglycerol	+	80.3	78.2

Table 91. The efficiency of 17:1 Chloroform:methanol and 2:1 Chloroform:methanol extraction method on the lipid standards: Ionization source used is electrospray ionization (ESI) and the HPLC column used is a reversed phase column (RP-HPLC). The values in this table is from the average 3 replicates and they represent percentage (%) recovery of lipid standards after the extraction compare to the same concentration of lipids spiked directly in the MS injection solvent. Legend AmF ammonium formate, AmAc ammonium acetate. The highest values for extraction efficiencies in both + and - modes of ESI are highlighted in green.

Lipid Standard	ESI mode	AmF	AmAc
Ceramide	-	75	83.8
Cardiolipin	-	70.9	79.3
Free Fatty Acid	-	76.1	74.5
Phosphatidylethanolamine	-	98	95
Phosphatidylglycerol	-	64	75.9
Phosphatidylinositol	-	79.3	82.5
Phosphatidylserine	-	71.5	84.8
Phosphatidylcholine	+	52.3	60.5
Phosphatidylsphingosine	+	78.4	75.2
Triacylglycerol	+	65.7	69.7

Table 10. The effect of high-energy collisional dissociation (CID) on the percentage of product-ion yield for commercial lipid standards: The values in this table represent the average of 3 replicates as the percentage (%) of the highest peak intensity value detected in all 6 replicates (3 replicates in CID, and 3 replicates in HCD). Legend: AmF ammonium formate, AmAc ammonium acetate. The highest values for product-ion yields in both + and - modes of ESI are highlighted in green.

Lipid Standard	ESI mode	AmF	AmAc
Ceramide	-	68.4	65.4
Cardiolipin	-	74.3	75.2
Free Fatty Acid	-	84.2	81.2
Phosphatidylethanolamine	-	85.1	73.1
Phosphatidylglycerol	-	68.4	67.1
Phosphatidylinositol	-	58.7	55.8
Phosphatidylserine	-	67.4	68.5
Phosphatidylcholine	+	92.5	65.3
Phosphatidylsphingosine	+	87.1	75.1
Triacylglycerol	+	91.4	84.9

Table 11. The effect of high-energy collisional dissociation (HCD) on the percentage of product-ion yield of the lipid standards: The values in this table represent the average of 3 replicates as the percentage (%) of the highest peak intensity value detected in all 6 replicates (3 replicates in CID, and 3 replicates in HCD). Legend: AmF ammonium formate, AmAc ammonium acetate. The highest values for product-ion yields in both + and - modes of ESI are highlighted in green.

Lipid Class	Fatty Acid Moieties	Ionization Type	MS Peak Area	Calculated m/z Values
PC	(16:0/10:0)	M+H	2.13E+08	650.4755
PC	(8:0/8:0)	M+H	2.30E+06	494.3241
PC	(8:0/8:0)	M+H	1.09E+05	496.3398
PC	(8:0/10:0)	M+H	6.38E+05	522.3554
PC	(8:0/10:0)	M+H	4.49E+05	524.3711
PC	(16:1/12:0)	M+H	1.58E+06	676.4912
PC	(16:0/12:0)	M+H	2.23E+06	678.5068
PC	(16:1/14:0)	M+H	3.33E+06	704.5225
PC	(16:0/14:0)	M+H	9.26E+05	706.5381
PC	(16:0/16:1)	M+H	6.91E+07	732.5538
PC	(16:0/18:1)	M+H	3.37E+07	760.5851
PC	(18:0/18:1)	M+H	6.38E+06	788.6164
PC	(16:1/10:0)	M+H	4.85E+05	648.4599
PC	(16:0/16:0)	M+H	5.29E+06	734.5694
PC	(18:0/16:0)	M+H	1.56E+06	762.6007
PC	(18:0/24:1)	M+H	3.10E+06	872.7103
PC	(20:0/24:1)	M+H	9.28E+05	900.7416
PC	(10:0/16:0)	M+H	4.39E+05	636.4963

Table 12. Lipid species of phosphatidylcholine identified by the optimized LC-MS/MS method. The lipid species represented here are from 7 growth time points (DME, D0, D1, D2, D4, D6, D8). Legend: DME stands for day mid-exponential phase. D stands for day and numeric values represent days of growth. The highlighted in yellow row is for the lipid standard of phosphatidylcholine.

Lipid Class	Fatty Acid Moieties	Ionization Type	MS Peak Area	Calculated m/z Values
So	(16:1)	M+H	1.26E+06	272.2584
So	(16:0)	M+H	4.64E+07	274.2741
So	(20:0)	M+H	3.71E+06	346.3316
So	(22:1)	M+H	4.55E+06	356.3523
So	(22:1)	M+H	3.13E+05	372.3472
So	(22:0)	M+H	2.16E+07	374.3629
So	(18:0)	M+H	5.43E+05	302.3054
So	(18:0)	M+H	1.13E+06	318.3003
So	(18:1)	M+H	3.11E+05	300.2897

Table 23. Lipid species of sphingomyelin identified by the developed LC-MS/MS method. The lipid species represented here are from 7 growth time points (DME, D0, D1, D2, D4, D6, D8). Legend: DME stands for day mid-exponential phase. D stands for day and numeric values represent days of growth. The highlighted in yellow row is for the lipid standard of sphingomyelin.

Lipid Class	Fatty Acid Moieties	Ionization Type	MS Peak Area	Calculated m/z Values
TG	(28:1/10:1/10:1)	M+NH4	1.27E+08	818.7232
TG	(10:0/10:0/22:1)	M+NH4	1.32E+07	738.6606
TG	(30:1/10:1/10:1)	M+NH4	2.06E+08	846.7545
TG	(30:0/10:1/10:1)	M+NH4	2.26E+08	848.7702
TG	(18:0/10:1/16:1)	M+NH4	2.62E+07	764.6763
TG	(18:0/10:1/16:0)	M+NH4	7.01E+07	766.6919
TG	(28:0/10:1/10:1)	M+NH4	4.13E+08	820.7389
TG	(16:0/16:0/16:0)	M+NH4	1.07E+07	824.7702
TG	(18:1/10:1/24:1)	M+NH4	1.21E+08	874.7858
TG	(18:0/10:1/24:0)	M+NH4	2.15E+08	878.8171
TG	(10:0/10:0/22:0)	M+NH4	1.67E+07	740.6763
TG	(16:0/10:1/22:0)	M+NH4	1.46E+08	822.7545

Table 34. Lipid species of triglyceride identified by the developed LC-MS/MS method. The lipid species represented here are from 7 growth time points (DME, D0, D1, D2, D4, D6, D8). Legend: DME stands for day mid-exponential phase. D stands for day and numeric values represent days of growth. The highlighted in yellow row is for the lipid standard of triglyceride.

Lipid Class	Fatty Acid Moieties	Ionization Type	MS Peak Area	Calculated m/z Values
Cer	(d18:1/17:0)	M-H	3.36E+07	550.5205
Cer	(16:0/16:0)	M-H	1.53E+05	526.4841
Cer	(14:1/16:0)	M-H	2.93E+05	528.427
Cer	(18:0/16:0)	M-H	3.98E+07	554.5154
Cer	(18:0/22:0)	M-H	4.35E+04	654.6042
Cer	(18:0/24:0)	M-H	3.27E+05	682.6355
Cer	(18:0/26:0)	M-H	1.03E+07	710.6668
Cer	(20:0/26:0)	M-H	1.16E+06	738.6981
Cer	(18:0/4:0)	M-H	2.46E+04	386.3276
Cer	(18:0/18:0)	M-H	3.31E+05	598.5416
Cer	(18:0/20:0)	M-H	1.58E+05	626.5729
Cer	(18:0/24:0)	M-H	5.54E+04	666.6406
Cer	(18:0/26:0)	M-H	5.18E+05	678.677
Cer	(18:0/26:0)	M-H	3.33E+06	694.6719
Cer	(16:0/30:0)	M-H	5.95E+05	722.7032
Cer	(12:0/4:0)	M-H	1.84E+05	302.2337
Cer	(20:0/16:0)	M-H	4.51E+05	582.5467
Cer	(20:1/18:0)	M-H	4.84E+05	640.5522
Cer	(14:0/18:0)	M-H	8.28E+04	542.479
Cer	(16:0/26:0)	M-H	8.81E+04	650.6457
Cer	(20:0/26:0)	M-H	4.52E+04	706.7083
Cer	(18:1/18:0)	M-H	2.54E+04	564.5361
Cer	(18:1/4:0)	M-H	3.86E+04	384.3119
Cer	(16:0/12:0)	M-H	8.39E+04	454.4266
Cer	(18:0/26:1)	M-H	5.44E+04	692.6562

Table 45. Lipid species of ceramide identified by the developed LC-MS/MS method. The lipid species represented here are from 7 growth time points (DME, D0, D1, D2, D4, D6, D8). Legend: DME stands for day mid-exponential phase. D stands for day and numeric values represent days of growth. The highlighted in yellow row is for the lipid standard of ceramide.

Lipid Class	Fatty Acid Moieties	Ionization Type	MS Peak Area	Calculated m/z Values
CL	(14:0/14:0/14:0/14:0)	M-H	2.18E+07	1239.84
CL	(14:0/14:0/14:0/12:0)	M-H	5.92E+05	1211.808
CL	(10:0/16:1/16:1/16:1)	M-H	7.58E+04	1261.824
CL	(12:0/18:1/12:0/16:1)	M-H	5.34E+04	1263.84
CL	(12:0/16:1/16:1/16:1)	M-H	3.33E+05	1289.855
CL	(16:1/16:1/16:0/12:0)	M-H	2.07E+05	1291.871
CL	(18:1/16:0/12:0/14:0)	M-H	4.16E+04	1293.887
CL	(18:1/16:1/12:0/16:1)	M-H	6.36E+05	1317.887
CL	(12:0/16:0/18:1/16:1)	M-H	2.32E+05	1319.902
CL	(16:1/16:1/16:1/16:1)	M-H	8.78E+05	1343.902
CL	(12:0/18:1/16:1/18:1)	M-H	5.20E+05	1345.918
CL	(18:1/18:1/16:0/12:0)	M-H	1.33E+05	1347.934
CL	(16:1/16:1/18:1/16:1)	M-H	2.86E+06	1371.934
CL	(18:1/16:0/16:1/16:1)	M-H	9.82E+05	1373.949
CL	(16:0/16:1/18:1/16:0)	M-H	1.14E+05	1375.965
CL	(10:0/16:0/20:0/20:1)	M-H	4.66E+05	1377.981
CL	(18:1/16:1/16:1/18:1)	M-H	3.93E+06	1399.965
CL	(18:1/16:1/16:0/18:1)	M-H	4.09E+05	1401.981
CL	(18:1/16:0/16:0/18:1)	M-H	6.33E+04	1403.996
CL	(18:1/16:1/18:1/18:1)	M-H	2.14E+06	1427.996
CL	(18:1/18:1/16:0/18:1)	M-H	1.32E+05	1430.012
CL	(18:1/18:1/18:1/18:1)	M-H	2.00E+06	1456.028
CL	(22:1/18:0/14:0/18:1)	M-H	1.91E+05	1460.059
CL	(8:0/20:0/16:0/20:0)	M-H	1.77E+05	1351.965

Table 56. Lipid species of cardiolipin identified by the developed LC-MS/MS method. The lipid species represented here are from 7 growth time points (DME, D0, D1, D2, D4, D6, D8). Legend: DME stands for day mid-exponential phase. D stands for day and numeric values represent days of growth. The highlighted in yellow row is for the lipid standard of cardiolipin.

Lipid Class	Fatty Acid Moieties	Ionization Type	MS Peak Area	Calculated m/z Values
FA	(19:0)	M-H	6.71E+07	297.2799
FA	(12:0)	M-H	2.60E+06	199.1704
FA	(16:1)	M-H	1.68E+07	253.2173
FA	(16:0)	M-H	1.84E+06	255.233
FA	(18:1)	M-H	2.98E+07	281.2486
FA	(18:0)	M-H	7.54E+06	283.2643
FA	(20:1)	M-H	5.83E+05	309.2799
FA	(20:0)	M-H	2.41E+06	311.2956
FA	(22:0)	M-H	8.20E+05	339.3269
FA	(24:0)	M-H	1.23E+06	367.3582
FA	(30:0)	M-H	9.86E+04	451.4521
FA	(10:0)	M-H	6.64E+04	171.1391
FA	(26:0)	M-H	2.65E+07	395.3895

Table 17. Lipid species of free fatty acid identified by the developed LC-MS/MS method. The lipid species represented here are from 7 growth time points (DME, D0, D1, D2, D4, D6, D8). Legend: DME stands for day mid-exponential phase. D stands for day and numeric values represent days of growth. The highlighted in yellow row is for the lipid standard of free fatty acid.

Lipid Class	Fatty Acid Moieties	Ionization Type	MS Peak Area	Calculated m/z Values
PE	(15:0/15:0)	M-H	3.30E+07	662.4766
PE	(16:0/10:0)	M-H	1.08E+05	606.414
PE	(16:1/12:0)	M-H	1.89E+05	632.4297
PE	(16:0/12:0)	M-H	2.62E+05	634.4453
PE	(18:1/12:0)	M-H	9.71E+04	660.461
PE	(16:1/16:1)	M-H	8.66E+06	686.4766
PE	(16:0/16:1)	M-H	1.65E+07	688.4923
PE	(16:1/18:1)	M-H	1.36E+07	714.5079
PE	(18:0/16:1)	M-H	2.74E+06	716.5236
PE	(18:1/18:1)	M-H	2.05E+06	742.5392
PE	(18:0/18:1)	M-H	1.52E+06	744.5549
PE	(20:1/18:1)	M-H	2.67E+05	770.5705
PE	(20:0/18:1)	M-H	1.95E+05	772.5862
PE	(16:1/10:0)	M-H	6.04E+04	604.3984
PE	(16:0/16:0)	M-H	3.18E+05	690.5079
PE	(18:0/16:0)	M-H	1.40E+05	718.5392
PE	(18:0/18:0)	M-H	6.33E+04	746.5705
PE	(26:0/16:1)	M-H	2.53E+05	828.6488
PE	(26:0/18:1)	M-H	1.68E+05	856.6801
PE	(16:1/14:1)	M-H	1.33E+05	658.4453

Table 68. Lipid species of phosphatidylethanolamine identified by the developed LC-MS/MS method. The lipid species represented here are from 7 growth time points (DME, D0, D1, D2, D4, D6, D8).

Legend: DME stands for day mid-exponential phase. D stands for day and numeric values represent days of growth. The highlighted in yellow row is for the lipid standard of phosphatidylethanolamine.

Lipid Class	Fatty Acid Moieties	Ionization Type	MS Peak Area	Calculated m/z Values
PG	(15:0/15:0)	M-H	6.89E+07	693.4712
PG	(16:0/16:1)	M-H	2.24E+05	719.4869
PG	(16:0/18:1)	M-H	6.40E+05	747.5182

Table 197. Lipid species of phosphatidylglycerol identified by the developed LC-MS/MS method. The lipid species represented here are from 7 growth time points (DME, D0, D1, D2, D4, D6, D8). Legend: DME stands for day mid-exponential phase. D stands for day and numeric values represent days of growth. The highlighted in yellow row is for the lipid standard of phosphatidylglycerol.

Lipid Class	Fatty Acid Moieties	Ionization Type	MS Peak Area	Calculated m/z Values
PI	(17:0/20:4)	M-H	2.94E+05	871.5342
PI	(16:0/10:0)	M-H	4.14E+05	725.4247
PI	(16:0/12:0)	M-H	1.21E+06	753.456
PI	(16:0/14:1)	M-H	1.56E+05	779.4716
PI	(18:0/12:0)	M-H	8.84E+05	781.4873
PI	(16:1/16:1)	M-H	6.34E+05	805.4873
PI	(16:0/16:1)	M-H	5.16E+06	807.5029
PI	(16:1/18:1)	M-H	3.71E+05	833.5186
PI	(16:0/18:1)	M-H	9.96E+06	835.5342
PI	(18:1/18:1)	M-H	2.64E+05	861.5499
PI	(18:0/18:1)	M-H	4.96E+06	863.5655
PI	(26:0/16:1)	M-H	2.19E+05	947.6594
PI	(26:0/18:1)	M-H	1.98E+05	975.6907
PI	(27:0/16:1)	M-H	4.68E+04	961.6751

Table 80. Lipid species of phosphatidylinositol identified by the developed LC-MS/MS method. The lipid species represented here are from 7 growth time points (DME, D0, D1, D2, D4, D6, D8). Legend: DME stands for day mid-exponential phase. D stands for day and numeric values represent days of growth. The highlighted in yellow row is for the lipid standard of phosphatidylinositol.

Lipid Class	Fatty Acid Moieties	Ionization Type	MS Peak Area	Calculated m/z Values
PS	(17:0/17:0)	M-H	1.98E+06	762.5291
PS	(16:0/16:1)	M-H	8.00E+05	732.4821
PS	(16:1/18:1)	M-H	2.72E+05	758.4978
PS	(16:0/18:1)	M-H	2.09E+06	760.5134
PS	(8:0p/16:0)	M-H	2.94E+04	606.3776

Table 91. Lipid species of phosphatidylserine identified by the developed LC-MS/MS method. The lipid species represented here are from 7 growth time points (DME, D0, D1, D2, D4, D6, D8). Legend: DME stands for day mid-exponential phase. D stands for day and numeric values represent days of growth. The highlighted in yellow row is for the lipid standard of phosphatidylserine.

2.4 Results and discussion

Like all other techniques, LC-MS/MS has its advantages and drawbacks. As we can see in Tables 5 and 6, although it is possible to identify all major classes of phospholipids using both NP-HPLC and RP-HPLC, it is impossible to achieve 100% ionization efficiency with either of these two columns. Overall, RP-HPLC allows to achieve higher ionization efficiencies than NP-HPLC (compare Tables 6 and 5, respectively). With both columns, the best result was obtained when mobile phase additive was ammonium formate in the positive mode, and ammonium acetate in the negative mode. Ionization efficiency is directly linked to the matrix effect in HPLC. In HPLC, the most frequent matrix effect is the ion suppression in which the target molecule does not get ionized to be detected by the first mass analyzer. Specially, the ionization efficiency is hindered when the ionization source is electrospray ionization, as compared to other harsher ionization methods such as atmospheric pressure chemical ionization (APCI). However, the drawback of the harsher methods of ionization is that molecular ions get fragments, so still the best choice of ionization is the soft ionization methods such as electrospray ionization [115]. More specifically ionization hindrance occurs in electrospray ionization when charges are added to target molecules in liquid phase where not all the target molecules gets charge and secondly ion suppression occurs during transformation of target molecules from liquid droplets to the gaseous phase [115].

The effect of all mobile phase additives is analyzed in the constant LC parameters such as mobile phases A and B, LC gradient, flow rate, temperature and pressure to prevent any error in determining the most effective additives. Our finding shows (table 6)

that optimal ionization is achieved in negative mode when only 10 mM of ammonium acetate is used as the sole additive without any kind of acid. For the positive mode, the result shows that optimal ionization is achieved when 10 mM of ammonium formate is used without any other additives. Due to difference in the chemical and physical properties of different lipid classes we excepted to have a random ionization efficiency of lipids with various additives, but it is interesting that a single additive give optimal ionization for almost all lipid classes that we targeted. Otherwise we had to run the sample with different mobile phases and with various additives to quantify the lipid classes, which would have been very time consuming. The values in tables 5 and 6 represents the average of 5 replicates run with each mobile phase additive and the percentage is relative to the highest peak intensity obtained in each set. Future studies can be done with different dilutions of lipid standards to evaluate the ionization efficiency, since one way to decrease the matrix effect is to dilute the sample adequately. Also, evaluation of these lipid standards ionizations with the same additives can be done with shot gun lipidomics to compare the shot gun with LC-MS/MS. Because, sometimes it is useful to just determine the concentration of different classes of lipids without analysis of the structure of each lipid species within a specific lipid class, since direct infusion is much faster and easier than LC-MS/MS method. Whereas LC-MS/MS requires longer time of experiment and data analysis after the experiment. Also, the other drawbacks of LC-MS/MS technique are the loss of some target molecules by the absorption of chromatographic support, and the decrease of the column performance over time [119].

Regardless of how the lipid samples are introduced into the Mass spectrometer whether it is directly injected or first separated by HPLC column; it is important that the

lipid species should be purified from other impurities during the extraction step prior to introduction into mass spectrometer. The impurities in the sample are the major cause of matrix effect and hindrance for isobaric species identification. Some example of these impurities in the lipid sample are: salts, carbohydrates, amines, peptides and metabolites [120]. The chemically diverse nature of lipids makes it difficult to extract them from other impurities. In general, most impurities have hydrophilic nature, thus mostly a mixture of polar and nonpolar organic solvent is used for extraction of lipids.

The major types of lipid extraction solvents reported in literature are chloroform, dichloromethane and *methyl-tert-butyl-ether* (MTBE) mixed with different quantity of methanol [121]. Each of the extraction method has its advantages and disadvantages. Although it has reported that a mixture of chloroform and methanol with ratios of 17:1 first step and 2:1 second step of extraction can extract all classes of lipids, but this method has two major disadvantages. First it is very toxic and it has been classified as a probable human carcinogen; although exposure to normal background level or under the threshold level (2 ppm or 7 mg/m^3) it is unlikely to result in major health problems [122]. The second issue with chloroform is that it has a higher density compare to water, thus lipid molecules together with chloroform stay in the bottom of extraction tube. Therefore, to get the lipid molecules the pipette tip or syringe tip must cross the insoluble layer of the extraction mixture. However, if even very small quantity of insoluble material is extracted together with lipids it can cause blockage of safe guard column, decrease the performance of HPLC column, and it can also clog the electrospray ionization nebulizer.

Despite the drawbacks of chloroform/methanol extraction method, when we compared the efficiency of all these different extraction methods (tables 7, 8 and 9) the result (table 9) shows that highest lipid standard recovery happens when chloroform/methanol method was used. The values in tables 7, 8 and 9 represent the average of 3 replicates of lipid standard recovery from the extraction of the 3 extraction methods. The percentage (%) values are compared to the same concentration of lipid standards when injected directly into the HPLC column. The concentration determination is based on the mass peak area related to each lipid class. The above-mentioned drawbacks of chloroform/methanol extraction method can be easily minimized or eliminated. For instance, if the chloroform is handled with caution inside the fume hood, its toxic effect can be minimized to normal level. The introduction of insoluble material can also be minimized if a thinner glass pipette is used.

The other two extraction solvents, namely MTBE and dichloromethane, are less toxic than chloroform. The acceptable threshold limit for dichloromethane is 50 ppm or 177 mg/m^3 which is almost 25 time higher than the acceptable threshold limit of chloroform [122]. Nevertheless, dichloromethane can also be carcinogenic if continuous exposure is experienced [122]. MTBE on the other hand is less toxic than either of dichloromethane and chloroform. Also, it has lower density than water, thus during extraction the pipette or syringe tip doesn't have to cross the insoluble layer, so not to introduce any insoluble material into the LC-MS/MS system.

Nevertheless, by comparing percentage recovery of lipid standards with the three extraction methods examined here, the highest percentage recovery of lipid standard of almost all lipid classes is achieved with chloroform/methanol method of extraction table 9. The second highest percent recovery of lipid standards is achieved with dichloromethane/methanol as the result shows in table 8. One of the reasons for similar percent recovery of lipid standards can be due to structure similarities of the two solvents, since dichloromethane has only one less chlorine atom than chloroform. Extraction with dichloromethane/methanol method can be used alternative to chloroform/methanol if the purpose of study is to just determine the different classes of lipids in a sample. However, if the purpose of study is the quantification of lipids, then the most appropriate solvent of extraction is chloroform/methanol method.

The result in table 7 shows that the least efficient extraction solvent among all 3 extraction methods is the MTBE method. Also, the result in table 7 shows that MTBE is not a suitable solvent of extraction for polar lipids, because two polar lipid classes phosphatidylinositol, and phosphatidylserine were not extracted at all.

After optimizing the ionization efficiency of the precursor ion with appropriate modifiers (tables 5 and 6), the next important factor for analysis of different lipid classes depends on finding a better fragmentation method for the MS-2 analysis. The generation of precursor ions by electrospray ionization (ESI) is usually done by adding a proton $[M+H]^+$ or a cation such as $[M+Na]^+$ or by removing a proton $[M-H]^-$ also, other multiple-charged ions such as $[M+2H]^{2+}$ are formed by ESI ionization. Isobaric species (species with same molecular weight, but different in acyl chains of various lipid species) together with oxidized lipid class and the multiple ion formed by a single lipid species makes the

assignment of the MS peaks to different lipid species difficult only based on the precursor/parent ion. Thus, further analysis of lipid species by MS/MS is crucial for identification of lipid species. The two most commonly used method for fragmentation or activation of precursor ion are higher-energy collisional dissociation (HCD) and collisional induced dissociation (CID). In both fragmentation methods, the parent ions accelerate due to the difference in electrical potential and collides with a neutral gas (CBAMS Orbitrap uses nitrogen gas for fragmentation) to fragment the parent ions into small parts which are then detected by second mass analyzer. We have tested both methods of fragmentation for positive and negative modes and our findings show in tables 10 and 11 that best result was achieved when HCD was used for positive mode and CID was used for negative mode.

After developing an optimized method of lipid identification and quantification, we successfully identified 10 different lipid classes in wild-type strain of *Saccharomyces cerevisiae* (see Tables 12 to 21). The lysoforms of some lipid classes were also detected, but we do not report them here because we did not have the appropriate internal standards to quantify them and, thus, we did not consider these molecules for further studies. The lipid species in each lipid class are sum of all unique species found when sample from growth points day mid-exponential (DME), days 0, 1, 2, 4, 6 and 8 were analyzed with our developed LC-MS/MS method. The reason that we collected all the unique species from various time points is that yeast cells make different lipid species as they age [86].

The fatty acid moieties of majority of lipid species identified in each class are about 16 to 18 carbons long and have even number of carbon. Most of species in each class identified with our method have already been reported separately when different studies target a subset of these lipid classes [123]. Our finding that the identified fatty acid moieties have even number of carbon is in parallel with previous studies [123]. The reason for this is that eukaryotes do not have odd number of carbon length in their fatty acid moieties [123].

The calculated mass over charge ratio (m/z) values reported in table numbers 12 through 21 are 4 digits after the decimal point. The precision in these values is due to the sensitivity of the LC-MS/MS developed. Two lipid species with same molecular weight can be unambiguously identified if they are different in their structure. The two otherwise isobaric species phosphatidylcholine (PC) table 12 and ceramide (CER) table 15 both having the same m/z value of 650 are well separated and characterized by this optimized method.

3.0 LC-MS/MS analysis of cellular lipidomes of wild-type and various mutant strains of *Saccharomyces cerevisiae* impaired in lipid metabolism cultured in the presence or absence of a longevity-extending plant extract 21

3.1 Introduction.

3.1-1 Background information on plant extract 21

The Titorenko lab has recently discovered six plant extracts that delay yeast chronological aging and extend the chronological lifespan of *Saccharomyces cerevisiae* [66]. These 6 plant extracts have the most potent life extending properties yet described. Among these 6 plant extracts the most potent life extending plant extract is plant extract 21 (PE21) [66]. This natural compound (PE21) is extracted from the bark of white willow, Salix alba. PE21 acts a geroprotector that decreases the rate at which yeast chronologically ages and extends the maximum chronological lifespan of yeast under non-caloric restriction conditions. PE21 slows yeast chronological aging because it attenuates Sch9, a protein kinase that is stimulated by both the nutrient-sensing TORC1 (target of rapamycin complex 1) signaling pathway and the sphingolipid-dependent Pkh1/2 (Pkb-activating kinase homolog) signaling pathway [66]. This natural compound achieves its geroprotector effect by 1) increasing mitochondrial respiration and membrane potential; 2) altering the intracellular concentrations of reactive oxygen species (ROS); 3) decreasing oxidative damage to cellular proteins, membrane lipids, and mitochondrial and nuclear genomes; 4) enhancing cell resistance to oxidative and thermal stresses; and 5) accelerating degradation of neutral lipids deposited in lipid droplets (LDs) [67]. These neutral and nonpolar lipids are steryl

esters and triacylglycerols are initially formed in the endoplasmic reticulum and then they are transported and stored in lipid droplets. These lipids are very hydrophobic and are prone to lipolytic degradation to generate metabolites required in the biosynthetic pathways of sphingolipids and phospholipids. New research highly suggests that the synthesis, the storage and the degradation of uncharged lipids are implicated in longevity extending processes [67].

Recent studies in the Titorenko lab have suggested that some pathways in lipid metabolism is altered when yeast cells are grown with this plant extract 21. The effect of plant extract 21 was analyzed on the lipidome of wilt type and various mutants related to lipid metabolism of *Saccharomyces cerevisiae* by determining the alternation of lipid composition by the developed LC-MS/MS method. Detailed information about possible lipid metabolism pathways effected by plant extract #21 and the related mutants is given in section 3.1-2 below.

3.1-2 Lipid metabolism pathways and various mutant strains of *Saccharomyces cerevisiae* impaired in these pathways

In the complex network of lipid metabolism of saccharomyces cerevisae, Phosphatidic acid (PA) serves as a common precursor to most of the other lipids [86]. PA is produced from glycerol-3-P through an intermediate lyso form of PA using two fatty acyl CoA reactions. These reactions are catalyzed in the endoplasmic reticulum by the GTP2- and SCT1-dependent glycerol-3-P acyltransferases. Lysoform of PA to PA conversion involves the catalysis of SLC1 and ALE1 acyltransferases as indicated in figure 3. Dihydroxyacetone-P is also used as substrate by glycerol-3-P acyltransferase, then the

product formed is converted to PA by AYR1 reductase from lipid droplets and AYR1 reductase from ER [86].

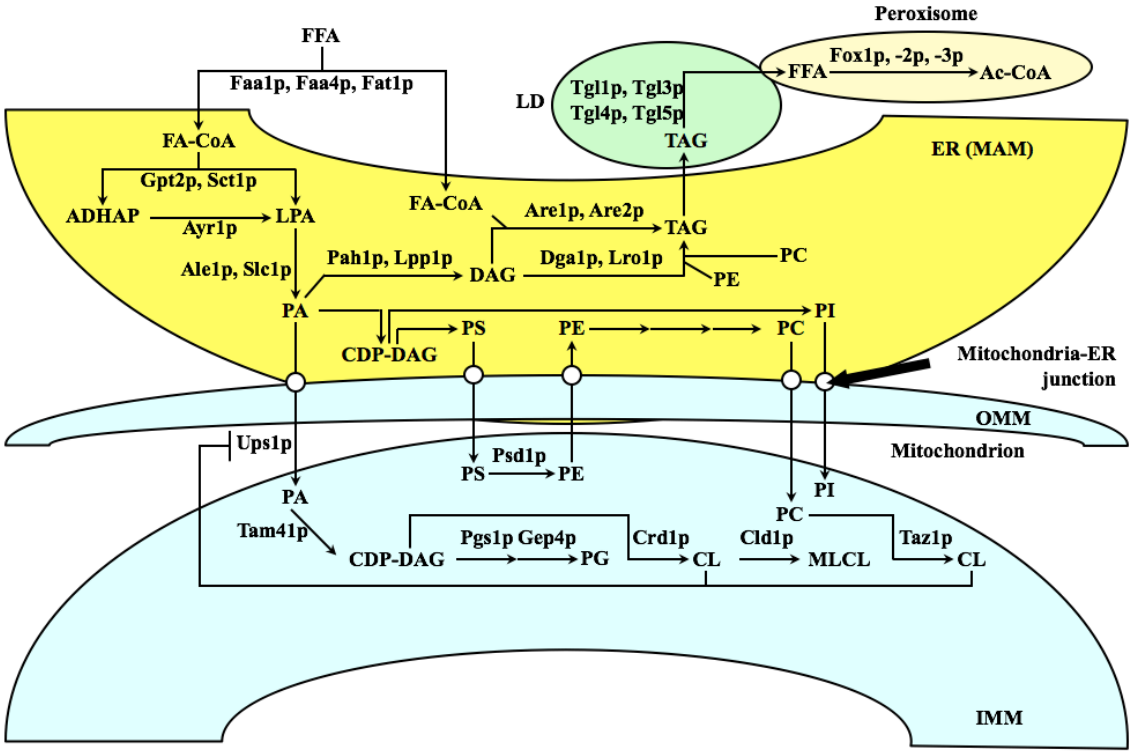

Figure 3. Lipid metabolism and inter-organelle transport in mitochondria, the endoplasmic reticulum (ER), lipid droplets (LD) and peroxisomes of the yeast S. cerevisiae. The arrows indicate the conversion of one lipid class to another lipid class and the enzyme(s) involve in the such pathways are indicated on top of the arrow. The letter P after each gene name indicates that it is the protein (enzyme) of that gene [69].

Phosphatidic acid (PA) is converted into the different lipid classes via two routes: CDP-DAG and DAG branches of this network as indicated in figure 3. The first subroutine, CDP-DAG, serves in the synthesis of all the phospholipids. PA is converted into CDP-DAG which then metabolized in the endoplasmic reticulum to produce PI and PS or in the mitochondria to produce PG and then CL [75-77]. This phosphatidylserine can then be shuttled to the mitochondria where it serves as an intermediate in the synthesis of PE. The latter is then converted into PC in the endoplasmic reticulum. The second subroutine,

DAG, serves in the synthesis of triacylglycerols and steryl esters. In this route, PA is converted to DAG in the endoplasmic reticulum followed by its conversion into TAG and SE. These neutral lipids are then shuttled by vesicles into lipid droplets where they are stored for future breakdown and replenishment of the PA, DAG and FFA pools [25-27].

Few enzymes and proteins of interest are involved in this complex network. Free fatty acids are converted into FFA-CoAs by two enzymes Faa1p and Faa4p [75, 77]. These FAA-CoA are then incorporated into phosphatidic acid by either Ale1p or Slc1p [75, 77]. The production of CL requires the shuttling of PA from the endoplasmic reticulum into the mitochondrial membrane. This lipid trafficking step occurs through Ups1p which associates with Mdm35 to form the shuttling complex [87]. The methylation of phosphatidylethanolamine to produce phosphatidylcholine in the endoplasmic reticulum is catalyzed by Cho2p [88]. Triacylglycerols are formed from diacylglycerols by an acylation step either with a transfer of acyl-CoA or acyl groups from glycerophospholipids. This reaction is catalyzed by either Dga1p, Are1p or Are2p. Tgl1p serves in the breakdown of ergosteryl esters within the plasma membrane or within lipid droplets [89 - 91]. Tgl1p as well as Tgl3p, Tgl4p, Tgl5p are lipases that are involved in the conversion of triacylglycerols into free fatty acids in lipid droplets [93 – 95]. Taz1p converts CL to MLCL through a transacylation step in the inner mitochondrial membrane [96].

3.2 Materials and Methods

3.2-1 Yeast strains

The wild-type strain *Saccharomyces cerevisiae* BY4742 (*MATα his3Δ1 leu2Δ0 lys2Δ0 ura3Δ0*). Mutant strains: SLC1 (*MATα SUC2 gal2 mal2 mel flo1 flo8-1 hap1 ho bio1 bio6*), TGL3 (BY4741; *Mat a; his3Δ1; leu2Δ0; met15Δ0; ura3Δ0; tgl3Δ YMR313c::kanMX4*), TGL1 (BY4741; *Mat a; his3Δ1; leu2Δ0; met15Δ0; ura3Δ0; tgl1Δ YMR313c::kanMX4*) TGL4 (*BY4742; Mat α; his3Δ1; leu2Δ0; lys2Δ0; ura3Δ0; tgl4Δ YKR089c::kanMX4*), TGL5 (BY4742; *Mat α; his3Δ1; leu2Δ0; lys2Δ0; ura3Δ0; tgl5Δ YOR081c::kanMX4*), DGA1 (*MATα SUC2 gal2 mal2 mel flo1 flo8-1 hap1 ho bio1 bio6; DGA1Δ*), ARE2 (*BY4742; Mat α; his3Δ1; leu2Δ0; lys2Δ0; ura3Δ0; are2Δ YKR089c::kanMX4*), CRD1 (*BY4742; Mat α; his3Δ1; leu2Δ0; lys2Δ0; ura3Δ0; crd1Δ YKR089c::kanMX4*), UPS1 (*BY4742; Mat α; his3Δ1; leu2Δ0; lys2Δ0; ura3Δ0; ups1Δ YKR089c::kanMX4*), TAZ1 (*BY4742; Mat α; his3Δ1; leu2Δ0; lys2Δ0; ura3Δ0; taz1Δ YKR089c::kanMX4*), CHO2 (*BY4742; Mat α; his3Δ1; leu2Δ0; lys2Δ0; ura3Δ0; cho2Δ YKR089c::kanMX4*). All these strains were bought from Thermo Scientific/Open Biosystems.

3.2-2 Media and growth conditions

Both the wild type and various mutant strains were grown in a synthetic minimal YNB medium (0.67% Yeast Nitrogen Base without amino acids) initially containing 2% glucose and supplemented with 20 mg/l histidine, 30 mg/l leucine, 30 mg/l lysine and 20 mg/l uracil. Cells were cultured at 30 ^{O}C with rotational shaking at 200 rpm in Erlenmeyer flasks at a “flask volume/medium volume” ratio of 5:1. The stock solution of aging-delaying

plant extract 21 (PE21) in ethanol was made on the day of adding this PE to cell cultures. This stock solution was added to growth medium immediately following cell inoculation into the medium. The final concentration of PE21 in growth medium was 0.1% (0.25 ml of 20% stock solution of PE21 per flask). The 20% PE21 stock solution was made by adding 2.5 grams of PE21 in 12.5 ml ethanol. The same condition was used for the control flasks, but instead of adding 0.25 ml of 20% stock solution of PE21 0.25 ml of 100% ethanol was added to give a percentage of 0.5% of ethanol in each flask.

3.2-3 Cell collection and lipid extraction of *Saccharomyces cerevisiae*

A hemocytometer (Hausser Scientific Catalog# 3200) was used to count yeast cells and to calculate the volume of cell culture containing 5.0 x 10^7 cells. Appropriate volume of cell culture was taken, and the cells were harvested by centrifugation in a Centra CL2 clinical centrifuge at 3,000 × g for 5 min at room temperature. The cell pellet was washed once in ice-cold nano-pure water and once in ice-cold 155 mM ammonium bicarbonate (pH 8.0), and the cells were subjected to centrifugation at 16,000 × g for 1 min at 4^{o}C. The cell pellet was stored at -80 ^{o}C until lipid extraction. For lipid extraction, the pelleted cells kept at -80 ^{o}C were thawed on ice before being re-suspended in 200 µl of ice-cold Nano-pure water. The re-suspended sample which contained 5 × 10^7 cells was transferred to a 15-mL high-strength glass screw top centrifuge tube with a Teflon lined cap (#0556912; Fisher Scientific). To each 15-mL high-strength glass tube the following was added: 1) 25 µL of the internal standard mix prepared in mixture of chloroform: methanol (both OPTIMA grade from Fisher Scientific used for LC-MS with CAS# 76-09-3 and 67-56-1), 2) 100 µL of 425-600 µM acid-washed glass beads to break open the cells

(#G8772; Sigma-Aldrich) and 600 µL of chloroform : methanol at a 17:1 ratio both from Fisher Scientific with OPTIMA grade and CAS# 76-09-3 and 67-56-1. The samples were then vortexed vigorously for 5 minute at room temperature to breakdown the cells and subjected to centrifugation in a Centra CL2 clinical centrifuge at 3,000 × g for 5 min at room temperature; this centrifugation allowed to separate the upper aqueous phase from the lower organic phase, which contained nonpolar lipids TAG, PC, PE and PG. The lower organic phase (400 µL) was then transferred to another 15-mL high-strength glass screw top centrifuge tube using pipette with polypropylene gel loading tips (Fisher scientific catalog# 13-611-115) with careful attention not to disrupt the glass beads or upper aqueous phase. 300 µL of chloroform-methanol (2:1) solution was added to the remaining upper aqueous phase to allow the extraction of sphingolipids and of polar lipids PA, PS, PI and CL. The samples were again vortexed vigorously at room temperature for 5 minutes. The initial separated organic band was kept at under the flow of nitrogen gas for the duration of the second vortexing. The samples were again centrifuged for 5 min at 3,000 × rpm at room temperature; the lower organic phase (200 µL) was then separated and added to the corresponding initial organic phase with pipette using the polypropylene gel loading tips. With both lower organic phases combined, the solvent was evaporated off by nitrogen gas flow. Once all solvent was evaporated, the tubes containing the lipid film were closed under the flow of nitrogen gas and stored in -80^{O}C.

Detection mode	Lipid classes	Lipid chain composition	Calculated M/Z values	Moles in samples
Negative	Ceramide	(18:1/17:0)	550.5204675	2.26E-09
	Cardiolipin	(14:0/14:0/14:0/14:0)	1239.839755	1.96E-09
	Free Fatty Acid	19:0	297.2799035	8.37E-09
	phosphatidylethanolamine	(15:0/15:0)	662.4766305	3.77E-09
	Phosphatidylglycerol	(15:0/15:0)	693.4712115	3.49E-09
	phosphatidylinositol	(17:0/20:4)	871.5342065	3.00E-11
	phosphatidylserine	(17:0/17:0)	762.5290605	3.18E-09
Positive	phosphatidylcholine	(13:0/13:0)	650.4755335	3.85E-09
	phytosphingosine	(16:1)	272.2584055	2.25E-09
	triacylglycerol	(28:1/10:1/10:1)	818.7232155	3.67E-09

Table 102. Internal lipid standards used for the experiment. Note: Internal lipid standards CL, CER, PI, SO, PE, PG, FFA, PS and PC were all from Avanti Polar Lipid, Alabaster, AL, USA. TAG internal standard originates from Larodan, Malmo, Sweden.

3.2-4 Sample preparation for LC-MS/MS

500 µL of acetonitrile: 2-propanol: H2O with ratio of (65:35:5) all with LC-MS grade from Fisher Scientific (catalog# A9551, A4611 and W6212) added to tubes containing the lipid film. Each tube was vortexed 3 times for 10 seconds each time and then all the samples were sonicated for 15 minutes and vortexed again as above and 100 µL from each sample was added to glass vials with inserts used for Agilent1100 Wellplate (note: it is important to eliminate all the air bubbles in the insert before putting the vials in the Agilent1100 Wellplate).

3.2-5 Liquid chromatography conditions

The LC–MS experiments were performed using an Agilent 1100 series LC system (Agilent Technologies) equipped with a binary pump, de-gaser and an autosamples. Lipid species were separated on a reverse-phase column CSH C18 (2.1 mm; 75 mm; pore size 130 Å; pH range of 1-11) (Waters, Milford, MA, USA) coupled to a CSH C18 VanGuard (Waters). The column was maintained at 55 °C at a flow-rate of 0.3 mL/min. The mobile phases consisted of (A) 60:40 (v/v) acetonitrile: water and (B) 90:10 (v/v) isopropanol: acetonitrile. For the positive mode ESI (+) both mobile phases A and B were mixed with 10 mM ammonium formate (0.631 g/L) from Fisher Scientific (catalog# A115-50). For the negative mode ESI (-) both mobile phases A and B were mixed with 10 mM ammonium acetate (0.771 g/L) from Fisher Scientific (catalog# 631-61-8). To enhance solubilizing of ammonium formate and ammonium acetate both salts were dissolved first in small volume of water (50 µl) before their addition in the mobile phases. Each mobile phase with modifiers (ammonium formate and ammonium acetate) was mixed, sonicated for 20 minutes to achieve complete dissolving of modifiers, mixed again, and then sonicated for another 20 minutes.

The separation of different lipid species by HPLC was achieved under the following HPLC gradient: 0 to 4 min 90%(A); 4 to 10 min 40%(A); 10 to 21 min 32% (A); 21 to 24 min 3 % (A); 24 to 33 min 90 % (A). A sample volume of 5 µl and 10 µl was used for the injection in ESI (+) and ESI (-) respectively. Samples were kept in the Agilent1100 Wellplate.

3.2-6 Mass spectrometry

Extracted lipids were separated by HPLC and analyzed with Thermo Orbitrap Velos Mass

Spectrometer equipped with ESI ion source (Thermo Scientific). Parent ions (MS-1) were detected in positive and negative modes using the FT analyzer at a resolution of 60,000. The MS-1 mass range used is from 150 – 2000 Dalton.

Ion Source type	ESI
Capillary Temperature ^{O}C	300
Source heater Temperature ^{O}C	300
Sheath Gas Flow	10
Aux Gas flow	5

Table 113. Thermo Orbitrap Velos mass spectrometer's tune file instrument settings. Legend: ESI stands for electrospray ionization.

Instrument polarity	Positive	Negative
Activation type	HCD	CID
Min. signal required	5000	5000
Isolation Width	2.0	2.0
Normalized Collision energy	55.0	35
Default charge state	2	2
Activation time	0.1	10

Table 124. Instrument method for MS-2 used in this experiment. Legend: HCD stands for High-energy-induced-collision-dissociation, and CID stands for collision-induced-dissociation.

3.2-7 Processing of raw data from LC-MS

Raw files from LC-MS were analyzed by Lipid Search software (V4.1) from Thermo Fisher. The Lipid Identification Software “Lipid Search” was used to identify different lipid classes with the help of Molecular Fragmentation Query Language based on the below (Table 4) parameters. In addition to the parameters below (Table 4) an extra manual filter was applied to eliminate any Fatty Acid with odd number of carbon and to eliminate any fatty acid with more than 1 double bond (polyunsaturated fatty acid).

Identification		
Database	Orbitrap	
Peak detection	Recall isotope (ON)	
Search option	Product search Orbitrap	
Search type	Product	
Experiment type	LC-MS	
Precursor tol	10 ppm	
Product tol	HCD (positive mode) 20 ppm	
	CID (negative mode) 0.5 da	
Quantitation		
Execute quantitation	ON	
Mz tol	-5.0; +5.0	
Tol type	ppm	
Filter		
Top rank filter	ON	
Main node filter	Main isomer peak	
m-score threshold	5.0	
c-score threshold	2.0	
FFA priority	ON	
ID quality filter	**A**	Lipid class & FA are completely identified
	B	Lipid class & some FA are identified
	C	Lipid class or FA are identified
	D	Lipid identified by other fragment ions (H_2O, etc)
Lipid Class		
HCD (positive)	PC, SO, TG	
CID (negative)	CER, CL, FA, PE, PG, PI, PS	
Ions		
HCD (positive)	+H, +NH_4, +Na	
CID (negative)	-H, -2H, +HCOO	

Table 135. The parameters for lipid search software (V 4.1) used in the experiment for lipid detection. Legend: HCD stands for High-energy-induced-collision-dissociation, and CID stands for collision-induced-dissociation.

3.3 Tables and figures of various lipid classes for wild-type cells treated with PE21 or remained untreated

LIPID CLASS	DME	D0	D1	D2	D4	D6	D8
PC	1.14E+00	8.78E+00	5.87E+00	5.28E-01	8.47E-01	7.54E-01	5.15E-01
SO	7.08E+01	3.39E+01	4.11E+01	2.27E+00	2.68E+01	4.79E+01	5.71E+01
TG	6.64E+00	1.01E+01	1.89E+01	4.65E-01	2.16E+01	2.64E+01	1.47E+01
CER	1.90E+00	5.80E+00	4.00E+00	1.82E-01	3.81E+00	7.71E-01	4.56E+00
CL	6.79E-01	1.44E+00	1.16E+00	6.79E-02	1.76E+00	1.25E+00	1.59E+00
FA	4.04E+00	1.67E+01	1.02E+01	5.53E-01	6.55E+00	8.41E+00	6.46E+00
PE	4.52E+00	6.45E+00	4.69E+00	8.68E+01	5.16E+00	2.44E+00	2.78E+00
PG	2.23E-02	4.55E-01	2.83E-01	1.41E-02	4.97E-02	1.94E-02	6.43E-03
PI	1.30E+00	3.84E+00	1.96E+00	7.90E-02	6.61E-01	4.31E-01	5.57E-01
PS	2.72E+00	5.62E+00	5.18E+00	5.17E-01	2.49E+01	3.97E+00	8.95E+00

Table 146. Mean percentage value of wild type control lipid species identified by developed LC-MS/MS method. The values are the mean (% of whole lipidome) of two experiments for the wild type strain taken at 7 time points (DME, D0, D1, D2, D4, D6, D8). The mean (%) values are shown in figures 4-13. Legend: DME stands for day mid-exponential. D stands for day and numeric values represent days of growth. Lipid class: Phosphatidylcholine, sphingosine, Triacylglycerol, Ceramide, Cardiolipin, Free Fatty Acid, Phosphatidylethanolamine, Phosphatidylglycerol, Phosphatidylinositol, Phosphatidylserine.

LIPID CLASS	DME	D0	D1	D2	D4	D6	D8
PC	0.0505935	0.4535511	0.2582072	0.2449733	0.0637053	0.129691737	0.2110605
SO	3.4121109	1.863243	2.4070247	0.1772678	1.849794	3.119837559	3.7796413
TG	0.3252402	0.6886521	1.203741	0.034841	1.5112929	1.418779605	1.7323119
CER	0.0440361	0.2210655	0.1673791	0.008917	0.1361826	0.037539913	0.1824743
CL	0.0421655	0.0752303	0.0597828	0.0037301	0.1165151	0.057574775	0.0358539
FA	0.2574151	1.1103996	0.7549778	0.0495599	0.5000848	0.681187833	0.2913811
PE	0.1757019	0.1895866	0.173524	6.0007662	0.2023507	0.066542081	0.9180897
PG	0.0013712	0.0198524	0.0145072	0.001113	0.003684	0.000961483	0.0045493
PI	0.0569928	0.1625117	0.073704	0.0041955	0.0373794	0.010241971	0.1437976
PS	0.0645074	0.1489661	0.1346236	0.0235393	1.2171991	0.162474513	2.3065374

Table 27. Standard deviation of wild type control lipid species identified by developed LC-MS/MS method. The values are calculated as the sample standard deviation (±%) of two experiments for the wild type strain taken at 7 time points (DME, D0, D1, D2, D4, D6, D8). Sample standard deviation was used because the sample is biological. These standard deviations are represented as error bars in figures 4-13. Legend: DME stands for day mid-exponential. D stands for day and numeric values represent days of growth. Lipid class: Phosphatidylcholine, Sphingosine, Triacylglycerol, Ceramide, Cardiolipin, Free Fatty Acid, Phosphatidylethanolamine, Phosphatidylglycerol, Phosphatidylinositol, Phosphatidylserine.

LIPID CLASS	DME	D0	D1	D2	D4	D6	D8
PC	1.81E+00	3.90E+00	3.26E+00	3.43E+00	1.87E+00	1.02E+00	7.85E-01
SO	6.71E+01	5.36E+01	3.21E+01	3.43E+01	3.33E+01	3.83E+01	5.58E+01
TG	2.03E+01	1.98E+01	2.67E+01	2.51E+01	7.80E+00	1.78E+01	1.25E+01
CER	2.94E+00	4.05E+00	4.36E+00	3.73E+00	2.09E+00	2.79E+00	3.11E+00
CL	1.93E-01	5.38E-01	5.41E-01	5.05E-01	5.53E-01	7.06E-01	6.11E-01
FA	1.32E+00	1.07E+00	1.46E+00	1.60E+00	6.40E-01	5.46E-01	9.93E-01
PE	5.49E+00	6.57E+00	1.07E+01	8.04E+00	6.70E+00	5.66E+00	3.96E+00
PG	1.10E-02	6.37E-02	2.03E-01	8.44E-02	6.23E-02	3.10E-02	0.00E+00
PI	2.38E+00	2.20E+00	3.57E+00	2.26E+00	1.34E+00	8.99E-01	7.90E-01
PS	1.37E+00	4.24E-01	9.75E+00	1.46E+01	4.20E+01	2.81E+01	1.50E+01

Table 28. Mean percentage value of wild type treated with PE21 lipid species identified by developed LC-MS/MS method. The values are the mean (% of whole lipidome) of two experiments for the wild type strain treated with PE21 taken at 7 time points (DME, D0, D1, D2, D4, D6, D8). The mean (%) values are shown in figures 4-13. Legend: DME stands for day mid-exponential. D stands for day and numeric values represent days of growth. Lipid class: Phosphatidylcholine, Sphingosine, Triacylglycerol, Ceramide, Cardiolipin, Free Fatty Acid, Phosphatidylethanolamine, Phosphatidylglycerol, Phosphatidylinositol, Phosphatidylserine.

LIPID CLASS	DME	D0	D1	D2	D4	D6	D8
PC	1.81E+00	3.90E+00	3.26E+00	3.43E+00	1.87E+00	1.02E+00	7.85E-01
SO	6.71E+01	5.36E+01	3.21E+01	3.43E+01	3.33E+01	3.83E+01	5.58E+01
TG	2.03E+01	1.98E+01	2.67E+01	2.51E+01	7.80E+00	1.78E+01	1.25E+01
CER	2.94E+00	4.05E+00	4.36E+00	3.73E+00	2.09E+00	2.79E+00	3.11E+00
CL	1.93E-01	5.38E-01	5.41E-01	5.05E-01	5.53E-01	7.06E-01	6.11E-01
FA	1.32E+00	1.07E+00	1.46E+00	1.60E+00	6.40E-01	5.46E-01	9.93E-01
PE	5.49E+00	6.57E+00	1.07E+01	8.04E+00	6.70E+00	5.66E+00	3.96E+00
PG	1.10E-02	6.37E-02	2.03E-01	8.44E-02	6.23E-02	3.10E-02	0.00E+00
PI	2.38E+00	2.20E+00	3.57E+00	2.26E+00	1.34E+00	8.99E-01	7.90E-01
PS	1.37E+00	4.24E-01	9.75E+00	1.46E+01	4.20E+01	2.81E+01	1.50E+01

Table 29. Standard deviation of wild type treated with PE21 lipid species identified by developed LC-MS/MS method. The values are calculated as the sample standard deviation (±%) of two experiments for the wild type strain treated with PE21 taken at 7 time points (DME, D0, D1, D2, D4, D6, D8). Sample standard deviation was used because the sample is biological. These standard deviations are represented as error bars in figures 4-13. Legend: DME stands for day mid-exponential. D stands for day and numeric values represent days of growth. Lipid class: Phosphatidylcholine, Sphingosine, Triacylglycerol, Ceramide, Cardiolipin, Free Fatty Acid, Phosphatidylethanolamine, Phosphatidylglycerol, Phosphatidylinositol, Phosphatidylserine.

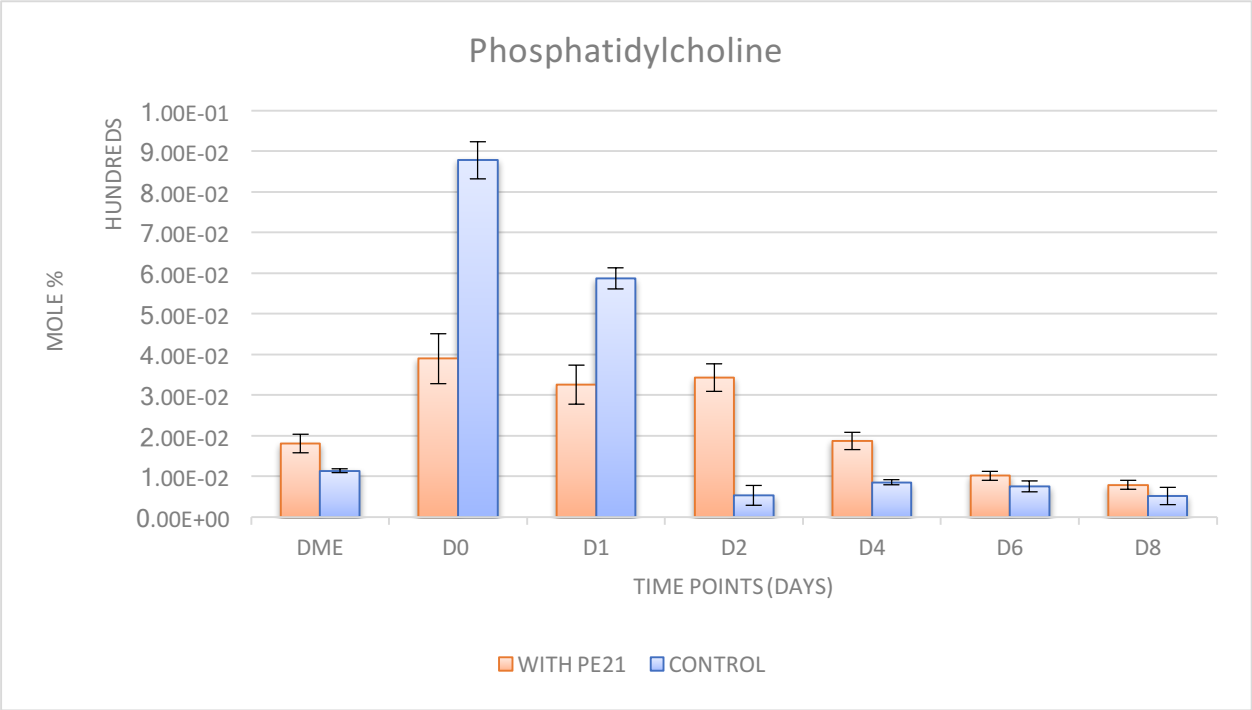

Figure 4. Mean percentage values of Phosphatidylcholine relative to the whole lipidome for wild-type control compared to wild-type treated with PE21, as measured by the developed LC-MS/MS method at 7 time points. Error bars presented are from Table 2 and Table 4. For growth conditions of control and treated with 21 refer to Materials and Methods in chapter 3 Legend: DME stands for day mid-exponential. D stands for day and numeric values represent days of growth. PE21 stands for plant extract 21.

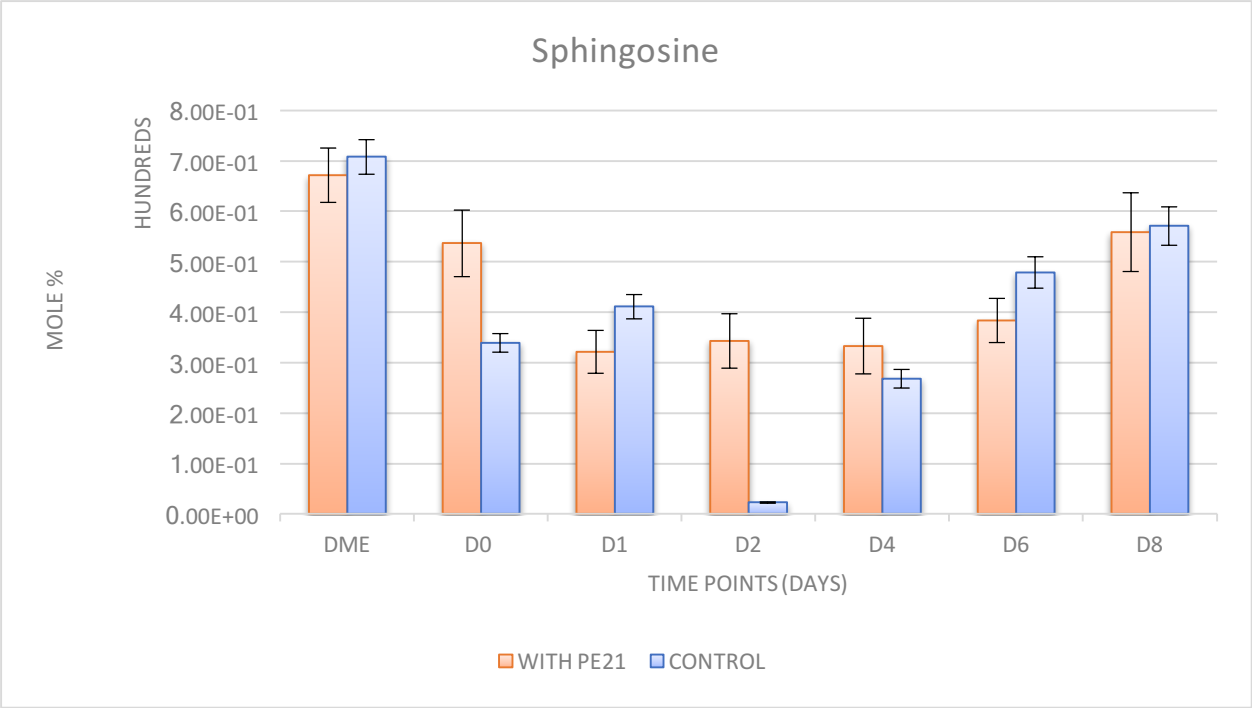

Figure 5. Mean percentage values of Sphingosine relative to the whole lipidome for wild-type control compared to wild-type treated with PE21, as measured by the developed LC-MS/MS method at 7 time points. Error bars presented are from Table 2 and Table 4. For growth conditions of control and treated with 21 refer to Materials and Methods in chapter 3 Legend: DME stands for day mid-exponential. D stands for day and numeric values represent days of growth. PE21 stands for plant extract 21.

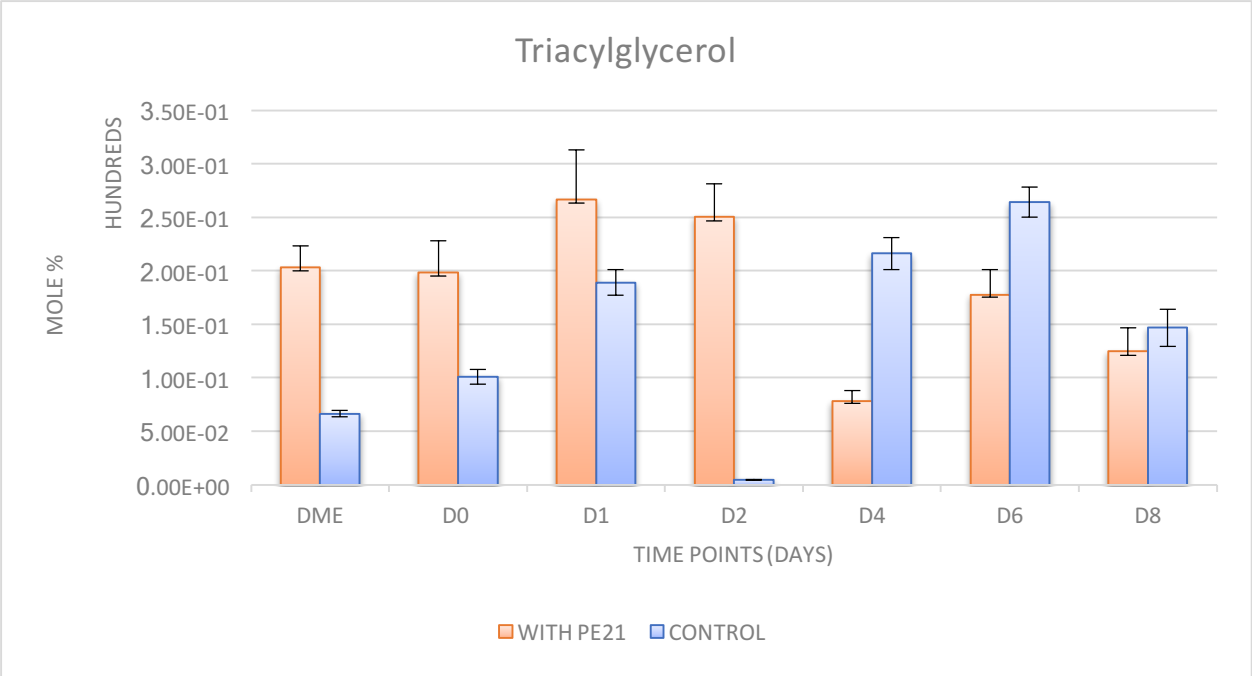

Figure 6. Mean percentage values of Triacylglycerol relative to the whole lipidome for wild-type control compared to wild-type treated with PE21, as meassured by the developed LC-MS/MS method at 7 time points. Error bars presented are from Table 2 and Table 4. For growth conditions of control and treated with 21 refer to Materials and Methods in chapter 3. Legend: DME stands for day mid-exponential. D stands for day and numeric values represent days of growth. PE21 stands for plant extract 21.

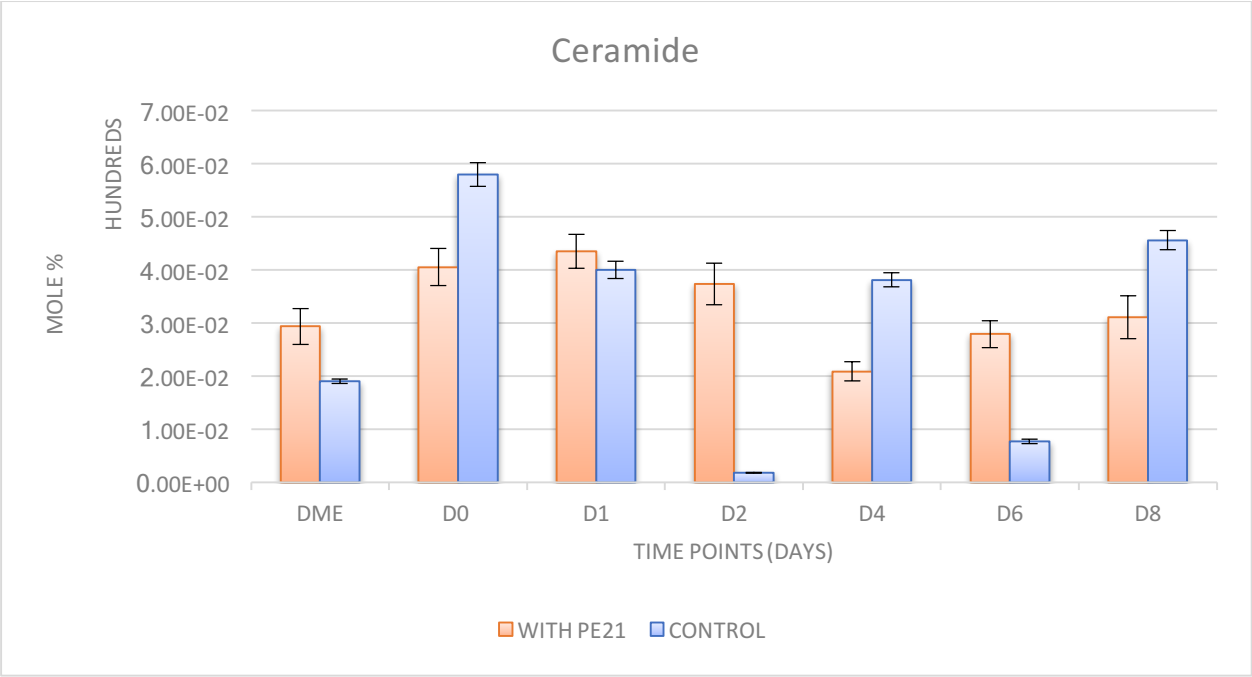

Figure 7. Mean percentage values of Ceramide relative to the whole lipidome for wild-type control compared to wild-type treated with PE21, as measured by the developed LC-MS/MS method at 7 time points. Error bars presented are from Table 2 and Table 4. For growth conditions of control and treated with 21 refer to Materials and Methods in chapter 3 Legend: DME stands for day mid-exponential. D stands for day and numeric values represent days of growth. PE21 stands for plant extract 21.

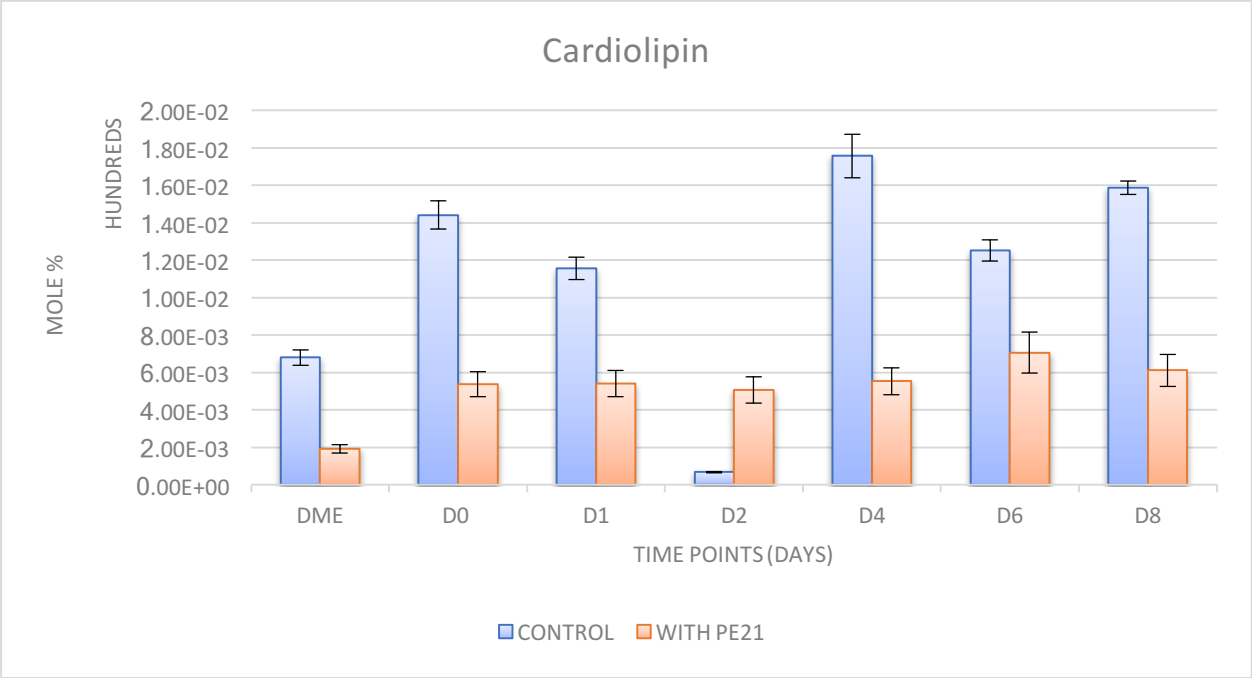

Figure 8. Mean percentage values of Cardiolipin relative to the whole lipidome for wild-type control compared to wild-type treated with PE21, as measured by the developed LC-MS/MS method at 7 time points. Error bars presented are from Table 2 and Table 4. For growth conditions of control and treated with 21 refer to Materials and Methods in chapter 3 Legend: DME stands for day mid-exponential. D stands for day and numeric values represent days of growth. PE21 stands for plant extract 21.

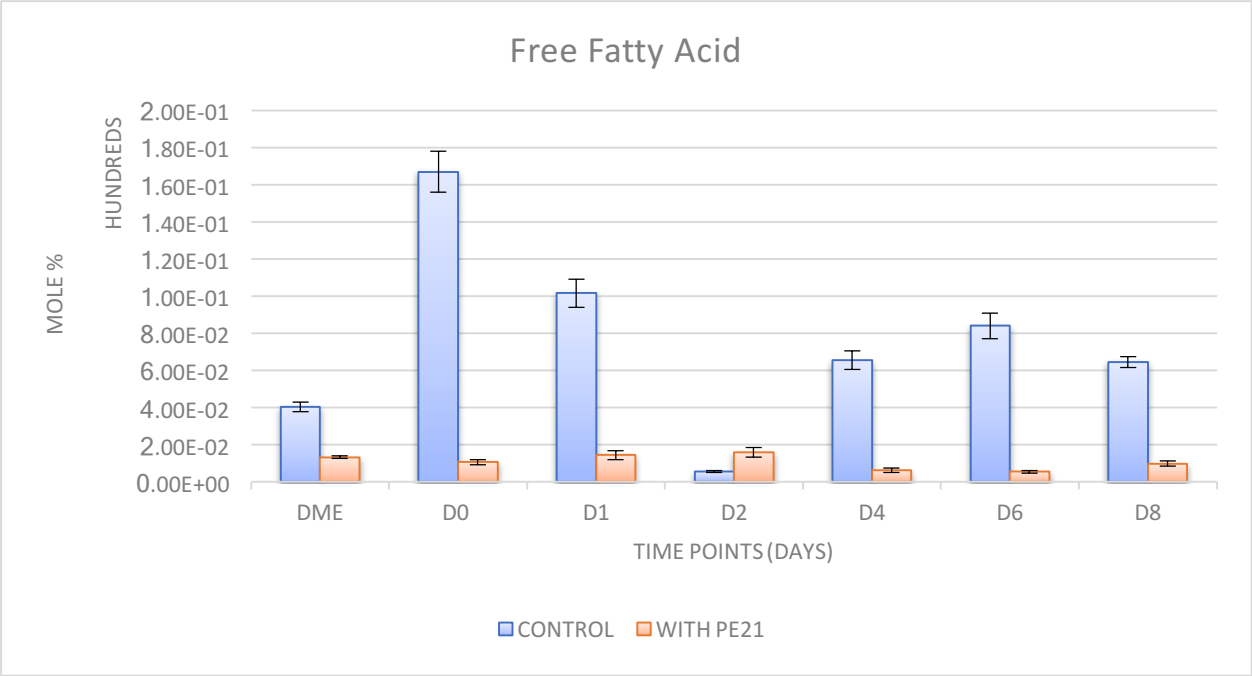

Figure 9. Mean percentage values of Free Fatty Acid relative to the whole lipidome for wild-type control compared to wild-type treated with PE21, as measured by the developed LC-MS/MS method at 7 time points. Error bars presented are from Table 2 and Table 4. For growth conditions of control and treated with 21 refer to Materials and Methods in chapter 3 Legend: DME stands for day mid-exponential. D stands for day and numeric values represent days of growth. PE21 stands for plant extract 21.

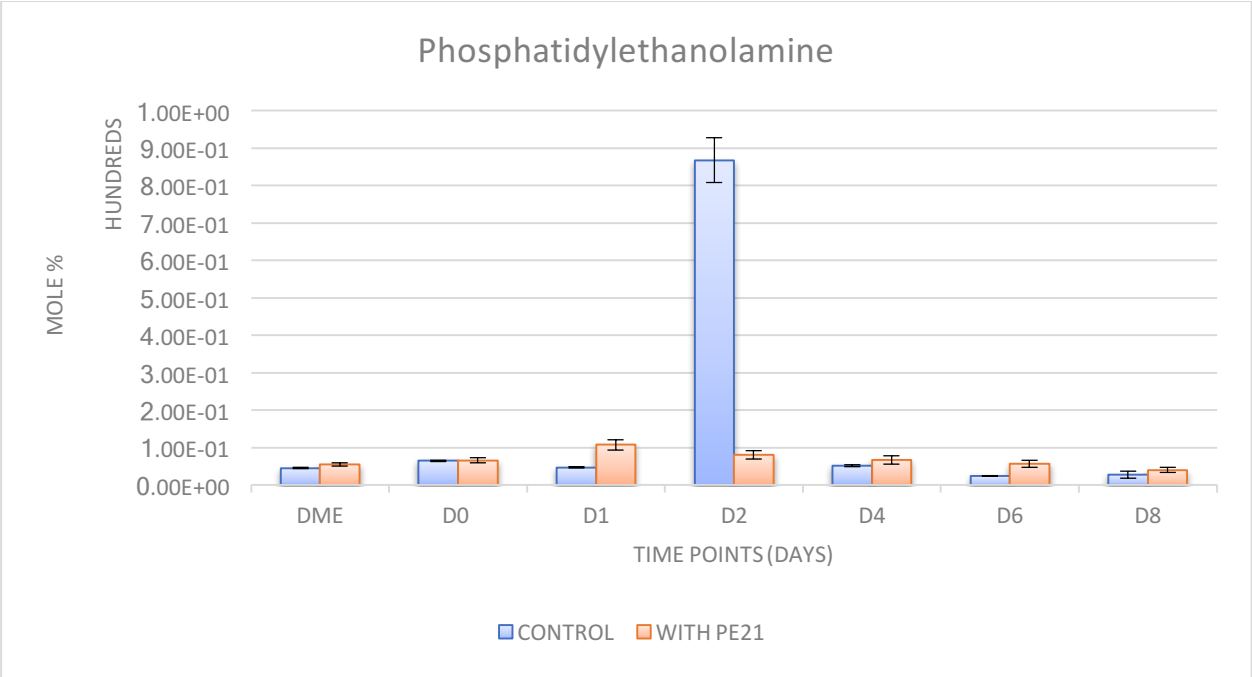

Figure 10. Mean percentage values of Phosphatidylethanolamine relative to the whole lipidome for wild-type control compared to wild-type treated with PE21, as measured by the developed LC-MS/MS method at 7 time points. Error bars presented are from Table 2 and Table 4. For growth conditions of control and treated with 21 refer to Materials and Methods in chapter 3 Legend: DME stands for day mid-exponential. D stands for day and numeric values represent days of growth. PE21 stands for plant extract 21.

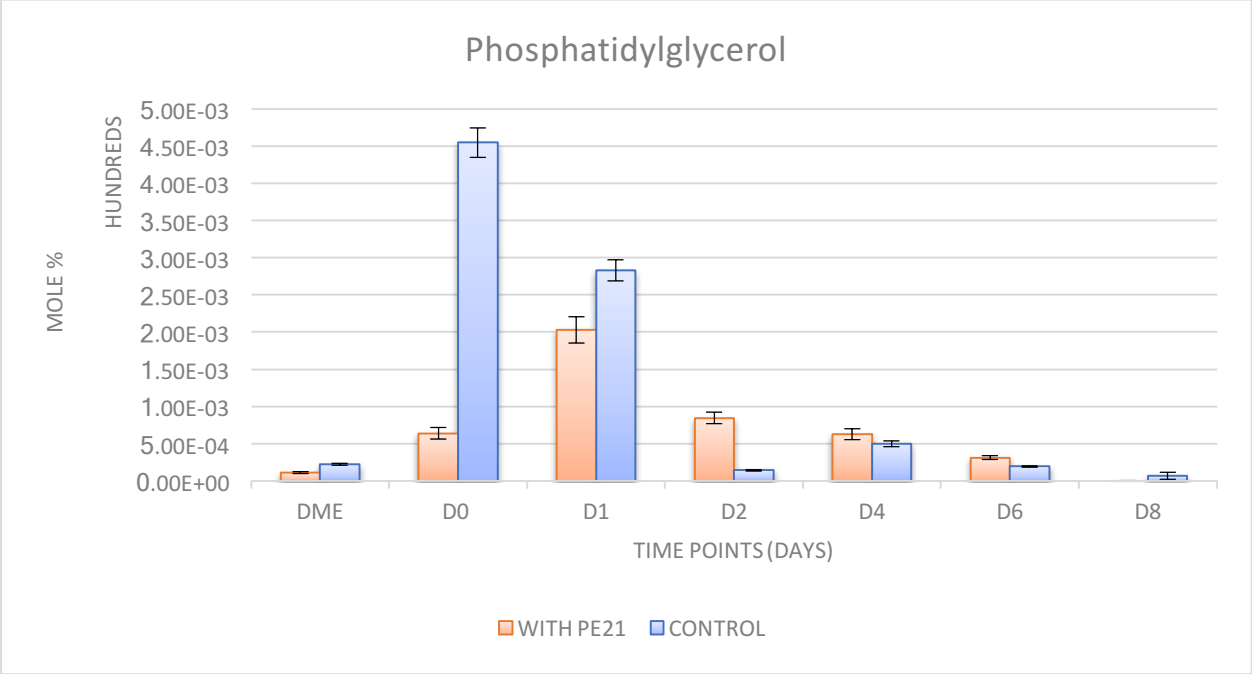

Figure 11. Mean percentage values of Phosphatidylglycerol relative to the whole lipidome for wild-type control compared to wild-type treated with PE21, as measured by the developed LC-MS/MS method at 7 time points. Error bars presented are from Table 2 and Table 4. For growth conditions of control and treated with 21 refer to Materials and Methods in chapter 3 Legend: DME stands for day mid-exponential. D stands for day and numeric values represent days of growth. PE21 stands for plant extract 21.

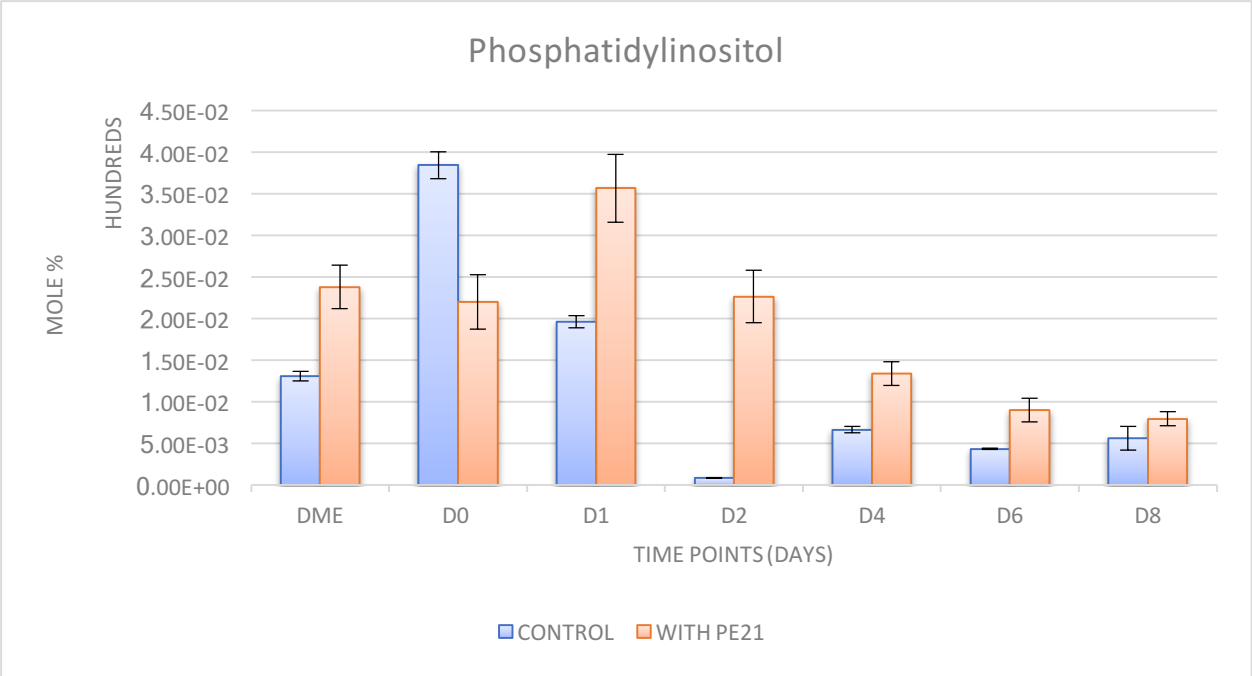

Figure 12. Mean percentage values of Phosphatidylinositol relative to the whole lipidome for wild-type control compared to wild-type treated with PE21, as measured by the developed LC-MS/MS method at 7 time points. Error bars presented are from Table 2 and Table 4. For growth conditions of control and treated with 21 refer to Materials and Methods in chapter 3 Legend: DME stands for day mid-exponential. D stands for day and numeric values represent days of growth. PE21 stands for plant extract 21.

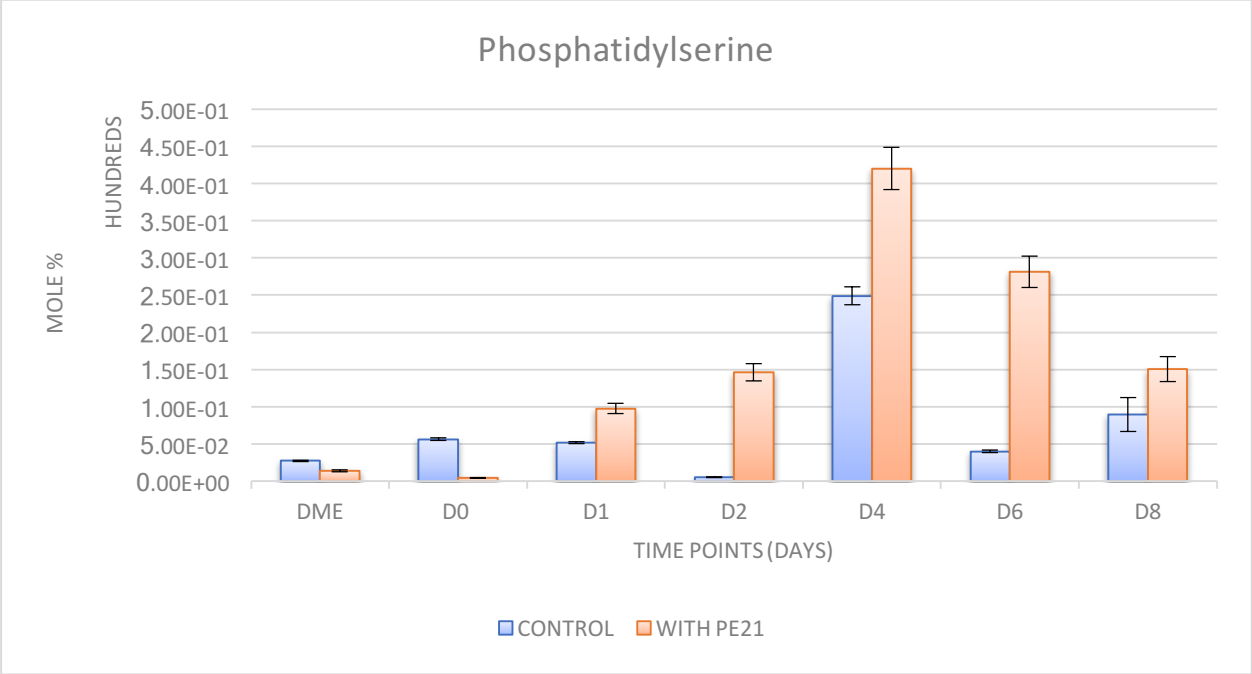

Figure 13. Mean percentage values of Triacylglycerol relative to the whole lipidome for wild-type control compared to wild-type treated with PE21, as measured by the developed LC-MS/MS method at 7 time points. Error bars presented are from Table 2 and Table 4. For growth conditions of control and treated with 21 refer to Materials and Methods in chapter 3 Legend: DME stands for day mid-exponential. D stands for day and numeric values represent days of growth. PE21 stands for plant extract 21.

3.3-1 Results and discussion of section 3.3.

Using the optimized LC-MS/MS method developed in Chapter 2 of this thesis, the effects of plant extract 21 on the lipidome of *Saccharomyces cerevisiae* is analyzed in this chapter. The findings of the study show that plant extract 21 considerably remodels the lipidome of *Saccharomyces cerevisiae*, thus the action of PE 21 should involve some aspects of the lipid metabolism pathways. Lipid metabolism pathways and inter-organelle transport in mitochondria, the endoplasmic reticulum (ER), lipid droplets (LD) and peroxisomes of the yeast S. cerevisiae involve numerous steps, each catalyzed by a known enzyme or several enzymes as it is illustrated in Figure 3.

The result in Figure 4 shows that PE21 increases the concentration of phosphatidylcholine (PC) late in life of chronologically aging yeast. PE 21 is involved in at least two different pathways to increase PC concentration in yeast when treated with PE21. These pathways are shown in Figure 3 as follows: 1) an increase of Cho2p and/or Opi3p concentration/activity; or 2) a decrease of Taz1p concentration/activity. Current studies in the Titorenko lab are addressing a hypothesis that the late-in-life increase of PC concentration plays an essential role in aging delay by PE21. These studies are aimed at answering the following 3 questions: 1) Will a mutation eliminating one of the enzymes involved in PC synthesis (such as Cho2p or Opi3p; Figure 3) impair the aging-delaying effect of PE21? 2) Will a mutation eliminating the enzyme involved in PC consumption (such as Taz1p; Figure 3) enhance the aging-delaying effect of PE21? 3) What are the concentrations of PC and other lipid classes in cells of each of these mutant strains?

Figures 5 and 7 shows that PE21 has a random effect on the concentration of sphingosine and ceramide lipid classes of yeast. Unlike other lipid classes, there is no an obvious trend of increasing or decreasing concentration of these two lipid classes as yeast cells age chronologically. Therefore, to conclude anything about possible role of PE21 on the remodeling of these two lipid classes more studies must be carried out on the mutant strains related to metabolism of these two lipid classes.

The result in Figure 6 shows that PE21 decreases the concentration of the neutral lipid triacylglycerol (TAG) in chronologically aging yeast. There are three possible ways of decreasing the concentration of TAG in yeast treated with PE21 (Figure 3). These different ways are as follows: 1) a decrease in the concentration/activity of enzymes Are1p and/or Are2p, 2) a decrease in the concentration/activity of enzymes Dga1p and/or Are2p or 3) an increase in the concentration/activity of enzymes Tgl1p, Tgl3p, Tgl4p and/or Tgl5p (Figure 3). Current studies in the Titorenko lab on various yeast mutant strains impaired in lipid metabolism are addressing the importance of the observed decreased TAG concentration in the aging-delaying ability of PE21 by answering the following 3 questions: 1) Will a mutation eliminating Are1p, Are2p, Dga1p or Lro1p enhance the aging-delaying effect of PE21? 2) Will a mutation eliminating Tgl1p, Tgl3p, Tgl4p or Tgl5p impair the aging-delaying effect of PE21? 3) What will be the concentrations of TAG and other lipid classes in cells of each of these mutant strains?

The result in Figure 8 shows that PE21 decreases the concentration of cardiolipin in the chronologically aging yeast. CL concentration can be decreased in yeast treated

with PE21 through a decrease in the concentration or activity of any of the following enzymes (Figure 1): Ups1p, Tam41p, Pgs1p, Gep4p, Crd1p, Cld1p or Taz1p. Current studies in the Titorenko lab on various yeast mutant strains impaired in lipid metabolism are addressing the importance of the early-in-life decreased CL concentration in the aging-delaying ability of PE21 by answering the following 2 questions: 1) Will a mutation eliminating an enzyme involved in CL synthesis (such as Ups1p, Tam41p, Pgs1p, Gep4p, Crd1p, Cld1p or Taz1p) enhance the aging-delaying effect of PE21? 2) What would be the concentrations of CL and other lipid classes in cells of each of these mutant strains?

Figure 9 shows that PE21 markedly decreases the concentration of free fatty acids. Since the concentration of TAG is also decreased by PE21, we can exclude the effect of PE21 on the enzymes Tg1p, Tg3p, Tg4p and Tg5p (all of which reside in lipid droplets). Most likely, PE21 directs the conversion of free fatty acids into different classes of phospholipids such as PE, PC, PI, PS and PG. Indeed, the results show that PE21 increases the concentration of these lipid classes. To further investigate a possible mechanism through which PE21 decreases the concentration of free fatty acids, many mutant strains impaired in the metabolism of free fatty acids are currently investigated in the Titorenko lab.

The result in Figure 10 shows that PE21 increases the concentration of phosphatidylethanolamine (PE) in chronologically aging yeast. PE21 can increase the concentration of PE in two different ways (Figure 1). The ways include the following: 1) an increase in the concentration or activity of Psd1p or 2) a decrease in the concentration

or activity of Cho2p and/or Opi3p. Current studies in the Titorenko lab on various yeast mutant strains impaired in lipid metabolism are addressing the importance of the observed increased PE concentration in the aging-delaying ability of PE21 by answering the following 3 questions: 1) Will a mutation eliminating an enzyme involved in PE synthesis (such as Psd1p) eliminate the aging-delaying effect of PE21? 2) Will a mutation eliminating an enzyme involved in PE consumption (such as Cho2p or Opi3p) enhance the aging-delaying effect of PE21? 3) What would be the concentrations of PE and other lipid classes in cells of each of these mutant strains?

The result in Figure 11 shows that PE21 does not have consistent effect on the concentrations of phosphatidylglycerol (PG), ceramides and sphingosine (Figures 5 and 7). To further narrow down the effect of PE21 on the concentration of PG, more studies need be done on mutant strains impaired in PG metabolism in *Saccharomyces cerevisiae*.

The result in Figure 12 shows that PE21 increases the concentration of phosphatidylinositol (PI). PE21 can only increase the concentration of PI by increasing the concentration and/or activity of Cds1p and/or Pis1p (Figure 3). Current studies in the Titorenko lab on various yeast mutant strains impaired in lipid metabolism are addressing the importance of the PE21-dependent increase of PI by answering the following 2 questions: 1) Will mutations eliminating enzymes involved in PI synthesis (such as Cds1p or Pis1p) eliminate the aging-delaying effect of PE21? 2) What will be the concentrations of PI and other lipid classes in cells of each of these mutant strains?

Figure 13 shows that PE21 increases the concentration of phosphatidylserine (PS) in chronologically aging yeast. PE21 can increase PS concentration in two different ways.

These two ways are as follows: 1) an increase in the concentration or activity of Cds1p and/or Cho1p or 2) a decrease in the concentration or activity of Psd1p (Figure 3). Current studies in the Titorenko lab on various yeast mutant strains impaired in lipid metabolism are addressing the importance of the PE21-dependent increase in PS concentration by answering the following three questions: 1) Will mutations eliminating enzymes involved in PS synthesis (such as Cds1p or Cho1p) eliminate the aging-delaying effect of PE21? 2) Will a mutation eliminating Psd1p, an enzyme involved in PS consumption, enhance the aging-delaying effect of PE21? 3) What would be the concentrations of PS and other lipid classes in cells of each of these mutant strains?

In sum, our findings indicate that PE21 remodels the lipid composition of wild-type *Saccharomyces cerevisiae*. Specifically, PE21 increases the concentration of PI, PS, PG, PC and PE. Because PA is the precursor for all phospholipids, PE21 is likely to somehow intensify the flow of PA into the endoplasmic reticulum and/or mitochondria where the synthesis of these lipids occurs.

TAG synthesis occurs in the endoplasmic reticulum, thus the observed PE21-dependent decrease in TAG concentration suggests that PE21 may decrease the flow of PA into the endoplasmic reticulum. Previous studies in the Titorenko lab on a decrease in CL concentration have revealed that such change in CL abundance can change mitochondrial functionality [124]. Specifically, it has been demonstrated that a decline in CL concentration can stimulate mitochondrial respiration and membrane potential and also to decrease mitochondrial production of reactive oxygen species [124].

Current studies in the Titorenko lab are focused on analysis of possible mechanisms through which PE21 causes such remodeling of yeast lipidome. One

hypothesis is that PE21 may increase yeast chronological lifespan by decreasing the concentration of free fatty acids. Such decline in the abundance of free fatty acid may decrease the rate of liponecrosis, which is a programmed cell death elicited in response to elevated intracellular concentrations of free fatty acids. This mechanism is discussed in more details in Section 3.4.

3.4 Tables and figures of various lipid classes for wild-type and 4 mutant strains impaired in lipid metabolism when the cells were grown without PE21

LIPID CLASS	DME	D0	D1	D2	D4	D6	D8
PC	1.14E+00	8.78E+00	5.87E+00	5.28E-01	8.47E-01	7.54E-01	5.15E-01
SO	7.08E+01	3.39E+01	4.11E+01	2.27E+00	2.68E+01	4.79E+01	5.71E+01
TG	6.64E+00	1.01E+01	1.89E+01	4.65E-01	2.16E+01	2.64E+01	1.47E+01
CER	1.90E+00	5.80E+00	4.00E+00	1.82E-01	3.81E+00	7.71E-01	4.56E+00
CL	6.79E-01	1.44E+00	1.16E+00	6.79E-02	1.76E+00	1.25E+00	1.59E+00
FA	4.04E+00	1.67E+01	1.02E+01	5.53E-01	6.55E+00	8.41E+00	6.46E+00
PE	4.52E+00	6.45E+00	4.69E+00	8.68E+01	5.16E+00	2.44E+00	2.78E+00
PG	2.23E-02	4.55E-01	2.83E-01	1.41E-02	4.97E-02	1.94E-02	6.43E-03
PI	1.30E+00	3.84E+00	1.96E+00	7.90E-02	6.61E-01	4.31E-01	5.57E-01
PS	2.72E+00	5.62E+00	5.18E+00	5.17E-01	2.49E+01	3.97E+00	8.95E+00

Table 30. Mean percentage value of wild type lipid classes identified by developed LC-MS/MS method when grown without PE21. The values are the mean (% of whole lipidome) of two experiments for the wild type strain taken at 7 time points (DME, D0, D1, D2, D4, D6, D8). Legend: DME stands for day mid-exponential. D stands for day and numeric values represent days of growth. Lipid class: Phosphatidylcholine, sphingosine, Triacylglycerol, Ceramide, Cardiolipin, Free Fatty Acid, Phosphatidylethanolamine, Phosphatidylglycerol, Phosphatidylinositol, Phosphatidylserine.

LIPID CLASS	DME	D0	D1	D2	D4	D6	D8
PC	0.0505935	0.4535511	0.2582072	0.2449733	0.0637053	0.129691737	0.2110605
SO	3.4121109	1.863243	2.4070247	0.1772678	1.849794	3.119837559	3.7796413
TG	0.3252402	0.6886521	1.203741	0.034841	1.5112929	1.418779605	1.7323119
CER	0.0440361	0.2210655	0.1673791	0.008917	0.1361826	0.037539913	0.1824743
CL	0.0421655	0.0752303	0.0597828	0.0037301	0.1165151	0.057574775	0.0358539
FA	0.2574151	1.1103996	0.7549778	0.0495599	0.5000848	0.681187833	0.2913811
PE	0.1757019	0.1895866	0.173524	6.0007662	0.2023507	0.066542081	0.9180897
PG	0.0013712	0.0198524	0.0145072	0.001113	0.003684	0.000961483	0.0045493
PI	0.0569928	0.1625117	0.073704	0.0041955	0.0373794	0.010241971	0.1437976
PS	0.0645074	0.1489661	0.1346236	0.0235393	1.2171991	0.162474513	2.3065374

Table 31. Standard deviation of wild type lipid classes identified by developed LC-MS/MS method when grown without PE21. The values are calculated as the sample standard deviation (±%) of two experiments for the wild type strain taken at 7 time points (DME, D0, D1, D2, D4, D6, D8). Sample standard deviation was used because the sample is biological. Legend: DME stands for day mid-exponential. D stands for day and numeric values represent days of growth. Lipid class: Phosphatidylcholine, Sphingosine, Triacylglycerol, Ceramide, Cardiolipin, Free Fatty Acid, Phosphatidylethanolamine, Phosphatidylglycerol, Phosphatidylinositol, Phosphatidylserine.

LIPID CLASS	DME	D0	D1	D2	D4	D6	D8
PC	3.83E-01	2.00E+00	7.33E-01	1.37E+00	7.91E-01	2.96E-01	6.64E-02
SO	6.42E+01	4.80E+01	6.79E+01	6.26E+01	4.83E+01	6.90E+01	6.96E+01
TG	1.14E+01	1.89E+01	4.65E-01	2.16E+01	2.64E+01	1.47E+01	1.04E+01
CER	3.59E-01	3.76E+00	1.63E+00	2.47E+00	3.87E+00	2.56E+00	2.91E+00
CL	2.25E-01	6.68E-01	2.88E-01	6.31E-01	1.02E+00	6.55E-01	3.41E-01
FA	1.26E+01	2.02E+01	6.78E+00	6.73E+00	1.13E+01	8.90E+00	4.78E+00
PE	7.92E-01	1.94E+00	5.40E-01	8.76E-01	1.42E+00	7.65E-01	3.80E-01
PG	5.69E-03	2.45E-02	8.35E-03	2.38E-02	3.71E-02	1.09E-02	0.00E+00
PI	1.43E+00	2.12E+00	9.73E-01	6.76E-01	1.06E+00	4.03E-01	2.54E-01
PS	1.46E+00	1.91E+00	6.13E+00	5.13E+00	7.98E+00	4.36E+00	5.07E+00

Table 152. Mean percentage values for mutant strain 8 lipid classes identified by the developed LC-MS/MS method in cells grown without PE21. The values are the mean (% of whole lipidome) of two experiments for the wild type strain taken at 7 time points (DME, D0, D1, D2, D4, D6, D8). Legend: DME stands for day mid-exponential. D stands for day and numeric values represent days of growth. Lipid class: Phosphatidylcholine, sphingosine, Triacylglycerol, Ceramide, Cardiolipin, Free Fatty Acid, Phosphatidylethanolamine, Phosphatidylglycerol, Phosphatidylinositol, Phosphatidylserine. Mutant strain 8 is mutated in gene *tgl3* and it is a deletion mutation. The gene is expressed in lipid drops and it is responsible for breakdown of triacylglycerol.

LIPID CLASS	DME	D0	D1	D2	D4	D6	D8
PC	4.40E-02	1.96E-01	9.01E-02	1.57E-01	1.24E-01	3.39E-02	8.16E-03
SO	6.84E+00	7.96E+00	9.50E+00	6.66E+00	6.34E+00	8.48E+00	7.41E+00
TG	1.40E+00	1.57E+00	1.17E+00	1.31E+00	2.58E+00	5.86E-01	1.28E+00
CER	3.32E-02	4.16E-01	1.91E-01	2.44E-01	2.85E-01	2.99E-01	2.69E-01
CL	2.96E-02	8.77E-02	3.06E-02	9.92E-02	1.42E-01	8.06E-02	4.19E-02
FA	1.65E+00	2.82E+00	8.34E-01	1.18E+00	1.11E+00	1.32E+00	7.94E-01
PE	1.24E-01	1.91E-01	9.43E-02	1.38E-01	1.87E-01	1.07E-01	6.65E-02
PG	7.31E-04	2.57E-03	6.69E-04	2.35E-03	2.50E-03	1.28E-03	0.00E+00
PI	1.88E-01	2.60E-01	1.44E-01	8.31E-02	1.57E-01	6.33E-02	3.13E-02
PS	1.53E-01	2.35E-01	4.52E-01	5.37E-01	5.88E-01	2.94E-01	6.22E-01

Table 163. Standard deviation values for mutant strain 8 lipid classes identified by the developed LC-MS/MS method in cells grown without PE21. The values are calculated as the sample standard deviation (±%) of two experiments for the wild type strain taken at 7 time points (DME, D0, D1, D2, D4, D6, D8). Sample standard deviation was used because the sample is biological. Legend: DME stands for day mid-exponential. D stands for day and numeric values represent days of growth. Lipid class: Phosphatidylcholine, Sphingosine, Triacylglycerol, Ceramide, Cardiolipin, Free Fatty Acid, Phosphatidylethanolamine, Phosphatidylglycerol, Phosphatidylinositol, Phosphatidylserine. Mutant strain 8 is mutated in gene *tgl3* and it is a deletion mutation. The gene is expressed in lipid drops and it is responsible for breakdown of triacylglycerol.

LIPID CLASS	DME	D0	D1	D2	D4	D6	D8
PC	1.27E+00	2.94E+00	5.06E+00	1.88E+00	1.13E+00	1.47E+00	2.63E-01
SO	5.13E+01	2.96E+01	3.38E+01	4.01E+01	2.17E+01	5.93E+01	5.95E+01
TG	2.07E+01	3.58E+01	1.89E+01	1.53E+01	2.16E+01	2.64E+01	1.85E+01
CER	3.61E+00	3.60E+00	5.66E+00	2.70E+00	3.57E+00	4.31E+00	3.63E+00
CL	2.10E-01	2.52E-01	1.32E+00	5.30E-01	8.47E-01	9.99E-01	1.54E+00
FA	4.04E+00	9.64E+00	1.02E+01	5.53E-01	6.55E+00	8.41E+00	6.02E+00
PE	4.64E+00	3.03E+00	7.44E+00	3.03E+00	3.17E+00	2.16E+00	8.93E-01
PG	3.77E-02	6.41E-02	1.38E-01	3.11E-02	3.82E-02	4.71E-02	1.56E-02
PI	2.74E+00	3.57E+00	5.02E+00	2.39E+00	1.94E+00	1.38E+00	6.48E-01
PS	2.47E+00	3.33E+00	5.25E+00	1.66E+01	3.17E+01	3.31E+00	1.53E+00

Table 174. Mean percentage values for mutant strain 9 lipid classes identified by the developed LC-MS/MS method in cells grown without PE21. The values are the mean (% of whole lipidome) of two experiments for the wild type strain taken at 7 time points (DME, D0, D1, D2, D4, D6, D8). Legend: DME stands for day mid-exponential. D stands for day and numeric values represent days of growth. Lipid class: Phosphatidylcholine, sphingosine, Triacylglycerol, Ceramide, Cardiolipin, Free Fatty Acid, Phosphatidylethanolamine, Phosphatidylglycerol, Phosphatidylinositol, Phosphatidylserine. Mutant strain 9 is mutated in gene *tgl1* and it is a deletion mutation. The gene is expressed in lipid drops and it is responsible for breakdown of triacylglycerol.

LIPID CLASS	DME	D0	D1	D2	D4	D6	D8
PC	1.46E-01	3.37E-01	7.07E-01	2.47E-01	1.39E-01	1.45E-01	3.46E-02
SO	4.22E+00	4.91E+00	3.88E+00	5.95E+00	3.79E+00	6.80E+00	7.81E+00
TG	3.43E+00	5.00E+00	1.54E+00	2.67E+00	3.58E+00	1.41E+00	1.97E+00
CER	4.00E-01	3.77E-01	5.93E-01	3.16E-01	3.52E-01	4.77E-01	3.81E-01
CL	2.06E-02	2.68E-02	1.74E-01	6.08E-02	8.33E-02	1.75E-01	2.15E-01
FA	8.44E-01	1.51E+00	3.25E+00	1.47E+00	1.48E+00	1.80E+00	9.99E-01
PE	6.10E-01	4.24E-01	1.23E+00	4.23E-01	4.70E-01	3.40E-01	1.48E-01
PG	4.17E-03	4.73E-03	1.19E-02	2.10E-03	4.00E-03	5.50E-03	1.63E-03
PI	3.38E-01	4.10E-01	6.17E-01	3.14E-01	2.07E-01	2.41E-01	1.02E-01
PS	2.54E-01	3.25E-01	5.15E-01	1.43E+00	2.41E+00	1.99E-01	1.19E-01

Table 185. Standard deviation values for mutant strain 9 lipid classes identified by the developed LC-MS/MS method in cells grown without PE21. The values are calculated as the sample standard deviation (±%) of two experiments for the wild type strain taken at 7 time points (DME, D0, D1, D2, D4, D6, D8). Sample standard deviation was used because the sample is biological. Legend: DME stands for day mid-exponential. D stands for day and numeric values represent days of growth. Lipid class: Phosphatidylcholine, Sphingosine, Triacylglycerol, Ceramide, Cardiolipin, Free Fatty Acid, Phosphatidylethanolamine, Phosphatidylglycerol, Phosphatidylinositol, Phosphatidylserine. Mutant strain 9 is mutated in gene *tgl1* and it is a deletion mutation. The gene is expressed in lipid drops and it is responsible for breakdown of triacylglycerol.

LIPID CLASS	DME	D0	D1	D2	D4	D6	D8
PC	1.17E+00	1.61E+00	1.33E+00	1.29E+00	1.48E-01	1.45E-01	1.45E-01
SO	2.92E+01	6.63E+00	7.57E+00	1.50E+01	2.51E+01	2.59E+01	2.02E+01
TG	7.08E+00	1.01E+01	1.89E+01	4.65E-01	2.16E+01	2.64E+01	3.89E+01
CER	4.72E+00	2.38E+00	1.98E+00	1.76E+00	4.89E+00	4.89E+00	5.18E+00
CL	1.01E+00	8.91E-01	1.19E+00	1.04E+00	1.83E+00	1.79E+00	7.88E+00
FA	4.04E+00	9.63E+00	8.22E+00	5.53E-01	6.55E+00	8.41E+00	6.46E+00
PE	3.47E+00	2.85E+00	2.53E+00	2.06E+00	9.48E-01	9.69E-01	5.63E-01
PG	1.11E-02	4.18E-02	4.45E-02	5.50E-02	1.13E-02	1.12E-02	0.00E+00
PI	1.22E+00	7.44E-01	6.02E-01	4.27E-01	2.43E-01	2.47E-01	1.74E-01
PS	3.49E+01	6.49E+01	7.29E+01	6.72E+01	3.49E+01	3.49E+01	8.33E+00

Table 196. **Mean percentage values for mutant strain 87 lipid classes identified by the developed LC-MS/MS method in cells grown without PE21.** The values are the mean (% of whole lipidome) of two experiments for the wild type strain taken at 7 time points (DME, D0, D1, D2, D4, D6, D8). Legend: DME stands for day mid-exponential. D stands for day and numeric values represent days of growth. Lipid class: Phosphatidylcholine, sphingosine, Triacylglycerol, Ceramide, Cardiolipin, Free Fatty Acid, Phosphatidylethanolamine, Phosphatidylglycerol, Phosphatidylinositol, Phosphatidylserine. Mutant strain 87 is mutated in gene *tgl4* and it is a deletion mutation. The gene is expressed in lipid drops and it is responsible for breakdown of triacylglycerol.

LIPID CLASS	DME	D0	D1	D2	D4	D6	D8
PC	1.15E-01	2.54E-01	1.98E-01	1.91E-01	1.45E-02	1.79E-02	2.15E-02
SO	3.84E+00	9.84E-01	1.06E+00	1.48E+00	3.73E+00	2.55E+00	3.35E+00
TG	7.53E-01	1.11E+00	3.55E-01	1.64E-01	2.36E+00	2.76E+00	5.11E+00
CER	4.07E-01	2.35E-01	2.20E-01	2.06E-01	5.99E-01	5.99E-01	5.11E-01
CL	1.41E-01	1.25E-01	1.17E-01	1.46E-01	2.40E-01	2.97E-01	1.31E+00
FA	2.28E+00	1.68E+00	1.36E+00	9.07E-01	1.89E+00	1.35E+00	1.16E+00
PE	5.15E-01	3.74E-01	3.32E-01	2.36E-01	1.49E-01	1.19E-01	9.85E-02
PG	1.17E-03	4.89E-03	5.47E-03	5.43E-03	1.38E-03	1.31E-03	0.00E+00
PI	1.20E-01	9.77E-02	6.91E-02	7.47E-02	3.40E-02	2.84E-02	3.04E-02
PS	3.29E+00	5.80E+00	1.01E+01	5.09E+00	3.50E+00	3.27E+00	8.17E-01

Table 207. Standard deviation values for mutant strain 87 lipid classes identified by the developed LC-MS/MS method in cells grown without PE21. The values are calculated as the sample standard deviation (±%) of two experiments for the wild type strain taken at 7 time points (DME, D0, D1, D2, D4, D6, D8). Sample standard deviation was used because the sample is biological. Legend: DME stands for day mid-exponential. D stands for day and numeric values represent days of growth. Lipid class: Phosphatidylcholine, Sphingosine, Triacylglycerol, Ceramide, Cardiolipin, Free Fatty Acid, Phosphatidylethanolamine, Phosphatidylglycerol, Phosphatidylinositol, Phosphatidylserine. Mutant strain 87 is mutated in gene *tgl4* and it is a deletion mutation. The gene is expressed in lipid drops and it is responsible for breakdown of triacylglycerol.

LIPID CLASS	DME	D0	D1	D2	D4	D6	D8
PC	6.57E-01	1.79E+00	2.38E+00	3.11E+00	6.70E-01	5.65E-01	8.11E-01
SO	4.46E+01	2.69E+01	7.59E+00	1.98E+01	3.94E+01	3.75E+01	4.27E+01
TG	2.27E+01	1.01E+01	1.89E+01	4.65E-01	2.16E+01	2.64E+01	1.47E+01
CER	8.00E-01	1.48E+00	1.65E+00	2.90E+00	4.12E+00	6.34E+00	6.18E+00
CL	2.58E+00	3.21E+01	1.98E+01	9.42E+00	1.96E+00	3.93E+00	9.40E+00
FA	4.04E+00	4.07E+00	5.98E+00	5.53E-01	6.55E+00	8.41E+00	6.46E+00
PE	2.22E+00	1.93E+00	3.69E+00	3.51E+00	1.69E+00	1.57E+00	2.27E+00
PG	0.00E+00	2.90E-02	5.64E-02	3.97E-02	1.59E-02	1.33E-02	2.61E-02
PI	2.21E+00	1.70E+00	1.97E+00	2.91E+00	1.67E+00	1.17E+00	1.43E+00
PS	1.38E+01	1.39E+01	4.53E+01	3.69E+01	2.77E+01	2.46E+01	2.02E+01

Table 218. Mean percentage value of mutant strain 88 lipid classes identified by developed LC-MS/MS method when grown without PE21. The values are the mean (% of whole lipidome) of two experiments for the wild type strain taken at 7 time points (DME, D0, D1, D2, D4, D6, D8). Legend: DME stands for day mid-exponential. D stands for day and numeric values represent days of growth. Lipid class: Phosphatidylcholine, sphingosine, Triacylglycerol, Ceramide, Cardiolipin, Free Fatty Acid, Phosphatidylethanolamine, Phosphatidylglycerol, Phosphatidylinositol, Phosphatidylserine. Mutant strain 88 is mutated in gene *tgl5* and it is a deletion mutation. The gene is expressed in lipid drops and it is responsible for breakdown of triacylglycerol.

LIPID CLASS	DME	D0	D1	D2	D4	D6	D8
PC	1.09E-01	2.20E-01	3.53E-01	5.16E-01	6.59E-02	6.01E-02	1.20E-01
SO	6.63E+00	3.09E+00	7.46E-01	2.60E+00	6.20E+00	4.30E+00	5.61E+00
TG	2.05E+00	9.60E-01	9.70E-01	1.11E+00	2.02E-01	1.06E+00	2.51E-01
CER	5.90E-02	1.82E-01	1.73E-01	2.68E-01	5.29E-01	5.47E-01	5.72E-01
CL	2.13E-01	5.60E+00	2.93E+00	1.40E+00	2.58E-01	4.84E-01	1.08E+00
FA	5.01E-01	4.66E-01	1.05E+00	1.16E+00	2.39E+00	2.43E+00	1.20E+00
PE	2.91E-01	2.70E-01	5.17E-01	5.51E-01	1.94E-01	2.20E-01	2.41E-01
PG	0.00E+00	2.14E-03	6.59E-03	3.43E-03	2.04E-03	1.48E-03	2.09E-03
PI	2.35E-01	2.24E-01	2.75E-01	4.06E-01	1.64E-01	1.25E-01	2.49E-01
PS	1.45E+00	1.71E+00	3.05E+00	3.65E+00	2.90E+00	1.97E+00	1.87E+00

Table 3922. Standard deviation of mutant strain 88 lipid classes identified by developed LC-MS/MS method when grown without PE21. The values are calculated as the sample standard deviation (±%) of two experiments for the wild type strain taken at 7 time points (DME, D0, D1, D2, D4, D6, D8). Sample standard deviation was used because the sample is biological. Legend: DME stands for day mid-exponential. D stands for day and numeric values represent days of growth. Lipid class: Phosphatidylcholine, Sphingosine, Triacylglycerol, Ceramide, Cardiolipin, Free Fatty Acid, Phosphatidylethanolamine, Phosphatidylglycerol, Phosphatidylinositol, Phosphatidylserine. Mutant strain 88 is mutated in gene *tgl5* and it is a deletion mutation. The gene is expressed in lipid drops and it is responsible for breakdown of triacylglycerol.

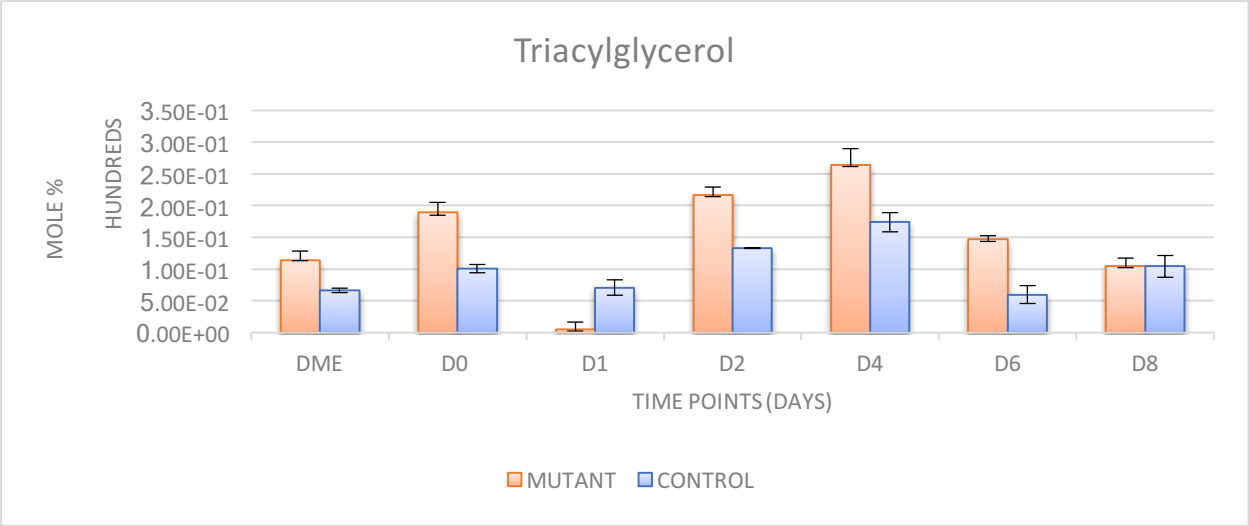

Figure 14. The mean mole % values of Triacylglycerol (TG) relative to the whole lipidome for wild-type strain compared to mutant strain 8 in cells grown without PE21. TG species were measured by the developed LC-MS/MS method at 7 time points. Error bars presented are from table 33 and mole % values are from table 32 for the mutant and tables 30 and 31 for wild type. For growth conditions of control and treated with 21 refer to Materials and Methods in chapter 3. Legend:DME stands for day mid-exponential. D stands for day and numeric values represent days of growth. PE21 stands for plant extract 21. Mutant strain 8 is mutated in gene *tgl3* and it is a deletion mutation. The gene is expressed in lipid drops and it is responsible for breakdown of triacylglycerol. Control stands for wild type *Saccharomyces cerevisiae*. The mean and n value of standard deviation is from 2 experiments.

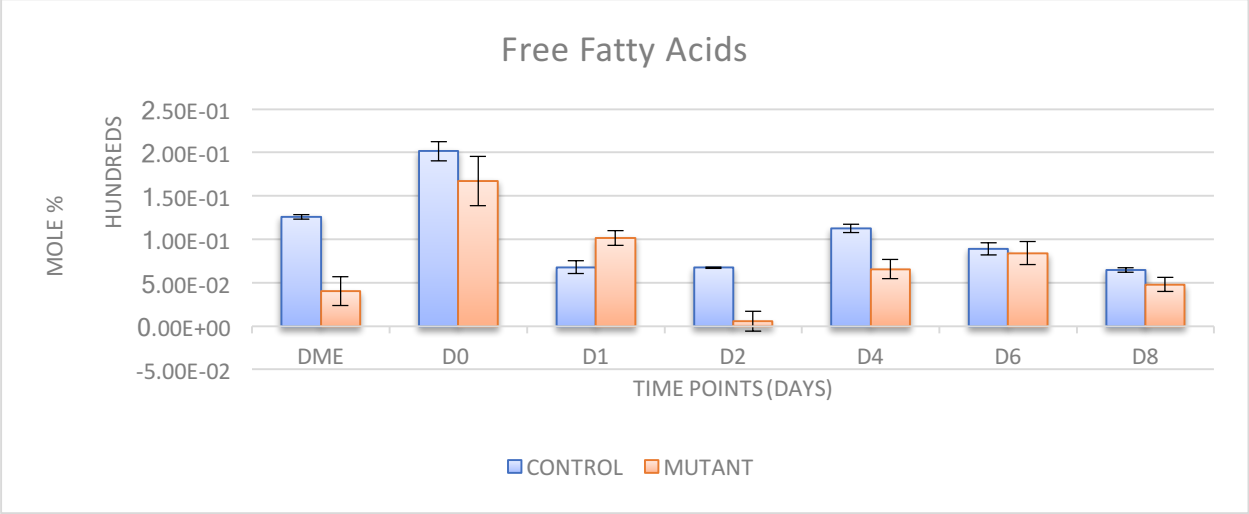

Figure 15. The mean mole % values of Free fatty acid (FFA) relative to the whole lipidome for wild-type strain compared to mutant strain 8 in cells grown without PE21. FFA species were measured by the developed LC-MS/MS method at 7 time points. Error bars presented are from table 33 and mole % values are from table 32 for the mutant and tables 30 and 31 for wild type. For growth conditions of control and treated with 21 refer to Materials and Methods in chapter 3. Legend:DME stands for day mid-exponential. D stands for day and numeric values represent days of growth. PE21 stands for plant extract 21. Mutant strain 8 is mutated in gene *tgl3* and it is a deletion mutation. The gene is expressed in lipid drops and it is responsible for breakdown of triacylglycerol. Control stands for wild type *Saccharomyces cerevisiae*. The mean and n value of standard deviation is from 2 experiments.

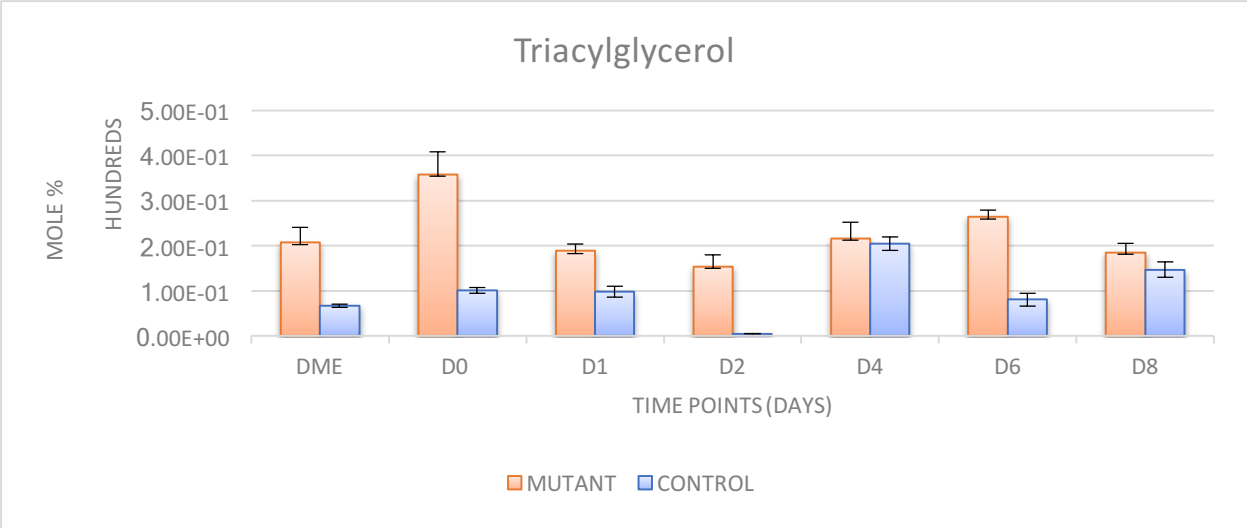

Figure 16. The mean mole % values of Triacylglycerol (TG) relative to the whole lipidome for wild-type strain compared to mutant strain 9 when in cells grown without PE21. TG species were measured by the developed LC-MS/MS method at 7 time points. Error bars presented are from table 35 and mole % values are from table 34 for the mutant and tables 30 and 31 for wild type. For growth conditions of control and treated with 21 refer to Materials and Methods in chapter 3. Legend: DME stands for day mid-exponential. D stands for day and numeric values represent days of growth. PE21 stands for plant extract 21. Mutant strain 9 is mutated in gene *tgl1* and it is a deletion mutation. The gene is expressed in lipid drops and it is responsible for breakdown of triacylglycerol. Control stands for wild type *Saccharomyces cerevisiae*. The mean and n value of standard deviation is from 2 experiments.

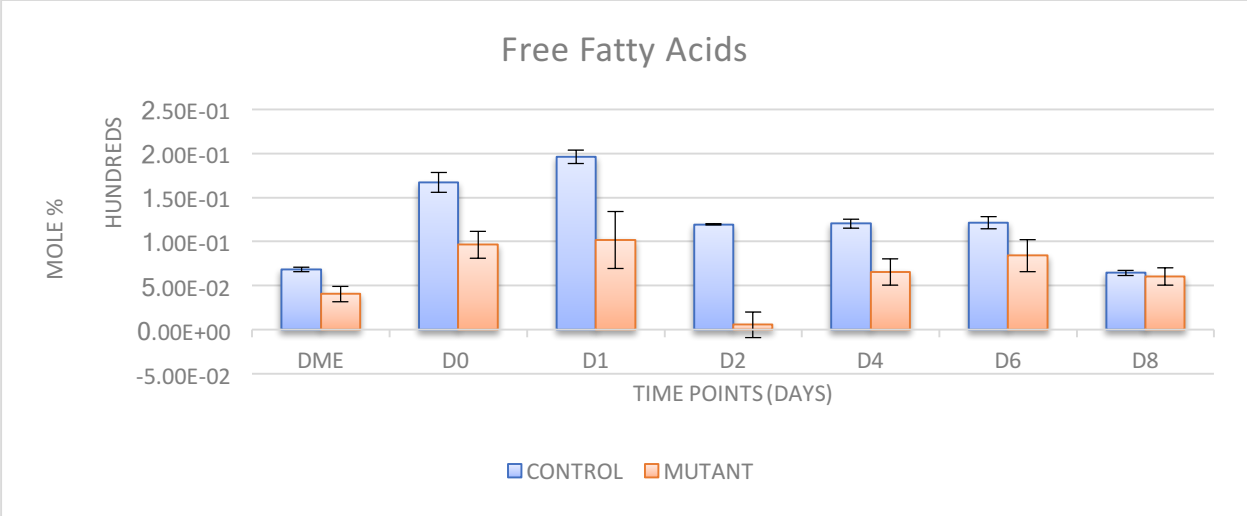

Figure 17. The mean mole % values of Free fatty acids (FFA) relative to the whole lipidome for wild-type strain compared to mutant strain 9 in cells grown without PE21. FFA species were measured by the developed LC-MS/MS method at 7 time points. Error bars presented are from table 35 and mole % values are from table 34 for the mutant and tables 30 and 31 for wild type. For growth conditions of control and treated with 21 refer to Materials and Methods in chapter 3. Legend:DME stands for day mid-exponential. D stands for day and numeric values represent days of growth. PE21 stands for plant extract 21. Mutant strain 9 is mutated in gene *tgl1* and it is a deletion mutation. The gene is expressed in lipid drops and it is responsible for breakdown of triacylglycerol. Control stands for wild type *Saccharomyces cerevisiae*. The mean and n value of standard deviation is from 2 experiments.

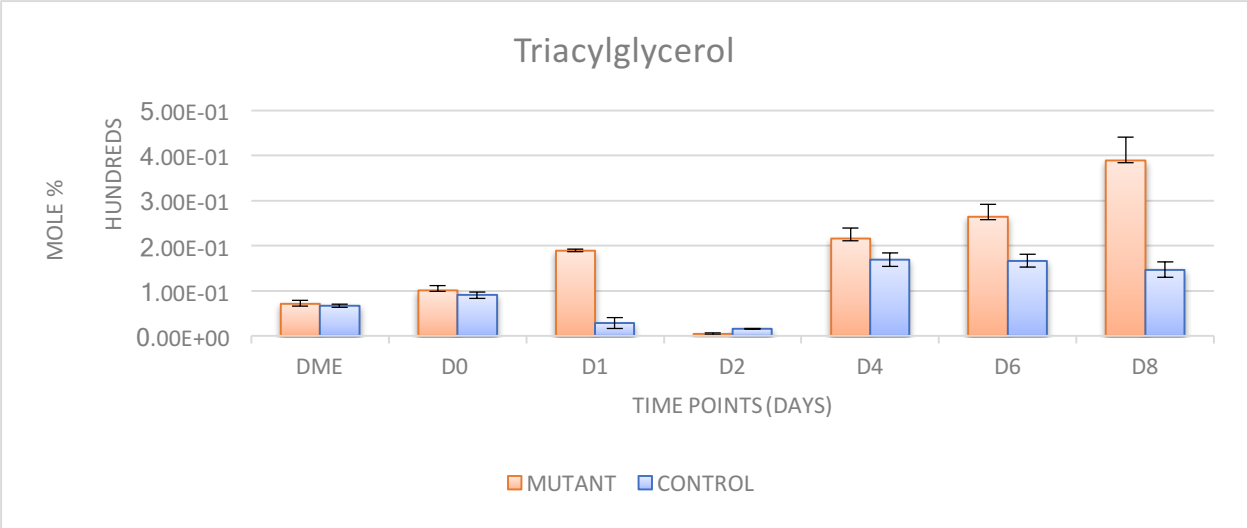

Figure 18. The mean mole % values of Triacylglycerol (TG) relative to the whole lipidome for wild-type strain compared to mutant strain 87 in cells grown without PE21. TG species were measured by the developed LC-MS/MS method at 7 time points. Error bars presented are from table 37 and mole % values are from table 36 for the mutant and tables 30 and 31 for wild type. For growth conditions of control and treated with 21 refer to Materials and Methods in chapter 3. Legend:DME stands for day mid-exponential. D stands for day and numeric values represent days of growth. PE21 stands for plant extract 21. Mutant strain 87 is mutated in gene *tgl4* and it is a deletion mutation. The gene is expressed in lipid drops and it is responsible for breakdown of triacylglycerol. Control stands for wild type *Saccharomyces cerevisiae*. The mean and n value of standard deviation is from 2 experiments.

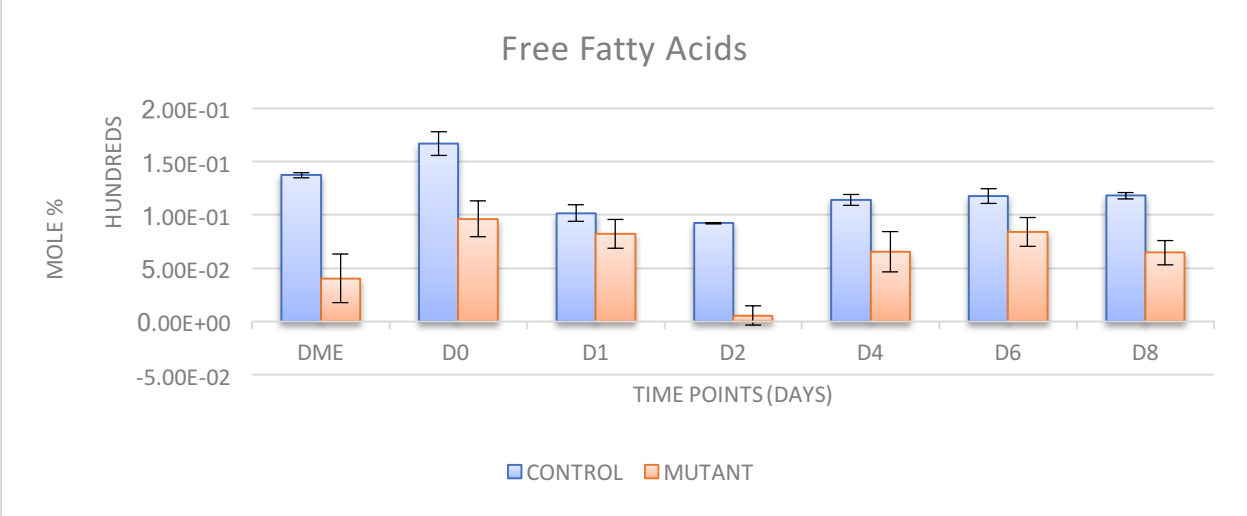

Figure 19. The mean mole % values of Free Fatty Acids (FFA) relative to the whole lipidome for wild-type strain compared to mutant strain 87 when in cells grown without PE21. FFA species were measured by the developed LC-MS/MS method at 7 time points. Error bars presented are from table 37 and mole % values are from table 36 for the mutant and tables 30 and 31 for wild type. For growth conditions of control and treated with 21 refer to Materials and Methods in chapter 3. Legend:DME stands for day mid-exponential. D stands for day and numeric values represent days of growth. PE21 stands for plant extract 21. Mutant strain 87 is mutated in gene *tgl4* and it is a deletion mutation. The gene is expressed in lipid drops and it is responsible for breakdown of triacylglycerol. Control stands for wild type *Saccharomyces cerevisiae*. The mean and n value of standard deviation is from 2 experiments.

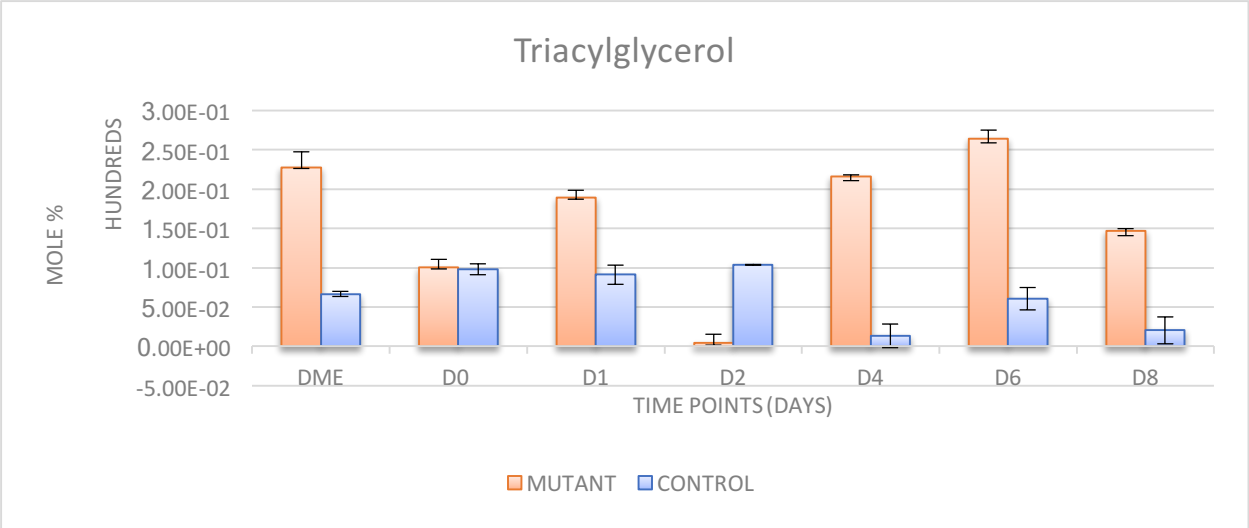

Figure 20. The mean mole % values of Triacylglycerol (TG) relative to the whole lipidome for wild-type strain compared to mutant strain 88 in cells were grown without PE21. TG species were measured by the developed LC-MS/MS method at 7 time points. Error bars presented are from table 39 and mole % values are from table 38 for the mutant and tables 30 and 31 for wild type. For growth conditions of control and treated with 21 refer to Materials and Methods in chapter 3. Legend:DME stands for day mid-exponential. D stands for day and numeric values represent days of growth. PE21 stands for plant extract 21. Mutant strain 88 is mutated in gene *tgl5* and it is a deletion mutation. The gene is expressed in lipid drops and it is responsible for breakdown of triacylglycerol. Control stands for wild type *Saccharomyces cerevisiae*. The mean and n value of standard deviation is from 2 experiments.

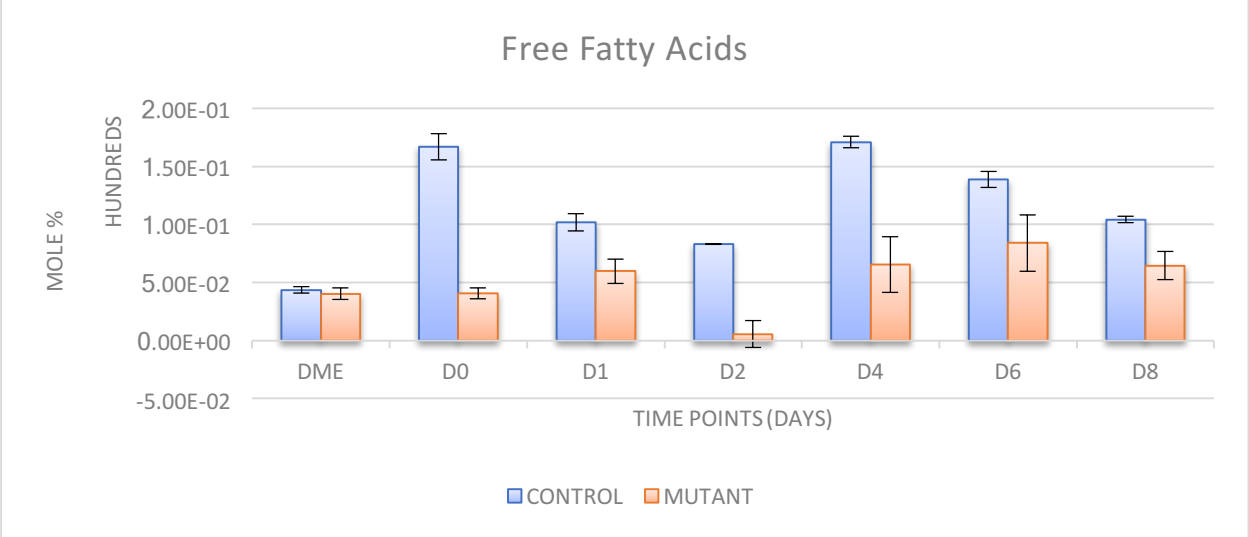

Figure 21. The mean mole % values of Free Fatty Acids (FFA) relative to the whole lipidome for wild-type strain compared to mutant strain 88 in cells e grown without PE21. FFA species were measured by the developed LC-MS/MS method at 7 time points. Error bars presented are from table 39 and mole % values are from table 38 for the mutant and tables 30 and 31 for wild type. For growth conditions of control and treated with 21 refer to Materials and Methods in chapter 3. Legend:DME stands for day mid-exponential. D stands for day and numeric values represent days of growth. PE21 stands for plant extract 21. Mutant strain 88 is mutated in gene *tgl5* and it is a deletion mutation. The gene is expressed in lipid drops and it is responsible for breakdown of triacylglycerol. Control stands for wild type *Saccharomyces cerevisiae*. The mean and n value of standard deviation is from 2 experiments.

3.5 Tables and figures of various lipid classes for wild-type and 4 mutant strains impaired in lipid metabolism when the cells were cultured with PE21

LIPID CLASS	DME	D0	D1	D2	D4	D6	D8
PC	1.81E+00	3.90E+00	3.26E+00	3.43E+00	1.87E+00	1.02E+00	7.85E-01
SO	6.71E+01	5.36E+01	3.21E+01	3.43E+01	3.33E+01	3.83E+01	5.58E+01
TG	2.03E+01	1.98E+01	2.67E+01	2.51E+01	7.80E+00	1.78E+01	1.25E+01
CER	2.94E+00	4.05E+00	4.36E+00	3.73E+00	2.09E+00	2.79E+00	3.11E+00
CL	1.93E-01	5.38E-01	5.41E-01	5.05E-01	5.53E-01	7.06E-01	6.11E-01
FA	1.32E+00	1.07E+00	1.46E+00	1.60E+00	6.40E-01	5.46E-01	9.93E-01
PE	5.49E+00	6.57E+00	1.07E+01	8.04E+00	6.70E+00	5.66E+00	3.96E+00
PG	1.10E-02	6.37E-02	2.03E-01	8.44E-02	6.23E-02	3.10E-02	0.00E+00
PI	2.38E+00	2.20E+00	3.57E+00	2.26E+00	1.34E+00	8.99E-01	7.90E-01
PS	1.37E+00	4.24E-01	9.75E+00	1.46E+01	4.20E+01	2.81E+01	1.50E+01

Table 40. Mean percentage value of wild type lipid classes identified by developed LC-MS/MS method when grown with PE21. The values are the mean (% of whole lipidome) of two experiments for the wild type strain taken at 7 time points (DME, D0, D1, D2, D4, D6, D8). Legend: DME stands for day mid-exponential. D stands for day and numeric values represent days of growth. Lipid class: Phosphatidylcholine, sphingosine, Triacylglycerol, Ceramide, Cardiolipin, Free Fatty Acid, Phosphatidylethanolamine, Phosphatidylglycerol, Phosphatidylinositol, Phosphatidylserine.

LIPID CLASS	DME	D0	D1	D2	D4	D6	D8
PC	1.81E+00	3.90E+00	3.26E+00	3.43E+00	1.87E+00	1.02E+00	7.85E-01
SO	6.71E+01	5.36E+01	3.21E+01	3.43E+01	3.33E+01	3.83E+01	5.58E+01
TG	2.03E+01	1.98E+01	2.67E+01	2.51E+01	7.80E+00	1.78E+01	1.25E+01
CER	2.94E+00	4.05E+00	4.36E+00	3.73E+00	2.09E+00	2.79E+00	3.11E+00
CL	1.93E-01	5.38E-01	5.41E-01	5.05E-01	5.53E-01	7.06E-01	6.11E-01
FA	1.32E+00	1.07E+00	1.46E+00	1.60E+00	6.40E-01	5.46E-01	9.93E-01
PE	5.49E+00	6.57E+00	1.07E+01	8.04E+00	6.70E+00	5.66E+00	3.96E+00
PG	1.10E-02	6.37E-02	2.03E-01	8.44E-02	6.23E-02	3.10E-02	0.00E+00
PI	2.38E+00	2.20E+00	3.57E+00	2.26E+00	1.34E+00	8.99E-01	7.90E-01
PS	1.37E+00	4.24E-01	9.75E+00	1.46E+01	4.20E+01	2.81E+01	1.50E+01

Table 41. Standard deviation of wild type lipid classes identified by developed LC-MS/MS method when grown with PE21. The values are calculated as the sample standard deviation (±%) of two experiments for the wild type strain taken at 7 time points (DME, D0, D1, D2, D4, D6, D8). Sample standard deviation was used because the sample is biological. Legend: DME stands for day mid-exponential. D stands for day and numeric values represent days of growth. Lipid class: Phosphatidylcholine, Sphingosine, Triacylglycerol, Ceramide, Cardiolipin, Free Fatty Acid, Phosphatidylethanolamine, Phosphatidylglycerol, Phosphatidylinositol, Phosphatidylserine.

LIPID CLASS	DME	D0	D1	D2	D4	D6	D8
PC	8.29E-01	1.26E+00	5.93E-01	2.09E+00	1.87E+00	3.02E+00	1.04E+00
SO	7.90E+01	6.73E+01	7.43E+01	4.28E+01	4.33E+01	3.79E+01	2.14E+01
TG	2.03E+01	1.98E+01	2.67E+01	2.51E+01	7.80E+00	1.78E+01	1.25E+01
CER	2.13E+00	3.29E+00	1.50E+00	3.19E+00	2.57E+00	2.18E+00	0.00E+00
CL	1.08E-01	3.69E-01	3.67E-01	1.56E+00	2.24E+00	4.29E+00	0.00E+00
FA	1.20E+00	1.07E+00	1.06E+00	1.60E+00	6.40E-01	5.46E-01	0.00E+00
PE	1.13E+00	2.28E+00	1.24E+00	2.98E+00	3.38E+00	4.34E+00	0.00E+00
PG	0.00E+00	0.00E+00	0.00E+00	0.00E+00	0.00E+00	3.64E-02	0.00E+00
PI	3.81E+00	4.74E+00	2.04E+00	4.69E+00	5.15E+00	3.20E+00	0.00E+00
PS	2.20E+00	6.56E+00	2.97E+00	1.01E+01	2.71E+01	2.22E+01	0.00E+00

Table 42. Mean percentage values for mutant strain 8 lipid classes identified by the developed LC-MS/MS method in cells grown with PE21. The values are the mean (% of whole lipidome) of two experiments for the wild type strain taken at 7 time points (DME, D0, D1, D2, D4, D6, D8). Legend: DME stands for day mid-exponential. D stands for day and numeric values represent days of growth. Lipid class: Phosphatidylcholine, sphingosine, Triacylglycerol, Ceramide, Cardiolipin, Free Fatty Acid, Phosphatidylethanolamine, Phosphatidylglycerol, Phosphatidylinositol, Phosphatidylserine. Mutant strain 8 has the entire gene *Tgl3* deleted. The protein product of this gene resides in lipid droplets and is responsible for breakdown of triacylglycerol.

LIPID CLASS	DME	D0	D1	D2	D4	D6	D8
PC	7.67E-02	1.87E-01	1.04E-01	2.40E-01	2.15E-01	4.74E-01	1.28E-01
SO	8.75E+00	7.72E+00	1.17E+01	5.26E+00	5.68E+00	4.35E+00	2.81E+00
TG	1.27E+00	6.14E-01	9.42E-01	4.15E+00	1.04E+00	2.29E+00	
CER	2.62E-01	2.43E-01	1.75E-01	2.35E-01	2.54E-01	2.41E-01	
CL	1.60E-02	4.85E-02	4.51E-02	2.58E-01	2.20E-01	6.00E-01	
FA	8.07E-02	2.43E-01	1.40E-01	2.89E-01	2.09E-01	1.16E-01	
PE	1.38E-01	2.99E-01	1.73E-01	4.17E-01	3.87E-01	6.07E-01	
PG	0.00E+00	0.00E+00	0.00E+00	0.00E+00	0.00E+00	4.68E-03	
PI	3.99E-01	7.86E-01	3.02E-01	7.78E-01	5.90E-01	3.67E-01	
PS	2.57E-01	4.42E-01	2.19E-01	9.99E-01	2.50E+00	2.05E+00	

Table 233. Standard deviation values for mutant strain 8 lipid classes identified by the developed LC-MS/MS method in cells grown with PE21. The values are calculated as the sample standard deviation (±%) of two experiments for the wild type strain taken at 7 time points (DME, D0, D1, D2, D4, D6, D8). Sample standard deviation was used because the sample is biological. Legend: DME stands for day mid-exponential. D stands for day and numeric values represent days of growth. Lipid class: Phosphatidylcholine, Sphingosine, Triacylglycerol, Ceramide, Cardiolipin, Free Fatty Acid, Phosphatidylethanolamine, Phosphatidylglycerol, Phosphatidylinositol, Phosphatidylserine. Mutant strain 8 has the entire gene *Tgl3* deleted. The protein product of this gene resides in lipid droplets and is responsible for breakdown of triacylglycerol.

LIPID CLASS	DME	D0	D1	D2	D4	D6	D8
PC	3.49E+00	2.05E+00	4.08E+00	3.38E+00	4.65E+00	3.94E+00	4.20E+00
SO	6.41E+01	3.92E+01	2.64E+01	5.31E+01	2.06E+01	4.26E+01	2.99E+01
TG	2.03E+01	3.38E+01	3.27E+01	2.51E+01	1.88E+01	1.78E+01	2.43E+01
CER	9.89E-01	2.24E+00	2.81E+00	8.62E-01	3.55E+00	2.60E+00	2.83E+00
CL	5.05E-01	3.80E-01	7.15E-01	9.08E-01	3.34E+00	1.71E+00	1.78E+00
FA	1.32E+00	8.14E-01	1.46E+00	9.54E-01	6.40E-01	5.46E-01	9.97E-01
PE	7.40E+00	2.84E+00	5.25E+00	4.17E+00	7.69E+00	5.06E+00	3.97E+00
PG	0.00E+00	0.00E+00	1.32E-02	2.67E-02	7.76E-02	4.54E-02	4.90E-02
PI	7.40E+00	4.42E+00	4.19E+00	4.18E+00	4.59E+00	3.75E+00	4.68E+00
PS	7.81E+00	7.14E+00	1.80E+01	1.33E+01	3.35E+01	2.65E+01	2.23E+01

Table 244. Mean percentage values for mutant strain 9 lipid classes identified by the developed LC-MS/MS method in cells grown with PE21. The values are the mean (% of whole lipidome) of two experiments for the wild type strain taken at 7 time points (DME, D0, D1, D2, D4, D6, D8). Legend: DME stands for day mid-exponential. D stands for day and numeric values represent days of growth. Lipid class: Phosphatidylcholine, sphingosine, Triacylglycerol, Ceramide, Cardiolipin, Free Fatty Acid, Phosphatidylethanolamine, Phosphatidylglycerol, Phosphatidylinositol, Phosphatidylserine. Mutant strain 9 has the entire gene *Tgl1* deleted. The protein product of this gene resides in lipid droplets and is responsible for breakdown of triacylglycerol.

LIPID CLASS	DME	D0	D1	D2	D4	D6	D8
PC	3.65E-01	3.58E-01	4.68E-01	5.60E-01	4.95E-01	6.89E-01	6.24E-01
SO	6.72E+00	4.82E+00	3.03E+00	5.66E+00	2.02E+00	6.33E+00	3.93E+00
TG	1.74E+00	4.45E+00	3.21E+00	1.59E+00	1.85E+00	9.61E-01	3.82E+00
CER	1.05E-01	2.35E-01	2.60E-01	1.11E-01	2.62E-01	2.25E-01	2.79E-01
CL	6.64E-02	3.73E-02	8.79E-02	1.43E-01	3.83E-01	2.39E-01	2.96E-01
FA	1.97E-01	1.07E-01	2.34E-01	1.09E-01	1.19E-01	7.44E-02	1.14E-01
PE	6.85E-01	4.47E-01	6.02E-01	6.56E-01	1.08E+00	7.51E-01	6.94E-01
PG	0.00E+00	0.00E+00	8.88E-04	2.14E-03	9.06E-03	3.64E-03	3.61E-03
PI	5.92E-01	7.33E-01	5.16E-01	4.11E-01	8.02E-01	6.55E-01	7.36E-01
PS	7.23E-01	6.60E-01	1.66E+00	1.63E+00	3.51E+00	2.94E+00	2.86E+00

Table 255. Standard deviation values for mutant strain 9 lipid classes identified by the developed LC-MS/MS method when cells were grown with PE21. The values are calculated as the sample standard deviation (±%) of two experiments for the wild type strain taken at 7 time points (DME, D0, D1, D2, D4, D6, D8). Sample standard deviation was used because the sample is biological. Legend: DME stands for day mid-exponential. D stands for day and numeric values represent days of growth. Lipid class: Phosphatidylcholine, Sphingosine, Triacylglycerol, Ceramide, Cardiolipin, Free Fatty Acid, Phosphatidylethanolamine, Phosphatidylglycerol, Phosphatidylinositol, Phosphatidylserine. Mutant strain 9 has the entire gene *Tgl1* deleted. The protein product of this gene resides in lipid droplets and is responsible for breakdown of triacylglycerol.

LIPID CLASS	DME	D0	D1	D2	D4	D6	D8
PC	1.30E+00	1.69E+00	1.17E+00	1.08E+00	1.04E+00	1.11E+00	7.63E-01
SO	1.09E+01	1.56E+01	5.34E+00	2.57E+01	2.68E+01	9.46E+00	3.89E+00
TG	2.03E+01	1.98E+01	2.67E+01	2.51E+01	7.80E+00	1.78E+01	1.25E+01
CER	1.54E+00	2.22E+00	1.15E+00	1.35E+00	1.06E+00	9.02E-01	5.97E-01
CL	1.63E+00	1.23E+00	1.83E+00	1.30E+00	4.37E+00	3.37E+00	5.39E+00
FA	3.33E-01	3.18E-01	2.26E-01	2.89E-01	1.63E-01	1.32E-01	9.67E-02
PE	3.53E+00	3.35E+00	2.95E+00	2.06E+00	1.56E+00	1.58E+00	1.39E+00
PG	0.00E+00	0.00E+00	7.41E-03	7.26E-03	2.40E-02	3.12E-02	3.31E-02
PI	5.43E+00	3.60E+00	2.65E+00	2.02E+00	1.75E+00	1.56E+00	1.06E+00
PS	8.19E+01	6.55E+01	8.13E+01	5.84E+01	6.08E+01	8.36E+01	8.42E+01

Table 266. Mean percentage values for mutant strain 87 lipid classes identified by the developed LC-MS/MS method in cells grown with PE21. The values are the mean (% of whole lipidome) of two experiments for the wild type strain taken at 7 time points (DME, D0, D1, D2, D4, D6, D8). Legend: DME stands for day mid-exponential. D stands for day and numeric values represent days of growth. Lipid class: Phosphatidylcholine, sphingosine, Triacylglycerol, Ceramide, Cardiolipin, Free Fatty Acid, Phosphatidylethanolamine, Phosphatidylglycerol, Phosphatidylinositol, Phosphatidylserine. Mutant strain 87 has the entire gene *Tgl4* deleted. The protein product of this gene resides in lipid droplets and is responsible for breakdown of triacylglycerol.

LIPID CLASS	DME	D0	D1	D2	D4	D6	D8
PC	1.12E-01	2.50E-01	1.84E-01	1.06E-01	1.63E-01	1.55E-01	8.12E-02
SO	1.27E+00	2.18E+00	5.25E-01	3.59E+00	3.98E+00	1.49E+00	3.83E-01
TG	9.53E-02	9.21E-01	1.18E+00	8.29E-01	5.93E-01	2.61E-01	5.49E-01
CER	1.39E-01	1.64E-01	8.50E-02	1.08E-01	1.11E-01	6.07E-02	6.26E-02
CL	2.01E-01	1.72E-01	2.56E-01	1.71E-01	7.64E-01	4.14E-01	7.54E-01
FA	3.49E-02	3.64E-02	3.76E-02	3.31E-02	2.85E-02	1.74E-02	1.35E-02
PE	3.04E-01	3.84E-01	5.15E-01	2.36E-01	2.18E-01	2.35E-01	1.48E-01
PG	0.00E+00	0.00E+00	7.76E-04	8.04E-04	1.61E-03	2.89E-03	2.65E-03
PI	6.66E-01	5.97E-01	4.62E-01	2.83E-01	2.74E-01	2.32E-01	1.76E-01
PS	8.08E+00	8.42E+00	9.01E+00	6.12E+00	7.82E+00	7.74E+00	5.67E+00

Table 277. Standard deviation values for mutant strain 87 lipid classes identified by the developed LC-MS/MS method in cells grown with PE21. The values are calculated as the sample standard deviation (±%) of two experiments for the wild type strain taken at 7 time points (DME, D0, D1, D2, D4, D6, D8). Sample standard deviation was used because the sample is biological. Legend: DME stands for day mid-exponential. D stands for day and numeric values represent days of growth. Lipid class: Phosphatidylcholine, Sphingosine, Triacylglycerol, Ceramide, Cardiolipin, Free Fatty Acid, Phosphatidylethanolamine, Phosphatidylglycerol, Phosphatidylinositol, Phosphatidylserine. Mutant strain 87 has the entire gene *Tgl4* deleted. The protein product of this gene resides in lipid droplets and is responsible for breakdown of triacylglycerol.

LIPID CLASS	DME	D0	D1	D2	D4	D6	D8
PC	1.52E+00	4.66E+00	1.63E+00	2.57E+00	1.75E+00	1.41E+00	1.06E+00
SO	1.73E+01	3.42E+01	1.49E+01	1.43E+01	5.52E+00	6.43E+00	9.57E+00
TG	2.42E+01	1.98E+01	2.67E+01	2.51E+01	7.80E+00	1.78E+01	1.25E+01
CER	2.60E+00	6.53E+00	2.39E+00	2.55E+00	1.07E+00	1.00E+00	5.15E-01
CL	1.55E+00	8.33E+00	4.94E+00	3.05E+01	1.10E+01	1.72E+01	7.84E+00
FA	6.54E-01	1.07E+00	7.95E-01	8.20E-01	2.72E-01	2.35E-01	1.27E-01
PE	5.12E+00	1.25E+01	4.26E+00	4.64E+00	2.41E+00	2.43E+00	1.26E+00
PG	0.00E+00	0.00E+00	5.09E-02	3.83E-02	6.08E-02	6.50E-02	6.49E-02
PI	4.14E+00	8.31E+00	3.84E+00	3.23E+00	2.21E+00	1.62E+00	1.15E+00
PS	4.59E+01	3.60E+00	4.09E+01	3.48E+01	6.98E+01	6.84E+01	7.69E+01

Table 288. Mean percentage value of mutant strain 88 lipid classes identified by developed LC-MS/MS method when grown with PE21. The values are the mean (% of whole lipidome) of two experiments for the wild type strain taken at 7 time points (DME, D0, D1, D2, D4, D6, D8). Legend: DME stands for day mid-exponential. D stands for day and numeric values represent days of growth. Lipid class: Phosphatidylcholine, sphingosine, Triacylglycerol, Ceramide, Cardiolipin, Free Fatty Acid, Phosphatidylethanolamine, Phosphatidylglycerol, Phosphatidylinositol, Phosphatidylserine. Mutant strain 88 has the entire gene *Tgl5* deleted. The protein product of this gene resides in lipid droplets and is responsible for breakdown of triacylglycerol.

LIPID CLASS	DME	D0	D1	D2	D4	D6	D8
PC	1.22E-01	6.52E-01	2.28E-01	3.16E-01	2.75E-01	1.38E-01	1.86E-01
SO	1.71E+00	4.49E+00	2.47E+00	1.76E+00	7.72E-01	1.07E+00	1.50E+00
TG	2.78E+00	1.58E+00	2.80E+00	4.93E-01	1.25E+00	2.37E-01	4.02E-01
CER	3.42E-01	6.05E-01	1.61E-01	1.72E-01	1.12E-01	6.75E-02	4.76E-02
CL	2.71E-01	1.09E+00	4.85E-01	3.75E+00	1.93E+00	1.70E+00	1.37E+00
FA	7.64E-02	2.26E-01	1.32E-01	8.06E-02	3.80E-02	3.91E-02	2.00E-02
PE	6.59E-01	1.33E+00	6.69E-01	4.94E-01	2.76E-01	3.40E-01	2.08E-01
PG	0.00E+00	0.00E+00	6.55E-03	4.01E-03	5.25E-03	4.79E-03	8.35E-03
PI	3.57E-01	9.53E-01	6.04E-01	4.52E-01	2.35E-01	1.86E-01	1.41E-01
PS	4.81E+00	3.33E-01	4.54E+00	3.65E+00	6.46E+00	4.61E+00	5.67E+00

Table 4929. Standard deviation of mutant strain 88 lipid classes identified by developed LC-MS/MS method when grown with PE21. The values are calculated as the sample standard deviation (±%) of two experiments for the wild type strain taken at 7 time points (DME, D0, D1, D2, D4, D6, D8). Sample standard deviation was used because the sample is biological. Legend: DME stands for day mid-exponential. D stands for day and numeric values represent days of growth. Lipid class: Phosphatidylcholine, Sphingosine, Triacylglycerol, Ceramide, Cardiolipin, Free Fatty Acid, Phosphatidylethanolamine, Phosphatidylglycerol, Phosphatidylinositol, Phosphatidylserine. Mutant strain 88 has the entire gene *Tgl5* deleted. The protein product of this gene resides in lipid droplets and is responsible for breakdown of triacylglycerol.

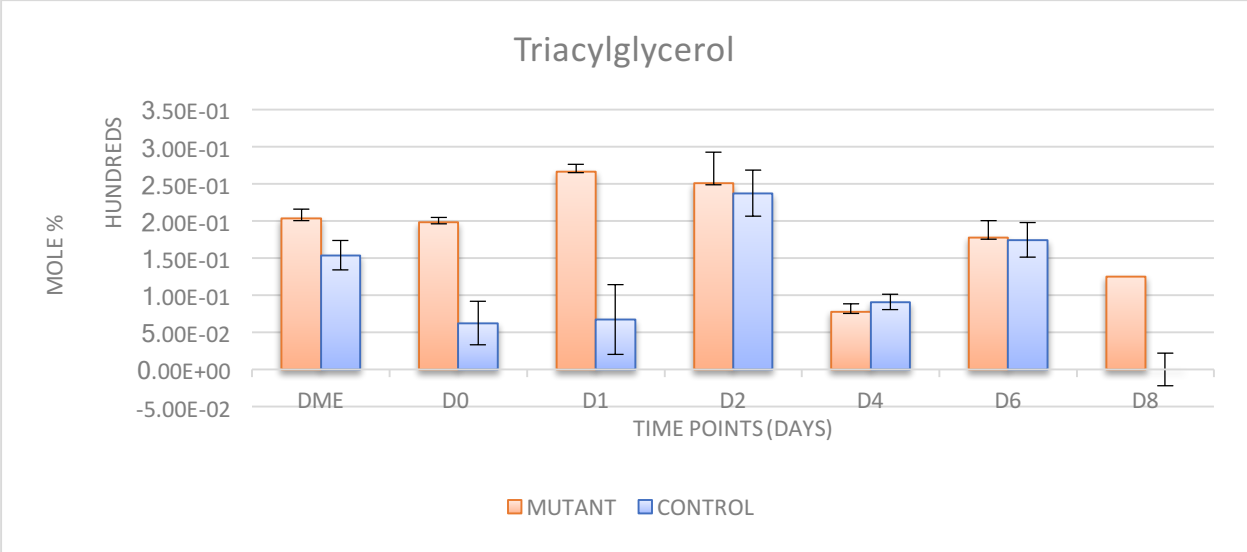

Figure 22. The mean mole % values of Triacylglycerol (TG) relative to the whole lipidome for wild-type strain compared to mutant strain 8 (*tgl3Δ*) when in cells grown with PE21. TG species were measured by the developed LC-MS/MS method at 7 time points. Error bars presented are from table 43 and mole % values are from table 42. For growth conditions of control and treated with 21 refer to Materials and Methods in chapter 3. Legend: DME stands for day mid-exponential. D stands for day and numeric values represent days of growth. PE21 stands for plant extract 21. Mutant strain 8 is mutated in gene *tgl3* and it is a deletion mutation. The gene is expressed in lipid drops and it is responsible for breakdown of triacylglycerol. Control stands for wild type *Saccharomyces cerevisiae*. The mean and n value of standard deviation are from 2 experiments.

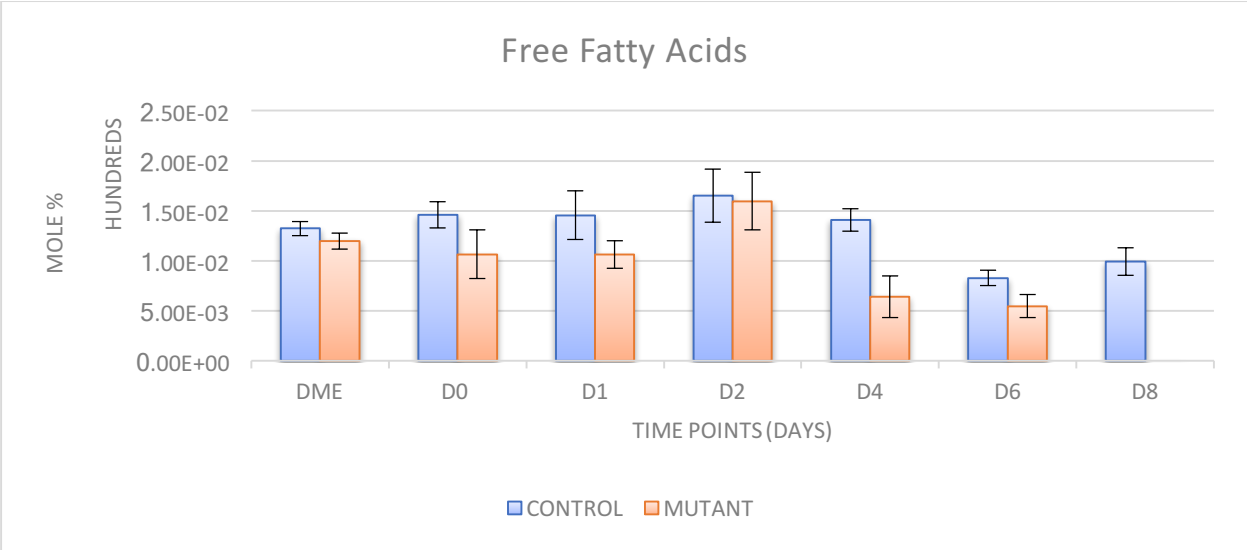

Figure 23. The mean mole % values of Free fatty acid relative to the whole lipidome for wild-type strain compared to mutant strain 8 (*tgl3Δ*) in cells grown with PE21. FFA species were measured by the developed LC-MS/MS method at 7 time points. Error bars presented are from table 43 and mole % values are from table 42. For growth conditions of control and treated with 21 refer to Materials and Methods in chapter 3. Legend: DME stands for day mid-exponential. D stands for day and numeric values represent days of growth. PE21 stands for plant extract 21. Mutant strain 8 is mutated in gene *tgl3* and it is a deletion mutation. The gene is expressed in lipid drops and it is responsible for breakdown of

triacylglycerol. Control stands for wild type *Saccharomyces cerevisiae*. The mean and n value of standard deviation are from 2 experiments.

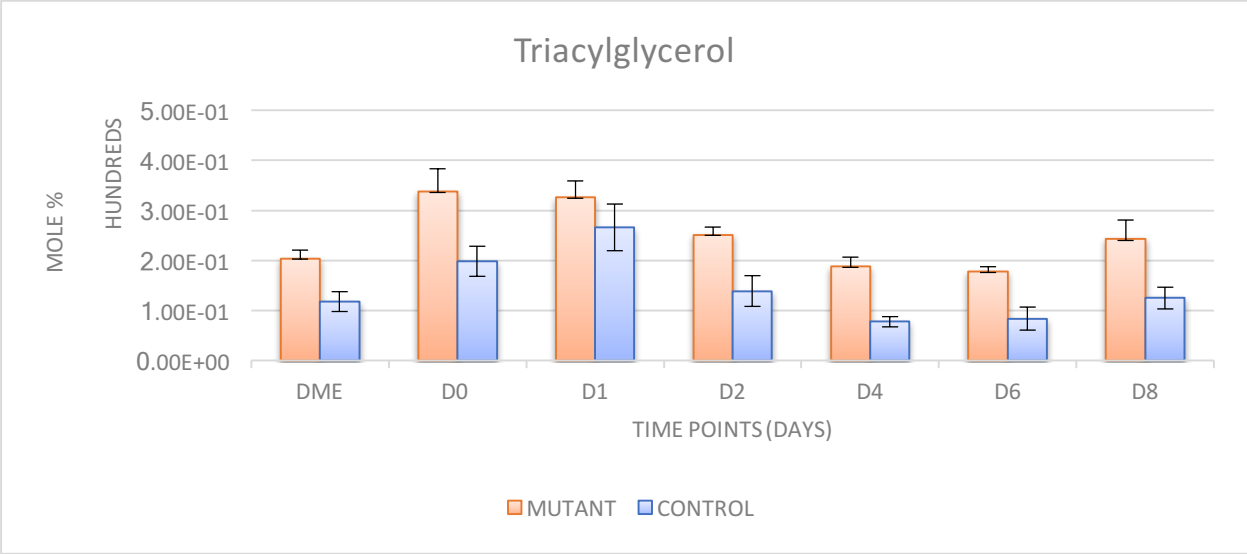

Figure 24. The mean mole % values of Triacylglycerol (TG) relative to the whole lipidome for wild-type strain compared to mutant strain 9 (*tgl1Δ*) in cells grown with PE21. TG species were measured by the developed LC-MS/MS method at 7 time points. Error bars presented are from table 45 and mole % values are from table 44. For growth conditions of control and treated with 21 refer to Materials and Methods in chapter 3. Legend: DME stands for day mid-exponential. D stands for day and numeric values represent days of growth. PE21 stands for plant extract 21. Mutant strain 9 is mutated in gene *tgl1* and it is a deletion mutation. The gene is expressed in lipid drops and it is responsible for breakdown of triacylglycerol. Control stands for wild type *Saccharomyces cerevisiae*. The mean and n value of standard deviation are from 2 experiments.

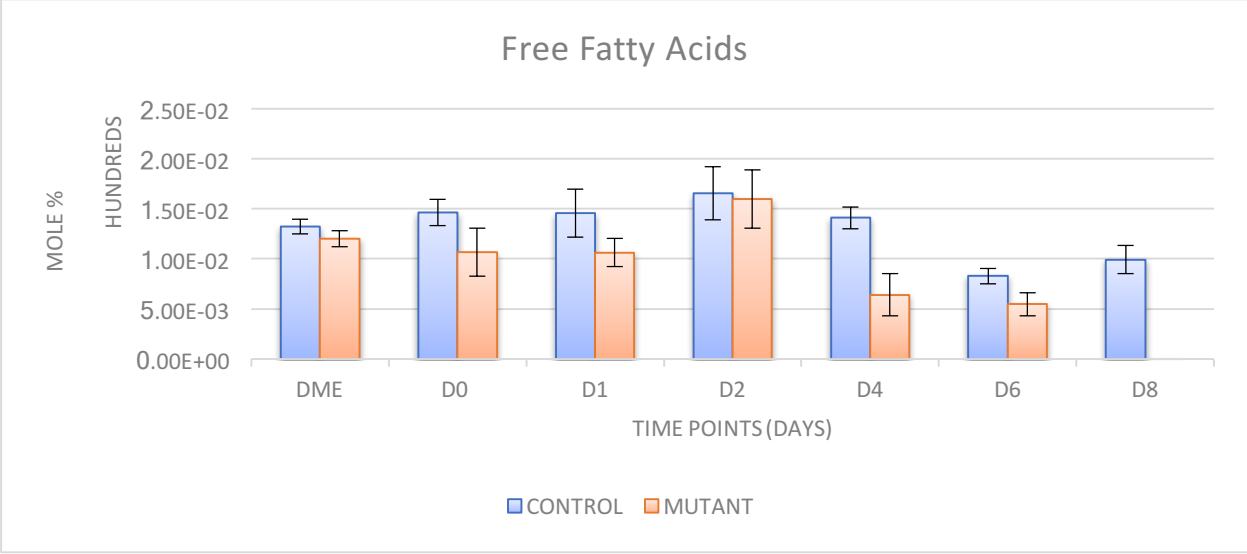

Figure 25. The mean mole % values of Free fatty acids (FFA) relative to the whole lipidome for wild-type strain compared to mutant strain 9 (*tgl1Δ*) in cells grown with PE21. FFA species were measured by the developed LC-MS/MS method at 7 time points. Error bars presented are from table 45 and mole % values are from table 44. For growth conditions of control and treated with 21 refer to Materials and Methods in chapter 3. Legend: DME stands for day mid-exponential. D stands for day and numeric values represent days of growth. PE21 stands for plant extract 21. Mutant strain 9 is mutated

in gene *tgl1* and it is a deletion mutation. The gene is expressed in lipid drops and it is responsible for breakdown of triacylglycerol. Control stands for wild type *Saccharomyces cerevisiae*. The mean and n value of standard deviation are from 2 experiments.

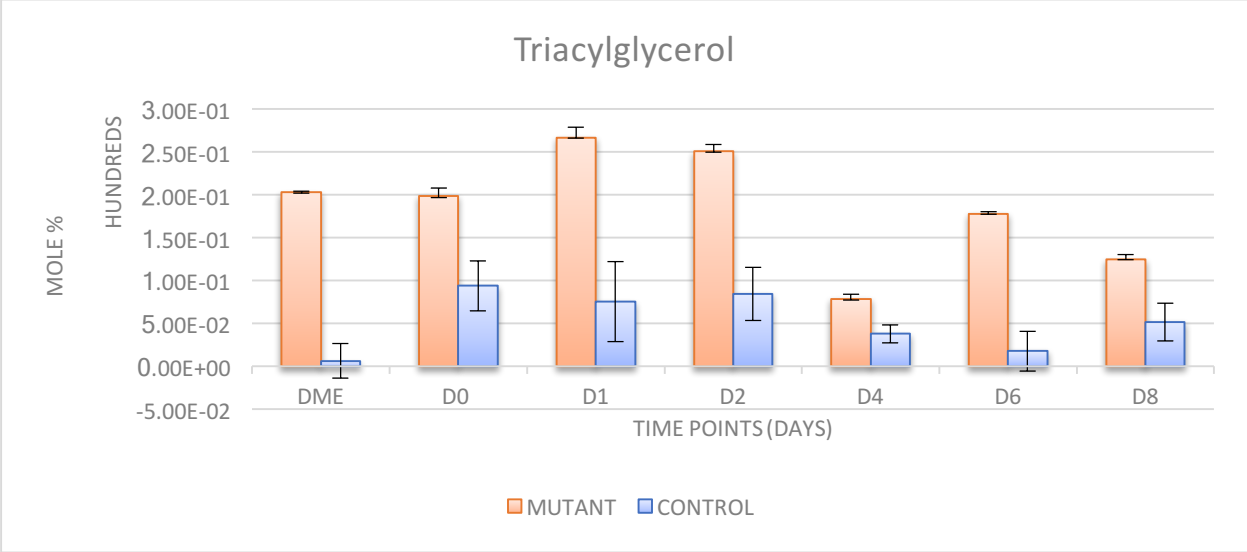

Figure 26. The mean mole % values of Triacylglycerol (TG) relative to the whole lipidome for wild-type strain compared to mutant strain 87 (*tgl4Δ*) in cells grown with PE21. TG species were measured by the developed LC-MS/MS method at 7 time points. Error bars presented are from table 47 and mole % values are from table 46. For growth conditions of control and treated with 21 refer to Materials and Methods in chapter 3. Legend: DME stands for day mid-exponential. D stands for day and numeric values represent days of growth. PE21 stands for plant extract 21. Mutant strain 87 is mutated in gene *tgl4* and it is a deletion mutation. The gene is expressed in lipid drops and it is responsible for breakdown of triacylglycerol. Control stands for wild type *Saccharomyces cerevisiae*. The mean and n value of standard deviation are from 2 experiments.

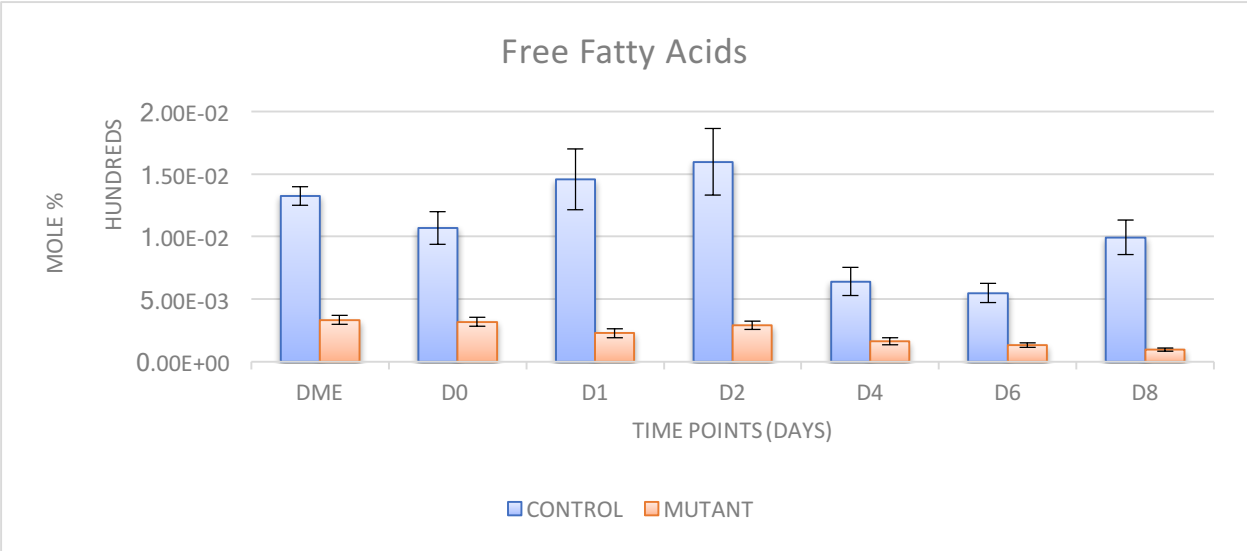

Figure 27. The mean mole % values of Free Fatty Acids (FFA) relative to the whole lipidome for wild-type strain compared to mutant strain 87 (*tgl4Δ*) in cells grown with PE21. FFA species were measured by the developed LC-MS/MS method at 7 time points. Error bars presented are from table 47 and mole % values are from table 46. For growth conditions of control and treated with 21 refer to Materials and Methods in chapter 3. Legend: DME stands for day mid-exponential. D stands for day

and numeric values represent days of growth. PE21 stands for plant extract 21. Mutant strain 87 is mutated in gene *tgl4* and it is a deletion mutation. The gene is expressed in lipid drops and it is responsible for breakdown of triacylglycerol. Control stands for wild type *Saccharomyces cerevisiae*. The mean and n value of standard deviation are from 2 experiments.

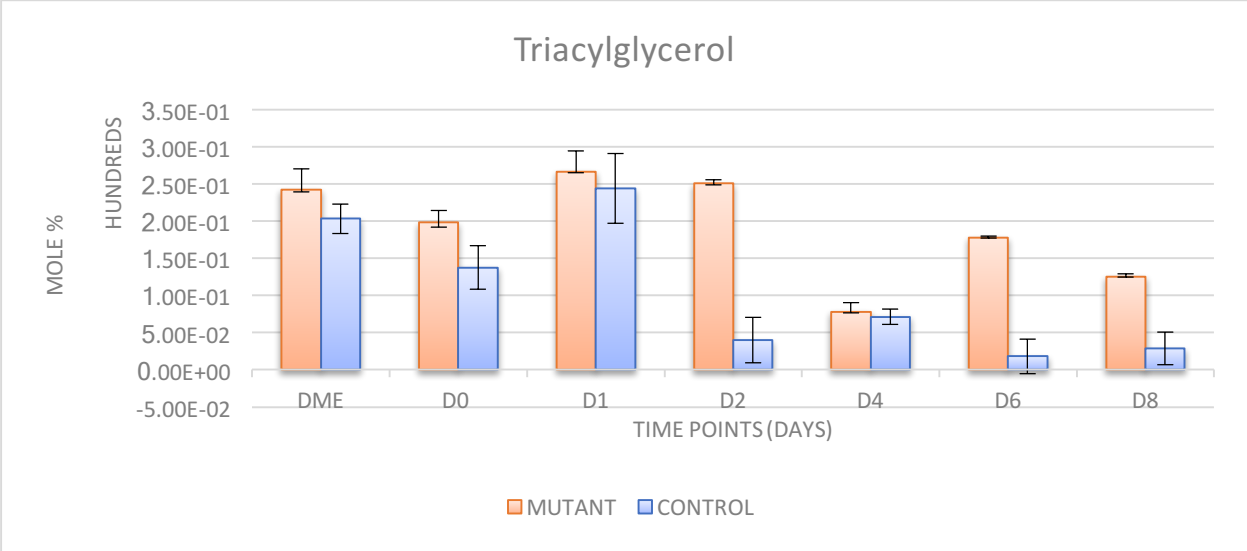

Figure 28. The mean mole % values of Triacylglycerol (TG) relative to the whole lipidome for wild-type strain compared to mutant strain 88 (*tgl5Δ*) when in cells grown with PE21. TG species were measured by the developed LC-MS/MS method at 7 time points. Error bars presented are from table 49 and mole % values are from table 48. For growth conditions of control and treated with 21 refer to Materials and Methods in chapter 3. Legend: DME stands for day mid-exponential. D stands for day and numeric values represent days of growth. PE21 stands for plant extract 21. Mutant strain 88 is mutated in gene *tgl5* and it is a deletion mutation. The gene is expressed in lipid drops and it is responsible for breakdown of triacylglycerol. Control stands for wild type *Saccharomyces cerevisiae*. The mean and n value of standard deviation are from 2 experiments.

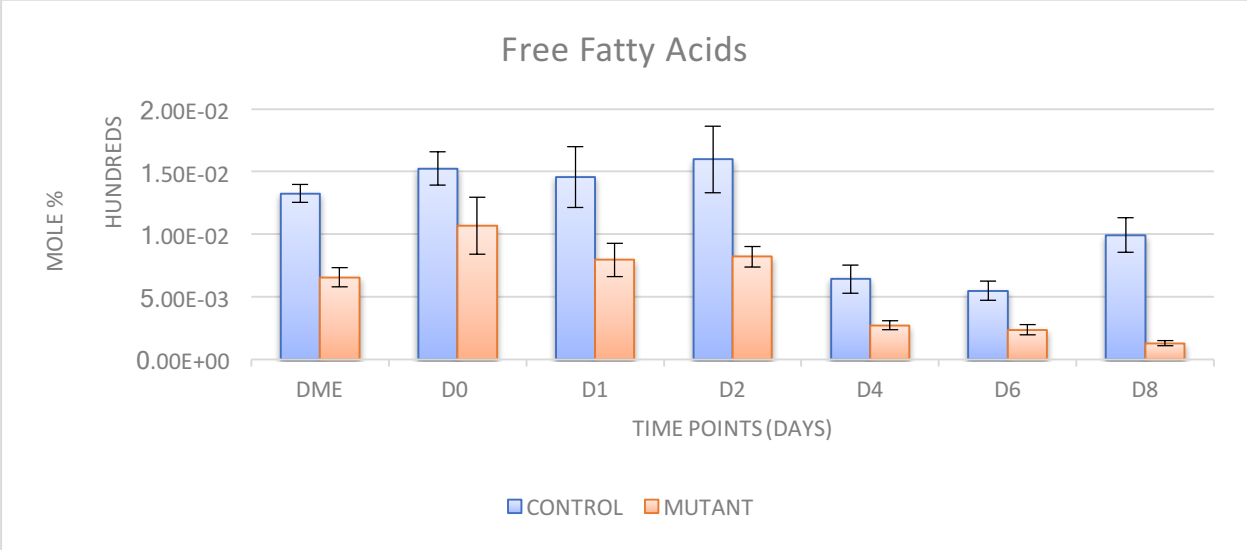

Figure 29. The mean mole % values of Free Fatty Acids relative to the whole lipidome for wild-type strain compared to mutant strain 88 (*tgl5Δ*) in cells grown with PE21. FFA species were measured by the developed LC-MS/MS method at 7 time points. Error bars presented are from table 49 and mole % values are from table 48. For growth conditions of control and treated with 21 refer to Materials and

Methods in chapter 3. Legend: DME stands for day mid-exponential. D stands for day and numeric values represent days of growth. PE21 stands for plant extract 21. Mutant strain 88 is mutated in gene *tgl5* and it is a deletion mutation. The gene is expressed in lipid drops and it is responsible for breakdown of triacylglycerol. Control stands for wild type *Saccharomyces cerevisiae*. The mean and n value of standard deviation are from 2 experiments.

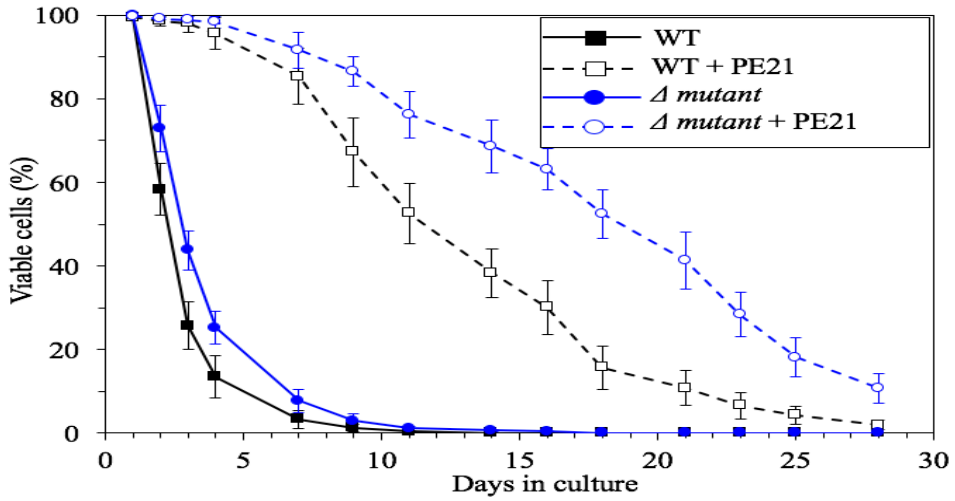

Figure 30. Viability curves of wild-type strain and the mutant strain 9 (*tgl1Δ*) cultured with and without PE21. Both mutant strain and wildtype cells were cultured initially in nutrient-rich YP medium containing 2% glucose, then the cells were transferred to a synthetic minimal YNB medium containing 2% glucose. The viability percentage values are relative to the number of viable cells at post-diauxic phase. The values reported are the mean of duplicate experiments. Mutant strain 9 is mutated in gene *tgl1* and it is a deletion mutation. The gene is expressed in lipid drops and it is responsible for breakdown of triacylglycerol. Legends: YNB stands for yeast nitrogen base (without amino acids). YP stands for yeast extract and peptone.

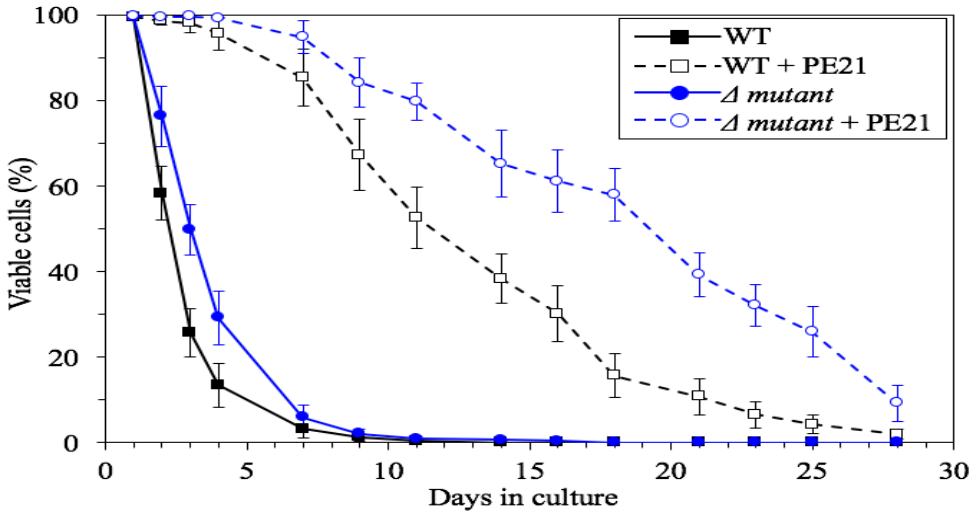

Figure 31. Viability curves of wild-type strain and the mutant strain 8 (*tgl3Δ*) cultured with and without PE21. Both mutant strain and wildtype cells were cultured initially in nutrient-rich YP medium containing 2% glucose, then the cells were transferred to a synthetic minimal YNB medium containing 2% glucose. The viability percentage values are relative to the number of viable cells at post-diauxic phase. The values reported are the mean of duplicate experiments. Mutant strain 8 is mutated I n gene *tgl3* and it is a deletion mutation. The gene is expressed in lipid drops and it is responsible for breakdown of triacylglycerol. Legends: YNB stands for yeast nitrogen base (without amino acids). YP stands for yeast extract and peptone.

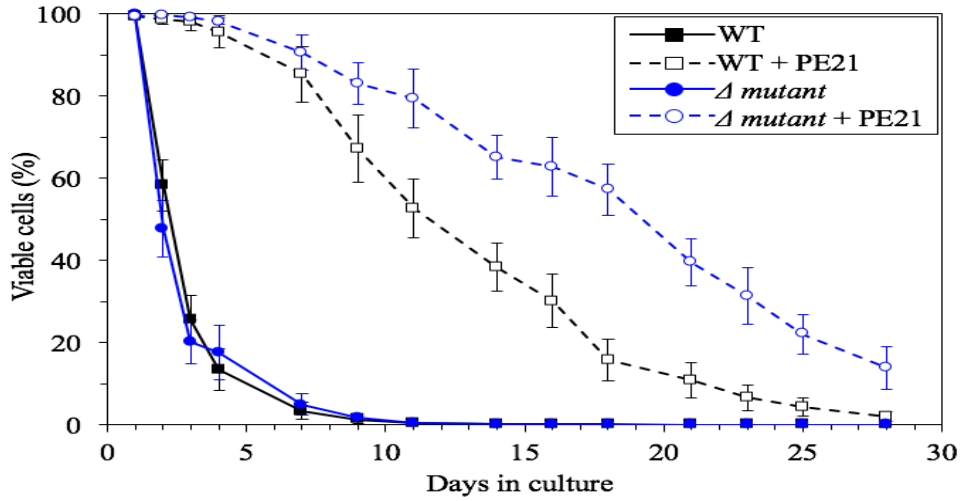

Figure 32. Viability curves of wild-type strain and the mutant strain 87 (*tgl4Δ*) cultured with and without PE21. Both mutant strain and wildtype cells were cultured initially in nutrient-rich YP medium containing 2% glucose, then the cells were transferred to a synthetic minimal YNB medium containing 2% glucose. The viability percentage values are relative to the number of viable cells at post-diauxic phase. The values reported are the mean of duplicate experiments. Mutant strain 87 is mutated in gene *tgl4* and it is a deletion mutation. The gene is expressed in lipid drops and it is responsible for breakdown of triacylglycerol. Legends: YNB stands for yeast nitrogen base (without amino acids). YP stands for yeast extract and peptone.

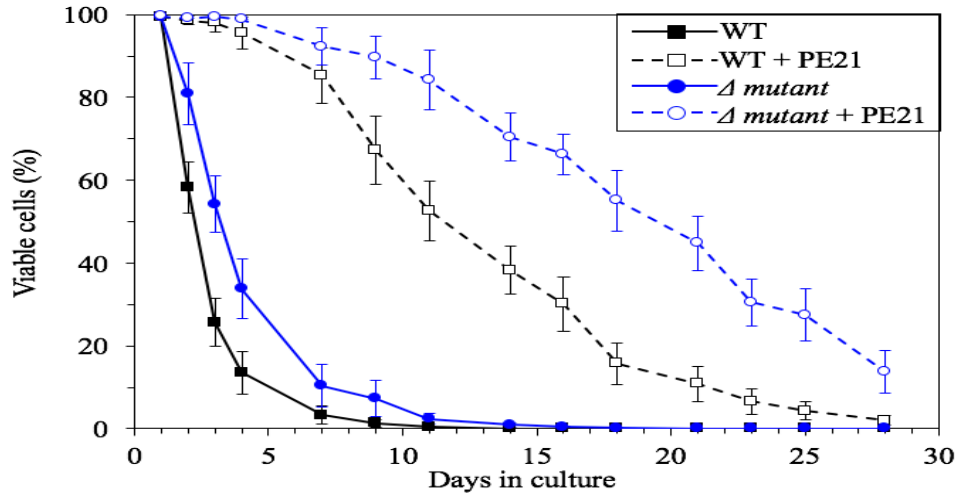

Figure 33. Viability curves of wild-type strain and the mutant strain 88 (*tgl5Δ*) cultured with and without PE21. Both mutant strain and wildtype cells were cultured initially in nutrient-rich YP medium containing 2% glucose, then the cells were transferred to a synthetic minimal YNB medium containing 2% glucose. The viability percentage values are relative to the number of viable cells at post-diauxic phase. The values reported are the mean of duplicate experiments. Mutant strain 88 is mutated in gene *tgl5* and it is a deletion mutation. The gene is expressed in lipid drops and it is responsible for breakdown of triacylglycerol. Legends: YNB stands for yeast nitrogen base (without amino acids). YP stands for yeast extract and peptone.

3.6 Results and discussion of sections 3.4 and 3.5

Tables 30, 32, 34, 36 and 38 provide data on the mole percentages of 10 lipid classes of wild-type and 4 mutant strains that lack different isoforms of triacylglycerol lipases. The values reported in each table represent the mean of two experiments. The tables correspond to different strains as follows: 30 (wild-type strain), 32 (strain 8, *tgl3Δ*), 34 (strain 9, *tgl1Δ*), 36 (strain 87, *tgl4Δ*) and 38 (strain 88, *tgl5Δ*). Tables 31, 33, 35, 37, and 39 show the standard deviation values of duplicate experiments for wild-type and these 4 mutant strains. The results shown in these tables indicate that standard deviations for different lipid classes vary between 5% to 20%. It is very unlikely that this variation is due to a detection or quantification error of the lipid analysis method developed by me; indeed, when the known concentrations of lipid standards were analyzed, there was less than 3% of variation between the 5 replicates as indicated in Section 2.0.

Although the total cellular lipidomes of 11 mutants were defined and compared to the total cellular lipidome of wild-type strain, the study focus of my thesis was on 4 mutant strains. These total cellular lipidomes of 12 strains were analyzed when yeast cells were cultured with or without PE21. As mentioned earlier, the mutants were deficient in the acyl transferase enzymes involved in different pathways of lipid metabolism. The future study will focus on the effects of PE21 on specific pathways of lipid metabolism through which PE21 extends yeast CLS.

Herein, the focus of the study is on 4 mutant strains. These mutant strains were impaired in 4 different enzymes, each of which catalyzes the breakdown of triacyclglycerols into free fatty acids. These enzymes reside in lipid droplets, which serve as a site for the storage of triacylglycerol molecules. In each of these 4 mutant strains,

the concentration of FFA is known to be lower than that in wild-type strain whereas the concentration of TAG is known to be higher than that in wild-type strain. The reason that these specific mutant strains were chosen for this study is that our finding presented in Section 3.3 (Figure 9) have revealed that PE21 considerably decreases the concentration of FFA. Unpublished data from the Titorenko suggest a hypothesis in which PE21 may increase yeast CLS because it decreases the rate of an age-related liponecrotic mode of programmed cell death (PCD).

Liponecrosis is a newly discovered subroutine of PCD, which is triggered by an accumulation of palmitoleic acid (POA) and some other species of free fatty acids [125]. Excessive amounts of exogenous POA are either incorporated into 1) phospholipids (PL) found in intracellular membranes; or 2) neutral lipids (NL), such as triacylglycerols (TAG), found in lipid droplets (Figure 3). The buildup of POA-containing PLs in the plasma membrane (PM) disrupts the asymmetrical distribution of certain phospholipid species, thus leading to a decline in the concentration of phosphatidylethanolamine (PE) within the extracellular leaflet of the PM [125]. This triggers the Rim101 pathway, which is activated either in response to 1) alkalinizing of extracellular medium; or 2) changes in the asymmetry of the membrane leaflets [125]. Activated Rim101 stimulates transcription of the Rsp1 gene leading to an increase in the amounts of Rbs1p protein [125]. This stimulates shuttling of PE from the extracellular leaflet to the intracellular leaflet of the PM. This depletion of PE in the extracellular leaflet of the PM increases its permeability, thus allowing small molecules to diffuse into the cell and to induce liponecrosis [125]. POA-containing PLs can also be found in mitochondrial membranes. This disrupts

mitochondrial functionality and leads to the production of reactive oxygen species that damage macromolecules and organelles and commits the cell to liponecrosis [125].

Because POA and other unsaturated FFAs are prone to age-related oxidative damage, their incorporation into phospholipids is detrimental for the cells because it induces liponecrotic cell death [126]. Several cellular processes can protect yeast from these toxic FFAs and liponecrosis. These cellular processes include: 1) an incorporation of the toxic FFAs into triacylglycerols to alleviate oxidative damage to macromolecules in other cellular locations [126]; 2) an oxidation of these FFAs in peroxisomes to reduce their flow into phospholipids [125]; 3) a degradation of dysfunctional mitochondria through mitophagy; or 4) a degradation of damaged macromolecules to maintain cellular homeostasis [125]. Liponecrosis is a subroutine of PCD, which consists of a genetically programmed set of cellular processes that occur in a defined sequence of events. These processes can be modulated through mutations in genes encoding various proteins involved in lipid metabolism and maintenance of functional mitochondria [125].

The results in Figures 30, 31, 32, and 33 of Section 3.5 support the above hypothesis. As we can see, all 4 mutant strains deficient in different triacylglycerol lipases live longer than wild-type strain cultured with without PE21. The difference between CLSs of wild-type and mutant strains is low in the absence of PE21; such difference is considerably enhanced in the presence of PE21. This finding suggests that the ability of PE21 to delay yeast chronological aging can be enhanced by decreasing the concentration of FFAs derived from the hydrolysis of TAG. Because FFAs elicit liponecrosis, it is likely that PE21 delays yeast chronological aging by delaying the onset of age-related liponecrosis.

The 10 analyzed lipid classes of these 4 mutants are tabulated in both Sections 3.4 (without PE21) and 3.5 (with PE21). As mentioned earlier, the focus of this study was on 4 mutant strains which have impaired enzymes responsible for the lipolytic breakdown of TAG in lipid droplets. The results described in Section 3.4 (without PE21; Figures 14, 16, 15 and 20) show that the concentration of TAG is higher in all 4 mutant strains in comparison with wild-type strain, whereas the concentration of FFAs is lower in comparison with wild-type strain. Similar findings are reported in Section 3.5 (with PE21; Figures 22, 24, 26 and 28). Indeed, TAG concentration in cells of each of the 4 mutants is higher in comparison wild-type strain, while the concentration of FFAs is lower in comparison with wild-type strain. The values shown in these figures represent the mean of two replicates and the n value for standard deviation is 2. In sum, these findings support the notion that each of the 4 mutant strains has a low rate of TAG lipolysis in lipid droplets.

Future studies should focus on the investigation of mechanisms underlying the essential role of lipid metabolism in yeast chronological aging delay by PE21. Specifically, it would need to be tested how the deletions of genes encoding enzymes involved in different aspects of lipid metabolism influence the concentration of different lipid classes and how these mutations impact CLS of yeast culture with or without PE21.

Discussion of the thesis

In this thesis, an optimized LC-MS/MS method has been developed. This method was successfully used to identify and quantify 10 different lipid classes of *Saccharomyces cerevisiae*. Prior to analysis of lipid sample by mass spectrometer, it was important to isolate and purify lipid species from other components of yeast cells which are the major source of matrix effect and isobaric peaks in mass spectrometry.

Currently, there are 3 most widely used methods of lipid extraction. Herein, all 3 methods were tested and compared to find the most efficient extraction method for *S. cerevisiae* lipid classes. The results of all 3 extraction methods in section 2.0 suggest that the most efficient extraction method for all 10 lipid classes is still the gold-standard method that uses a mixture of chloroform and methanol for extraction.

The ionization efficiencies of most frequently used mobile phase additives are tested and compared in section 2.0. To minimize an error in assessing these efficiencies by each of the 3 methods, the LC-MS/MS parameters, mobile phases and re-solubilizing solvent were kept constant. The results presented in section 2.0 show that the most efficient ionization additives are ammonium formate in the positive mode and ammonium acetate in the negative mode. It has been reported in literature that the addition of minute concentrations of organic acids, such as formic acid and acetic acid, enhances the ionization of lipids by decreasing the matrix effects through lowering of pH in the sample. Nevertheless, our results show the above-mentioned organic salts without any acids give the optimal ionization for each of the 10 lipid classes analyzed.

Even though almost all published studies used the same mobile phases A and B containing the same additives for both positive and negative modes of ionization, our

results suggest that different organic salts must be added to obtain an optimal ionization efficiency for each of the ionization modes (Table 5).

Using the optimized lipid extraction and LC-MS/MS methods developed in this thesis, the effects of the willow bark extract (which is called PE21) on the lipidome of *Saccharomyces cerevisiae* was analyzed. The results in section 2.3 show that PE21 considerably remodels the lipid composition of the wild-type strain of *Saccharomyces cerevisiae*. Although PE21 alters the concentration of all 10-analyzed lipid classes, our focus of study was on FFA and its storage form triacylglycerol.

In section 3.0, the lipid profiles of 11 mutant strains were analyzed and compared to that of wild-type strain using cells cultured without and with PE21. The mutant strains studied are impaired in different pathways of lipid metabolism in various organelles of *Saccharomyces cerevisiae*. The purpose of this part of the study was to determine or narrow down the possible mechanism through which PE21 increases the CLS of *Saccharomyces cerevisiae*.

The result in section 3.0 shows that PE21 remodels the lipidome of all mutant strains, as compared to the corresponding mutant strains when the cells were cultured without PE21. The results for all mutant strains were compared with wild-type strain in the presence or absence of PE21; these data are tabulated in supplementary section. The results for 4 mutant strains impaired in FFA metabolism were studied more in detail, as described in section 3.0.

It has been hypothesized in Dr. Vladimir Titorenko's lab that one of the possible mechanisms through which PE21 increases the CLS of *Saccharomyces cerevisiae* is by decreasing the rate of liponecrosis. A detailed description of liponecrosis is provided in

section 3.0. The findings support this hypothesis for all 4 mutant strains. First, the concentrations of both TAG and FFA were analyzed in all mutant strains and compared to wild-type strain, using cells cultured with and without PE21. The data of these experiments confirm that in all 4 mutant strains the concentration of TAG is increased and the concentration of FFA is decreased as compared to wild-type strain. Moreover, the CLSs of mutant strains having lower FFA concentrations were compared to that of wild-type strain. These experiments have revealed that the CLSs of all these mutant strains are higher than that of wild-type strain.

References

1. Kirkwood, T.B.L. (2005). Understanding the odd science of aging. *Cell* 120:437-447.
2. Guarente, L.P., Partridge, L. and Wallace, D.C. (Editors) (2008). *Molecular Biology of Aging*. Cold Spring Harbor Laboratory Press, Cold Spring Harbor, New York, 610 pages.
3. Fontana, L., Partridge, L. and Longo, V.D. (2010). Extending healthy life span - from yeast to humans. *Science* 328:321-326.
4. Masoro, E.J. and Austad, S.N. (Editors) (2011). *Handbook of the Biology of Aging.* 7th Edition. Academic Press (an imprint of Elsevier), Amsterdam, 572 pages.
5. Kirkwood, T.B.L., Boys, R.J., Gillespie, C.S., Proctor, C.J., Shanley, D.P. and Wilkinson, D.J. (2003). Towards an e-biology of ageing: integrating theory and data. *Nat. Rev. Mol. Cell Biol.* 4:243-249.
6. Greer, E.L. and Brunet, A. (2008). Signaling networks in aging. *J. Cell Sci.* 121:407-412.
7. Lin, S.-J. and Sinclair, D. (2008). Molecular mechanisms of aging: insights from budding yeast. In: Guarente, L.P., Partridge, L., Wallace, D.C. (Eds.), *Molecular Biology of Aging*. Cold Spring Harbor Laboratory Press, Cold Spring Harbor, New York, pp. 483-516.
8. Mair, W. and Dillin, A. (2008). Aging and survival: the genetics of life span extension by dietary restriction. *Annu. Rev. Biochem.* 77:727-754.

9. Puigserver, P. and Kahn, C.R. (2008). Mammalian metabolism in aging. In: Guarente, L.P., Partridge, L., Wallace, D.C. (Eds.), *Molecular Biology of Aging*. Cold Spring Harbor Laboratory Press, Cold Spring Harbor, New York, pp. 545-574.

10. Lopez-Otin, C., Blasco, M. A., Partridge, L., Serrano, M. & Kroemer, G. The hallmarks of aging. *Cell* 153, 1194–1217 (2013).

11. Bitterman, K.J., Medvedik, O. and Sinclair, D.A. (2003). Longevity regulation in *Saccharomyces cerevisiae*: linking metabolism, genome stability, and heterochromatin. *Microbiol. Mol. Biol. Rev.* 67:376-399.

12. Kenyon, C. (2005). The plasticity of aging: insights from long-lived mutants. *Cell* 120:449-460.

13. Guarente, L. (2006). Sirtuins as potential targets for metabolic syndrome. *Nature* 444:868-874.

14. Kaeberlein, M., Burtner, C.R. and Kennedy, B.K. (2007). Recent developments in yeast aging. *PLoS Genet.* 3:e84.

15. Wei, M., Fabrizio, P., Hu, J., Ge, H., Cheng, C., Li, L. and Longo, V.D. (2008). Life span extension by calorie restriction depends on Rim15 and transcription factors downstream of Ras/PKA, Tor, and Sch9. *PLoS Genet*. 4:e13.

16. Narasimhan, S.D., Yen, K. and Tissenbaum, H.A. (2009). Converging pathways in lifespan regulation. *Curr. Biol*. 19:R657-R666.

17. Piper, M.D., Selman, C., McElwee, J.J. and Partridge, L. (2008). Separating cause from effect: how does insulin/IGF signalling control lifespan in worms, flies and mice? *J. Intern. Med*. 263:179-191.

18. Puigserver, P. and Kahn, C.R. (2008). Mammalian metabolism in aging. In: *Molecular Biology of Aging* (Guarente LP, Partridge L, Wallace DC, eds). Cold Spring Harbor Laboratory Press, Cold Spring Harbor, New York, pp. 545-574.

19. Salih, D.A. and Brunet, A. (2008). FoxO transcription factors in the maintenance of cellular homeostasis during aging. *Curr. Opin. Cell Biol*. 20:126-136.

20. Wolff, S. and Dillin, A. (2006). The trifecta of aging in *Caenorhabditis elegans*. *Exp. Gerontol*. 41:894-903

21. Laplante, M. and Sabatini, D.M. (2009). mTOR signaling at a glance. *J. Cell Sci*. 122:3589-3594.

22. Shaw, R.J. (2009). LKB1 and AMP-activated protein kinase control of mTOR signalling and growth. *Acta Physiol*. 196:65-80.

23. Mirisola MG, Taormina G, Fabrizio P, Wei M, Hu J, Longo VD. Serine- and threonine/valine-dependent activation of PDK and Tor orthologs converge on Sch9 to promote aging. PLoS Genetics 2014; 10(2): e1004113.

24. Martin DE, Hall MN. The expanding TOR signaling network. Current Opinion in Cell Biology 2005; 17(2):158-66.

25. Díaz-Troya, S., Pérez-Pérez, M.E., Florencio, F.J. and Crespo, J.L. (2008). The role of TOR in autophagy regulation from yeast to plants and mammals. *Autophagy* 4:851-865.

26. Huber, A., Bodenmiller, B., Uotila, A., Stahl, M., Wanka, S., Gerrits, B., Aebersold, R. and Loewith, R. (2009). Characterization of the rapamycin-sensitive phosphoproteome reveals that Sch9 is a central coordinator of protein synthesis. *Genes Dev*. 23:1929-1943.

27. Pan, Y. and Shadel, G.S. (2009). Extension of chronological life span by reduced TOR signaling requires down-regulation of Sch9p and involves increased mitochondrial OXPHOS complex density. *Aging* 1:131-145.

28. Crespo JL, Hall MN. Elucidating TOR Signaling and Rapamycin Action: Lessons from *Saccharomyces cerevisiae*. Microbiology and Molecular Biology Reviews 2002; 66(4): 579±591.

29. Medvedik, O., Lamming, D.W., Kim, K.D. and Sinclair, D.A. (2007). MSN2 and MSN4 link calorie restriction and TOR to sirtuin-mediated lifespan extension in *Saccharomyces cerevisiae*. *PLoS Biol*. 5:e261.

30. Lee, P., Cho, B.R., Joo, H.S. and Hahn, J.S. (2008). Yeast Yak1 kinase, a bridge between PKA and stress-responsive transcription factors, Hsf1 and Msn2/Msn4. *Mol. Microbiol*. 70:882-895.

31. Smets, B., Ghillebert, R., De Snijder, P., Binda, M., Swinnen, E., De Virgilio, C. and Winderickx, J. (2010). Life in the midst of scarcity: adaptations to nutrient availability in *Saccharomyces cerevisiae*. *Curr. Genet*. 56:1-32.

32. Roosen, J., Engelen, K., Marchal, K., Mathys, J., Griffioen, G., Cameroni, E., Thevelein, J.M., De Virgilio, C., De Moor, B. and Winderickx, J. (2005). PKA and Sch9 control a molecular switch important for the proper adaptation to nutrient availability. *Mol. Microbiol*. 55:862-880.

33. Cheng, C., Fabrizio, P., Ge, H., Longo, V.D. and Li, L.M. (2007). Inference of transcription modification in long-live yeast strains from their expression profiles. *BMC Genomics* 8:219.

34. Cheng, C., Fabrizio, P., Ge, H., Wei, M., Longo, V.D. and Li, L.M. (2007). Significant and systematic expression differentiation in long-lived yeast strains. *PLoS One* 2:e1095.

35. Slattery, M.G., Liko, D. and Heideman, W. (2008). Protein kinase A, TOR, and glucose transport control the response to nutrient repletion in *Saccharomyces cerevisiae*. *Eukaryot. Cell* 7:358-367.

36. Santangelo, G.M. (2006). Glucose signaling in *Saccharomyces cerevisiae*. *Microbiol. Mol. Biol. Rev*. 70:253-282.

37. Gancedo, J.M. (2008). The early steps of glucose signalling in yeast. *FEMS Microbiol. Rev*. 32:673-704.

38. Masoro, E.J. (2002). *Caloric Restriction: A Key to Understanding and Modulating Aging*. Elsevier, Amsterdam.

39. Colman, R.J., Anderson, R.M., Johnson, S.C., Kastman, E.K., Kosmatka, K.J., Beasley, T.M., Allison, D.B., Cruzen, C., Simmons, H.A., Kemnitz, J.W. and Weindruch, R. (2009). Caloric restriction delays disease onset and mortality in rhesus monkeys. *Science* 325:201-204.

40. Sinclair, D.A. (2005). Toward a unified theory of caloric restriction and longevity regulation. *Mech. Ageing Dev*. 126:987-1002.

41. Min, K.J., Flatt, T., Kulaots, I. and Tatar, M. (2007). Counting calories in *Drosophila* diet restriction. *Exp. Gerontol*. 42:247-251.

42. Weindruch, R. and Walford, R.L. (1988). *The Retardation of Aging and Disease by Dietary Restriction*. Thomas, Springfield.

43. Zimmerman, J.A., Malloy, V., Krajcik, R. and Orentreich, N. (2003). Nutritional control of aging. *Exp. Gerontol*. 38:47-52.

44. Mair, W., Piper, M.D. and Partridge, L. (2005). Calories do not explain extension of life span by dietary restriction in *Drosophila*. *PLoS Biol*. 3:e223.

45. Piper, M.D., Mair, W. and Partridge, L. (2005). Counting the calories: the role of specific nutrients in extension of life span by food restriction. *J. Gerontol. A Biol. Sci. Med. Sci*. 60:549-555.

46. Blagosklonny, M.V. (2006). Aging and immortality: quasi-programmed senescence and its pharmacologic inhibition. *Cell Cycle* 5:2087-2102..

47. Blagosklonny, M.V. (2008). Aging: ROS or TOR. *Cell Cycle* 7:3344-3354.

48. Blagosklonny, M.V. (2009). TOR-driven aging: speeding car without brakes. *Cell Cycle* 8:4055-4059.

49. Kaeberlein M. Lessons on longevity from budding yeast. Nature 2010; 464:513-519.

50. Richardson A, Galvan V, Lin AL, Oddo S. How longevity research can lead to therapies for Alzheimer's disease: The rapamycin story. Experimental Gerontology 2015; 68:51-8.

51. Yakupoglu YK, Buell JF, Woodle S, Kahan BD. Individualization of immunosuppressive therapy. III. Sirolimus associated with a reduced incidence of malignancy. Transplantation Proceedings 2006; 38(2):358-61.

52. Powers, R.W. 3rd, Kaeberlein, M., Caldwell, S.D., Kennedy, B.K. and Fields, S. (2006). Extension of chronological life span in yeast by decreased TOR pathway signaling. *Genes Dev*. 20:174-184.

53. Bonawitz, N.D., Chatenay-Lapointe, M., Pan, Y. and Shadel, G.S. (2007). Reduced TOR signaling extends chronological life span via increased respiration and upregulation of mitochondrial gene expression. *Cell Metab*. 5:265-277.

54. Harrison, D.E., Strong, R., Sharp, Z.D., Nelson, J.F., Astle, C.M., Flurkey, K., Nadon, N.L., Wilkinson, J.E., Frenkel, K., Carter, C.S., Pahor, M., Javors, M.A., Fernandez, E. and Miller, R.A. (2009). Rapamycin fed late in life extends lifespan in genetically heterogeneous mice. *Nature* 460:392-395.

55. Bjedov, I., Toivonen, J.M., Kerr, F., Slack, C., Jacobson, J., Foley, A. and Partridge, L. (2010). Mechanisms of life span extension by rapamycin in the fruit fly *Drosophila melanogaster*. *Cell Metab*. 11:35-46.

56. Demidenko, Z.N., Zubova, S.G., Bukreeva, E.I., Pospelov, V.A., Pospelova, T.V. and Blagosklonny, M.V. (2009). Rapamycin decelerates cellular senescence. *Cell Cycle* 8:1888-1895.

57. Onken, B. and Driscoll, M. (2010). Metformin induces a dietary restriction-like state and the oxidative stress response to extend *C. elegans* healthspan via AMPK, LKB1, and SKN-1. *PLoS ONE* 5:e8758.

58. Anisimov, V.N., Berstein, L.M., Egormin, P.A., Piskunova, T.S., Popovich, I.G., Zabezhinski, M.A., Tyndyk, M.L., Yurova, M.V., Kovalenko, I.G., Poroshina, T.E., Semenchenko, A.V., Anisimov, V.N., Berstein, L.M., Egormin, P.A., Piskunova, T.S., Popovich, I.G., Zabezhinski, M.A., Tyndyk, M.L., Yurova, M.V., Kovalenko, I.G., Poroshina, T.E. and Semenchenko, A.V. (2008). Metformin slows down aging and extends life span of female SHR mice. *Cell Cycle* 7:2769-2773.

59. Ingram, D.K., Roth, G.S., Lane, M.A., Ottinger, M.A., Zou, S., de Cabo, R. and Mattison, J.A. (2006). The potential for dietary restriction to increase longevity in humans: extrapolation from monkey studies. *Biogerontology* 7:143-148.

60. Lane, M.A., Roth, G.S. and Ingram, D.K. (2007). Caloric restriction mimetics: a novel approach for biogerontology. *Methods Mol. Biol*. 371:143-149.

61. Petrascheck, M., Ye, X. and Buck, L.B. (2007). An antidepressant that extends lifespan in adult *Caenorhabditis elegans*. *Nature* 450:553-556.

62. Howitz, K.T., Bitterman, K.J., Cohen, H.Y., Lamming, D.W., Lavu, S., Wood, J.G., Zipkin, R.E., Chung, P., Kisielewski, A., Zhang, L.L., Scherer, B. and Sinclair, D.A. (2003). Small molecule activators of sirtuins extend *Saccharomyces cerevisiae* lifespan. *Nature* 425:191-196.

63. Wood, J.G., Rogina, B., Lavu, S., Howitz, K., Helfand, S.L., Tatar, M. and Sinclair, D. (2004). Sirtuin activators mimic caloric restriction and delay ageing in metazoans. *Nature* 430:686-689.

64. Baur, J.A., Pearson, K.J., Price, N.L., Jamieson, H.A., Lerin, C., Kalra, A., Prabhu, V.V., Allard, J.S., Lopez-Lluch, G., Lewis, K., Pistell, P.J., Poosala, S., Becker, K.G., Boss, O., Gwinn, D., Wang, M., Ramaswamy, S., Fishbein, K.W., Spencer, R.G., Lakatta, E.G., Le Couteur, D., Shaw, R.J., Navas, P., Puigserver, P., Ingram, D.K., de Cabo, R. and Sinclair, D.A. (2006). Resveratrol improves health and survival of mice on a high-calorie diet. *Nature* 444:337-342.

65. Burstein MT, Titorenko VI. A mitochondrially targeted compound delays aging in yeast through a mechanism linking mitochondrial membrane lipid metabolism to mitochondrial redox biology. Redox Biol 2014; 2:305-307.

66. Lutchman V, Dakik P, McAuley M, Cortes B, Ferraye G, Gontmacher L, Graziano D, Moukhariq FZ, Simard É, Titorenko VI. Six plant extracts delay yeast chronological aging through different signaling pathways. Oncotarget. 2016; 7: 50845-50863.

67. Lutchman V, Medkour Y, Samson E, Arlia-Ciommo A, Dakik P, Cortes B, Feldman R, Mohtashami S, McAuley M, Chancharoen M, Rukundo B, Simard É, Titorenko VI. Discovery of plant extracts that greatly delay yeast chronological aging and have different effects on longevity-defining cellular processes. Oncotarget. 2016; 7: 16542-16566.

68. Longo, V.D. and Kennedy, B.K. (2006). Sirtuins in aging and age-related disease. *Cell* 126:257-268.

69. Arlia-Ciommo A, Leonov A, Piano A, Svistkova V, Titorenko VI. Cellautonomous mechanisms of chronological aging in yeast *Saccharomyces cerevisiae*. Microbial Cell 2014; 1:163-178.

70. Bitterman, K.J., Medvedik, O. and Sinclair, D.A. (2003). Longevity regulation in *Saccharomyces cerevisiae*: linking metabolism, genome stability, and heterochromatin. *Microbiol. Mol. Biol. Rev*. 67:376-399.

71. Mair, W. and Dillin, A. (2008). Aging and survival: the genetics of life span extension by dietary restriction. *Annu. Rev. Biochem*. 77:727-754. 135. Masoro, E.J. (2005). Overview of caloric restriction and ageing. *Mech. Ageing Dev*. 126:913-922.

72. Sinclair, D.A. (2005). Toward a unified theory of caloric restriction and longevity regulation. *Mech. Ageing Dev*. 126:987-1002.

73. Longo VD, Shadel GS, Kaeberlein M, Kennedy B. Replicative and Chronological Aging in *Saccharomyces cerevisiae*. Cell Metab 2012; 16:18-31.

74. Fabrizio, P. and Longo, V.D. (2003). The chronological life span of *Saccharomyces cerevisiae*. *Aging Cell* 2:73-81.

75. Henry SA, Kohlwein SD, Carman GM. Metabolism and Regulation of Glycerolipids in the Yeast *Saccharomyces cerevisiae*. Genetics 2012; 190:317-349.

76. Carman GM, Han G. Regulation of Phospholipid Synthesis in the Yeast *Saccharomyces cerevisiae*. Annu Rev Biochem 2011; 80:859-883.

77. Klug L, Daum G. Yeast lipid metabolism at a glance. FEMS Yeast Res 2014; 14:369-388.

78. Hauff, K.D. and Hatch, G.M. (2006). Cardiolipin metabolism and Barth Syndrome. *Prog. Lipid Res*. 45:91-101.

79. Ott, M., Zhivotovsky, B., and Orrenius, S. (2007). Role of cardiolipin in cytochrome c release from mitochondria. *Cell Death Differ.* 14:1243-1247.

80. Houtkooper, R.H. and Vaz, F.M. (2008). Cardiolipin, the heart of mitochondrial metabolism. *Cell. Mol. Life Sci*. 65:2493-2506.

81. Schlame, M. (2008). Cardiolipin synthesis for the assembly of bacterial and mitochondrial membranes. *J. Lipid Res*. 49:1607-1620.

82. Gohil, V.M. and Greenberg, M.L. (2009). Mitochondrial membrane biogenesis: phospholipids and proteins go hand in hand. *J. Biol. Chem.*184:469-472. 198.

83. Joshi, A.S., Zhou, J., Gohil, V.M., Chen, S. and Greenberg, M.L. (2009). Cellular functions of cardiolipin in yeast. *Biochim. Biophys. Acta* 1793:212-218.

84. Schlame, M. and Ren, M. (2009). The role of cardiolipin in the structural organization of mitochondrial membranes. *Biochim. Biophys. Acta* 1788:2080-2083.

85. Osman, C., Voelker, D.R. and Langer, T. (2011). Making heads or tails of phospholipids in mitochondria. *J. Cell Biol*. 192:7-16.

86. Shevchenko A, Simons K. 2010. Lipidomics: coming to grips with lipid diversity. Nat. Rev. Mol. Cell Biol. 11:593–98.

87. Tamura, Y., Onguka, O., Hobbs, A. E. A., Jensen, R. E., Iijima, M., Claypool, S. M., & Sesaki, H. (2012). Role for Two Conserved Intermembrane Space Proteins, Ups1p and Up2p, in Intra-mitochondrial Phospholipid Trafficking. The Journal of Biological Chemistry, 287(19), 15205–15218.

88. Koadki, T. and Yamashita, S., Characterization of the methyltransferases in the yeast phosphatidylethanolamine methylation pathway by selective gene disruption. European Journal of Biochemistry, 185: 243–251.

89. Oelkers P, Cromley D, Padamsee M, Billheimer JT, Sturley SL. The *DGA1* Gene determines a second triglyceride synthetic pathway in yeast. J Biol Chem. 2002;277:8877–8881. doi: 10.1074/jbc.M111646200.

90. Zweytick, D., Leitner, E., Kohlwein, S. D., Yu, C., Rothblatt, J. and Daum, G., Contribution of Are1p and Are2p to steryl ester synthesis in the yeast *Saccharomyces cerevisiae*. European Journal of Biochemistry, 267: 1075–1082.

91. Köffel, R., Tiwari, R., Falquet, L., & Schneiter, R. (2005). The *Saccharomyces cerevisiae* YLL012/YEH1, YLR020/YEH2, and TGL1 Genes Encode a Novel Family of Membrane-Anchored Lipases That Are Required for Steryl Ester Hydrolysis. Molecular and Cellular Biology, 25(5), 1655–1668.

92. Wagner, A. and Daum, G. (2005). Formation and mobilization of neutral lipids in the yeast *Saccharomyces cerevisiae*. *Biochem. Soc. Trans*. 33:1174-1177.

93. Kurat, C.F., Natter, K., Petschnigg, J., Wolinski, H., Scheuringer, K., Scholz, H., Zimmermann, R., Leber, R., Zechner, R. and Kohlwein, S.D. (2006) Obese yeast: Triglyceride lipolysis is functionally conserved from mammals to yeast. *J. Biol. Chem.* 281:491-500.

94. Czabany, T., Athenstaedt, K. and Daum, G. (2007). Synthesis, storage and degradation of neutral lipids in yeast. *Biochim. Biophys. Acta* 1771:299-309.

95. Mullner, H. and Daum, G. (2004). Dynamics of neutral lipid storage in yeast. *Acta Biochim. Pol.* 51:323-347.

96. Gu, Z., Valianpour, F., Chen, S., Vaz, F. M., Hakkaart, G. A., Wanders, R. J. A. and Greenberg, M. L. (2004), Aberrant cardiolipin metabolism in the yeast *taz1* mutant: a model for Barth syndrome. Molecular Microbiology, 51: 149–158.

97. Brügger, B., Erben, G., Sandhoff, R., Wieland, F.T. and Lehmann, W.D. (1997). Quantitative analysis of biological membrane lipids at the low picomole level by nano-electrospray ionization tandem mass spectroscopy. *Proc. Natl. Acad. Sci. USA*

94:2339-2344.

98. Schneiter, R., Brügger, B., Sandhoff, R., Zellnig, G., Leber, A., Lampl, M., Athenstaedt, K., Hrastnik, C., Eder, S., Daum, G., Paltauf, F., Wieland, F.T. and Kohlwein, S.D. (1999). Electrospray ionization tandem mass spectrometry (ESIMS/MS) analysis of the lipid molecular species composition of yeast subcellular membranes reveals acyl chain-based sorting/remodeling of distinct molecular species en route to the plasma membrane. *J. Cell Biol*. 146:741-754.

99. Guo, T., Gregg, C., Boukh-Viner, T., Kyryakov, P., Goldberg, A., Bourque, S., Banu, F., Haile, S., Milijevic, S., San, K.H., Solomon, J., Wong, V. and Titorenko, V.I. (2007). A signal from inside the peroxisome initiates its division by promoting the remodeling of the peroxisomal membrane. *J. Cell Biol*. 177:289-303.

100. Russell, S.J. and Kahn, C.R. (2007). Endocrine regulation of ageing. *Nat. Rev. Mol. Cell Biol.* 8:681-691.

101. Cao, H., Gerhold, K., Mayers, J.R., Wiest, M.M., Watkins, S.M. and Hotamisligil, G.S. (2008). Identification of a lipokine, a lipid hormone linking adipose tissue to systemic metabolism. *Cell* 134:933-944.

102. Brugger B. Lipidomics: analysis of the lipid composition of cells and subcellular organelles by electrospray ionization mass spectrometry. Annu Rev Biochem. 2014;83:79–98.

103. Guo, T., Gregg, C., Boukh-Viner, T., Kyryakov, P., Goldberg, A., Bourque, S., Banu, F., Haile, S., Milijevic, S., San, K.H., Solomon, J., Wong, V. and Titorenko, V.I. (2007). A signal from inside the peroxisome initiates its division by promoting the remodeling of the peroxisomal membrane. *J. Cell Biol*. 177:289-303.

104. Russell, S.J. and Kahn, C.R. (2007). Endocrine regulation of ageing. Nat. Rev. Mol. Cell Biol. 8:681-691.

105. Cao, H., Gerhold, K., Mayers, J.R., Wiest, M.M., Watkins, S.M. and Hotamisligil, G.S. (2008). Identification of a lipokine, a lipid hormone linking adipose tissue to systemic metabolism. Cell 134:933-944.

106. Claypool, S.M., Oktay, Y., Boontheung, P., Loo, J.A. and Koehler, C.M. (2008). Cardiolipin defines the interactome of the major ADP/ATP carrier protein of the mitochondrial inner membrane. *J. Cell Biol*. 182:937-950.

107. Schneiter R, Bru¨gger B, Sandhoff R, Zellnig G, Leber A, et al. (1999) Electrospray ionization tandem mass spectrometry (ESI-MS/MS) analysis of the lipid molecular species composition of yeast subcellular membranes reveals acyl chain-based sorting/remodeling of distinct molecular species en route to the plasma membrane. J Cell Biol 146: 741–754.

108. Daum G, Lees ND, Bard M, Dickson R (1998) Biochemistry, cell biology and molecular biology of lipids of *Saccharomyces cerevisiae*. Yeast 14: 1471–1510. doi:10.1002/(SICI)1097-0061(199812)14:16,1471::AID-YEA353.3.0.CO;2- Y.

109. Czabany, T., Athenstaedt, K. and Daum, G. (2007). Synthesis, storage and degradation of neutral lipids in yeast. Biochim. Biophys. Acta 1771:299-309.

110. Brügger, B., Erben, G., Sandhoff, R., Wieland, F.T. and Lehmann, W.D. (1997). Quantitative analysis of biological membrane lipids at the low picomole level by nano-electrospray ionization tandem mass spectroscopy. Proc. Natl. Acad. Sci. USA 94:2339-2344.

111. Whitehouse CM, Dreyer RN, Yamashita M, Fenn JB. 1985. Electrospray interface for liquid chromatographs and mass spectrometers. Anal. Chem. 57:675–79

112. Van Pelt CK, Zhang S, Fung E, Chu I, Liu T, et al. 2003. A fully automated nano electrospray tandem mass spectrometric method for analysis of Caco-2 samples. Rapid Commun. Mass Spectrom. 17:1573–78.

113. Milne S, Ivanova P, Forrester J, Alex Brown H. Lipidomics: An analysis of cellular lipids by ESI-MS. Methods 2006 June 2006;39(2):92-103.

114. .B. Fenn, M. Mann, C.K. Meng, S.F. Wong, C.M. Whitehouse, Science 246 (1989) 64–71

115. Han X, Gross RW. 1994. Electrospray ionization mass spectroscopic analysis of human erythrocyte plasma membrane phospholipids. Proc. Natl. Acad. Sci. USA 91:10635–39.

116. Schuhmann K, Herzog R, Schwudke D, Metelmann-Strupat W, Bornstein SR, Shevchenko A. 2011. Bottom-up shotgun lipidomics by higher energy collisional dissociation on LTQ orbitrap mass spectrometers. Anal. Chem. 83:5480–87.
117. Li J, Hoene M, Zhao X, Chen S, Wei H, et al. 2013. Stable isotope-assisted lipidomics combined with nontargeted isotopomer filtering, a tool to unravel the complex dynamics of lipid metabolism. Anal. Chem. 85:4651–57.
118. Schwudke D, Schuhmann K, Herzog R, Bornstein SR, Shevchenko A. 2011. Shotgun lipidomics on high resolution mass spectrometers. Cold Spring Harb. Perspect. Biol. 3:a004614.
119. Deems R, BuczynskiMW, Bowers-Gentry R, Harkewicz R, Dennis EA. 2007. Detection and quantitation of eicosanoids via high performance liquid chromatography–electrospray ionization–mass spectrometry. Methods Enzymol. 432:59–82.
120. Panuwet, P., Hunter, R. E., D'Souza, P. E., Chen, X., Radford, S. A., Cohen, J. R., … Barr, D. B. (2016). Biological Matrix Effects in Quantitative Tandem Mass Spectrometry-Based Analytical Methods: Advancing Biomonitoring. Critical Reviews in Analytical Chemistry / CRC, 46(2), 93–105.
121. Folch, J., M. Lees, and G. H. Sloane Stanley. 1957. A simple method for the isolation and purification of total lipides from animal tissues. J. Biol. Chem. 226: 497–509.
122. International Agency for Research on Cancer. Chloroform. Some Halogenated Hydrocarbons; IARC Monographs on the Evaluation of the Carcinogenic Risk of

Chemicals to Humans, Vol. 20; World Health Organization: Lyon, France, 1979; pp 401-427.

123. Ejsing, C.S., Sampaio, J.L., Surendranath, V., Duchoslav, E., Ekroos, K., Klemm, R.W., Simons, K. and Shevchenko, A. (2009). Global analysis of the yeast lipidome by quantitative shotgun mass spectrometry. Proc. Natl. Acad. Sci. USA 106:2136- 2141.

124. Lutchman V, Medkour Y, Samson E, Arlia-Ciommo A, Dakik P, Cortes B, Feldman R, Mohtashami S, McAuley M, Chancharoen M, Rukundo B, Simard É, Titorenko VI. Discovery of plant extracts that greatly delay yeast chronological aging and have different effects on longevity-defining cellular processes. Oncotarget. 2016; 7(13):16542-16566.

125. Richard, V.R., Beach, A., Piano, A., Leonov, A., Feldman, R., Burstein, M.T., Kyryakov, P., Gomez-Perez, A., Arlia-Ciommo, A., Baptista, S., Campbell, C., Goncharov, D., Pannu, S., Patrinos, D., Sadri, B., Svistkova, V., Victor, A. and Titorenko, V.I. Mechanism of liponecrosis, a distinct mode of programmed cell death. Cell Cycle (2014) 13:3707-3726.

126. Medkour, Y., Dakik, P., McAuley, M., Mohammad, K., Mitrofanova, D. and Titorenko, V.I. Mechanisms underlying the essential role of mitochondrial membrane lipids in yeast chronological aging. Oxid. Med. Cell. Longev. (2017) 2017:2916985.